

CRYOGENIC QUALITY METER

George C. Marshall Space Flight Center
Huntsville, Alabama

FINAL REPORT
November 2, 1964

FACILITY FORM 608

N65 14025 (ACCESSION NUMBER)	
201 (PAGES)	1 (THRU)
CR-60065 (NASA CR OR TMX OR AD NUMBER)	14 (CATEGORY)

GPO PRICE \$ _____

OTS PRICE(S) \$ _____

Hard copy (HC) 6.00

Microfiche (MF) 1.25

Industrial / *Accufay* 650 ACKERMAN ROAD • COLUMBUS 2, OHIO

Contract No. NAS 9-11734
Contract Number 14-000000-1(1)
CRS 82-1343-04

CRYOGENIC QUALITY METER

Final Report

November 2, 1964

**Fluid Mechanics Section
Fluid Mechanics & Thermodynamics Branch
Propulsion Division
Propulsion & Vehicle Engineering Laboratory
Research & Development Operations
George C. Marshall Space Flight Center
Huntsville, Alabama**

C. D. Arnett	Principal C.O.R.
H. D. Burke	Alternate C.O.R.
A. M. Payne	Alternate C.O.R.

**Contract No. NAS8-11736
Control No. DCN 1-4-50-01210 & S1(1)
CPB 02-1263-64**

**Performed by
The Industrial Nucleonics Corporation
650 Ackerman Road
Columbus, Ohio 43202**

PREFACE

The work performed under this contract consists of an analytical study to determine the most practical method for measuring the quality of cryogenic propellants being vented to a vacuum ambient, and a device scheme for the measurement. Since any application imposes certain limitations in the instrument design, the contract application specifications for the design were those anticipated for the Saturn SIVB from launch through orbit.

Written by William B. Joyce
William Joyce
Technical Manager

Reviewed by Howard J. Evans
Howard Evans
Manager, Applied Physics Laboratory

Approved by William R. Clore
William R. Clore
Manager, Research, Development,
Engineering and Test Division

Contract Performance
Checked by Charles O. Badgett
Charles O. Badgett
Program Manager

TABLE OF CONTENTS

<u>Section Number</u>		<u>Page Number</u>
1.	INTRODUCTION	1-1
2.	FACTORS INFLUENCING DESIGN	2-1
2.1	Definition of Quality	2-1
2.2	Selected Physical Properties of Hydrogen and Oxygen	2-6
2.3	Explicit Specifications	2-13
2.4	Implicit Specifications	2-15
2.5	Mixing of Vented Fluid	2-19
2.6	General Measurement Principles	2-23
3.	APPROACHES STUDIES AND METHOD OF SCREENING	3-1
3.1	Approaches Studied	3-1
3.2	Basis of Selection of Approaches Studied	3-2
3.3	Method of Screening Approaches	3-3
4.	LESS PROMISING APPROACHES	4-1
4.1	Mechanical Techniques	4-1
4.1.1	Simple Pressure Measurement	4-1
4.1.2	Mechanical Reactance	4-1
4.1.3	Quality from Flow Measurements	4-4
4.2	Acoustical Techniques	4-10
4.2.1	Attenuation and Scattering	4-12

<u>Section Number</u>		<u>Page Number</u>
	4.2.2 Speed of Sound	4-18
	4.2.3 Dynamic Compressibility	4-29
4.3	Electromagnetic Techniques	4-31
	4.3.1 Capacitance	4-31
	4.3.2 Susceptibility (Atomic)	4-44
	4.3.3 Susceptibility (Nuclear)	4-47
	4.3.4 Nuclear Paramagnetic Resonance and Electron Paramagnetic Resonance	4-50
	4.3.5 Microwave Techniques	4-54
	4.3.6 Scattering of Light	4-59
	4.3.7 Spectroscopic Techniques	4-62
4.4	Thermal and Thermodynamic Techniques	4-64
	4.4.1 Heat Flow (Hot Wire Technology)	4-64
	4.4.2 Vaporization of Liquid	4-65
4.5	Nuclear Techniques	4-65
	4.5.1 Gamma Ray Transmission	4-68
	4.5.2 Beta Rays	4-71
	4.5.3 Alpha Particles	4-72
	4.5.4 Neutrons	4-74
4.6	Other Techniques	4-75
5.	PROMISING APPROACHES	5-1
5.1	Vaporization	5-1

<u>Section Number</u>	<u>Page Number</u>
5.2 Beta Transmission	5-9
5.3 Gamma Ray Scatter	5-15
5.4 Electronic Circuitry	5-27
5.4.1 Basic Concepts	5-27
5.4.2 Specific Description	5-30
5.4.2.1 Scintillator Assembly	5-30
5.4.2.2 Regulated Power Supply	5-31
5.4.2.3 Pulse Amplifier	5-31
5.4.2.4 Ratio Computer	5-31
5.4.2.5 Temperature Control	5-34
5.4.2.6 Grouping of Units	5-36
5.4.2.7 Errors	5-36
5.4.2.8 Weight	5-37
5.4.2.9 Solid-State Detector System	5-37
6. CONCLUSIONS	6-1
BIBLIOGRAPHY	

APPENDICES

<u>Section Number</u>		<u>Page Number</u>
A.	Response of a Parallel Plate Capacitor to Fuel Location	A-1
B.	Sources of Statistical Noise in Gamma Ray Attenuation or Scatter	B-1
C.	Scattering of Gamma Rays by Liquid vs. Scattering by Vapor	C-1
D.	The Relation Between the Source Strength and Detector Count Rate for the Gamma Ray Scatter Detector of Figure 19 (Section 5.3)	D-1
E.	Theory of Pulse Rate Ratio Computer	E-1

ILLUSTRATIONS

<u>Section Number</u>		<u>Page Number</u>
1.	Temperature-Entropy Diagram for Hydrogen	2-10
2.	Continuous Vent Orbital Coast Pressure History for Saturn 5/S-IVB	2-11
3.	Density vs Pressure for Saturated Hydrogen Vapor	2-12
4.	Liquid Disperser	2-22
5.	Mechanical Reactance	4-2
6.	Viscous Drag (Two-Phase Flow)	4-5
7.	Turbine Blade (Two-Phase Flow) - Separation of Phases	4-6
8.	Flow Through an Orifice (Two Phase Flow)	4-8
9.	Acoustical Quality Meter (Speed of Sound)	4-22
10.	Liquid Distribution in a Capacitor	4-34
11.	Capacitor Electric Field Structure	4-40
12.	Alignment of O ₂ Electric Moment by an External Field	4-45
13.	Heat Transfer Quality Meter	4-66
14.	Density Measuring Gauges	4-69
15.	Expansion Technique Quality Meter	5-2

<u>Section Number</u>		<u>Page Number</u>
16.	Vaporization Quality Meter	5-6
17.	Quality Control and Measurement System	5-8
18.	Beta Transmission Quality Meter	5-12
19.	Gamma Ray Scatter Quality Meter	5-17
20.	Block Diagram, Cryogenic Vent Quality Guage with Scintillation Photomultiplier	5-28
21.	Photomultiplier and Regulated Power Supply	5-32
22.	Pulse Amplifier	5-33
23.	Ratio Computer and Pressure Compensator	5-35
24.	Block Diagram, Cryogenic Vent Quality Gauge with Solid-State Detector	5-38
E-1	Basic Divider Circuit	E-3
E-2	Direction Indicator	E-4
E-3	Current Wave Forms	E-5

1. INTRODUCTION

While in orbit, a cryogenic fuel such as used in the Saturn S-IVB will suffer boil off. The boiled off fuel mass is vented to vacuum ambient. The quality of the fluid fuel boiled off is a figure of merit indicating what percent of the vented fuel is in the vapor rather than the liquid state. It is desirable that this figure of merit be as high as possible. Various possible approaches to the design of a quality gauge are examined. Based on this study, an optimum design is proposed.

The Saturns are an evolutionary series of launch vehicles leading toward the Saturn V which will place the 95,000 pound Apollo/Lem spacecraft on its trajectory toward the moon.¹ The Saturn I's are the first-generation space launch vehicles.

The Saturn I-B is a more powerful version of Saturn I, capable of boosting a 17-ton payload into low earth orbit. Its immediate mission is the flight testing of the Apollo/Lem spacecraft in earth orbit.

The second stage of the Saturn I-B is the S-IVB. Eventually, the S-IVB will become the third stage of the Saturn V. On the Saturn V, the S-IVB will be launched into a low earth orbit and shut down during systems checkout. After restart, it will accelerate the Apollo spacecraft to escape velocity. Before being jettisoned, the S-IVB is used in stabilizing the Lem in a turn around and docking maneuver preliminary to eventual lunar capture.

Superior numbers refer to similarly numbered references at the end of this report.

The S-IVB has a single liquid hydrogen/liquid oxygen engine rated at 200,000 pounds thrust. A common bulkhead separates the LH_2 from the LOX. Some other distinctive features result from the extended period (hours) during which the S-IVB parked in an orbit at about 100 miles altitude. Heat leaks into the fuel tank causing propellant vaporization thereby increasing tank pressure. To prevent eventual over-pressurization, energy is removed from the tank by continuously venting vapor overboard. Successful venting requires that vapor, but not liquid, be released.

Two particularly significant factors tending to introduce liquid into the vented fluid are (1) the turbulence produced by acceleration, vibration and maneuvering as the S-IVB is propelled into orbit, and (2) the lack of apparent gravity while in orbit. In the absence of g forces, the wetting cryogenics will tend to cover all surfaces inside the tank, including the mouth of any vent tube. As a result, release of liquid may be expected.

Three methods are used to avoid this loss of liquid. First, seventy-pound settling engines run for nearly a minute after the initial S-IVB shutdown and are expected to provide sufficient acceleration to settle the liquids in the "bottoms" of their tanks while any turbulence dies out.

The second method operates during the entire vent cycle of up to five hours while parked in orbit. Boiled off fluid is continuously vented to vacuum ambient. The vapor is piped from inside the tank to suitable exterior points where it is released through nozzles. The small

acceleration of the tank resulting from this venting tends to hold the fuel in the bottom of the tank and thereby insures that the inlet to the vent pipe remains free of liquid. The third method employs a turbine separator during the fast tank blowdown immediately before engine restart. During this blow-down period, the centrifugal action of the separator removes all but the smallest drops.

The several techniques just mentioned form a system which minimizes the amount of liquid escaping with the vented vapor. In order to evaluate the effectiveness of this system, a quality gauge or meter is needed.

Quality is defined as the ratio of the mass of the vapor, m_v , to the total mass (vapor mass plus liquid mass, m_l) being vented.

$$Q = \frac{m_v}{m_l + m_v} \quad (1-1)$$

At 100% quality, there is no liquid in the vapor. At 50%, the vented fluid carries an equal mass of vapor and liquid. Thus, quality is a direct indication of the success of the separation system.

This report analytically evaluates a large number of possible approaches to the design of a quality measurement meter. Most are rejected for reasons which are peculiar to the particular application. Three approaches are rated as promising. Device design details and performance figures are presented for the best method adaptable to the contract application specifications.

2. FACTORS INFLUENCING DESIGN

The final design of an instrument and the adaptability of a technology to the instrument and measurement is always dictated by the application. Three prime factors limit the number of choices of technology available for a specific use:

1. Nature of the process variations,
2. Nature of the environmental conditions and variations, and
3. The end use of the measured data.

Several of these factors as they effect design of the quality meter are examined below.

2.1 Definition of Quality

A brief definition of quality was given in the introduction, Equation (1-1). A precise definition includes a number of significant implications which will be considered in this section.

Heat flow into a cryogenic liquid will cause fluid boil off in any practical system. Theoretically, it is possible to contain the fluid in a sufficiently strong structure. However, in practice, the weight of such a restraining tank is enormous and completely impractical for spaceflight vehicles.

It is advantageous to program the amount of boil off. Insulation minimizes the heat flow to the liquid. The unavoidable minimum heat which does reach the fuel is removed by venting fluid, usually vapor. Optimum venting releases as much energy as possible while minimizing the mass of fuel lost; that is, the energy-mass ratio of the vented fuel is

maximized. For vapors or gases at low temperature and not too high pressure, this ratio is highest in the gaseous state and increases with increasing temperature and decreasing pressure. Hydrogen and oxygen are examples for they have negative Joule coefficients and positive Joule-Kelvin (Thompson) coefficients at the temperatures of interest.²

A vapor-liquid state is in equilibrium with a vapor pressure corresponding to the temperature inside the tank. Optimum venting efficiency occurs with the following procedure. A tube leads from outside the tank into the ullage. A pressure dropping valve is located at the interior end of the tube. The vapor (for example, hydrogen vapor) expands through the valve to a pressure slightly above the vacuum ambient. The associated cooling of the hydrogen extracts heat from the LH_2 in the tank if the vent tube passes through the fuel before piercing the tank wall. For a sufficiently long pass through the liquid, the vapor will extract heat until the vapor temperature reaches the liquid temperature. This represents the optimum energy-mass ratio for a passive vent system.

In the S-IVB application, it is essential that the vented vapor produce an accelerative thrust. Thus, the principle pressure drop occurs outside the tank at the end of the vent tubes. Internal expansion would greatly attenuate the thrust. Furthermore, at 100% quality, expansion from only 20 or 30 psi yields a very modest improvement in the energy-mass ratio. Thus, expansion external to the tank appears to be a well-justified compromise in return for positive fuel control in the tank.

On the other hand, if 50% or lower quality should occur, the internal expansion method would vaporize the vented fuel with the heat of vaporization drawn from the unvented liquid. A considerable improvement in the energy-mass ratio would result. This approach is analyzed further as a part of a recommended thermodynamic approach (Section 5).

With the present S-IVB design, the minimum allowable pressure of the vented vapor, at the termination of thermal contact with the fuel, is determined by thrust considerations and is nearly as great as the pressure in the tank. Subject to these restrictions, the optimum energy/mass ratio occurs when the vented fluid carries along no liquid. An index of this efficiency is quality defined as the ratio of the rate at which vapor is vented to the rate at which vapor plus liquid is vented:

$$Q = \frac{\bar{\rho}_v A s_v}{\bar{\rho}_v A s_v + \bar{\rho}_l A s_l} = \frac{\bar{\rho}_v s_v}{\bar{\rho}_v s_v + \bar{\rho}_l s_l} \quad (2-1)$$

where,

A = cross sectional area of the vent tube at the point of measurement

Q = quality

$\bar{\rho}_v$ = density of the vapor averaged over A. (The vapor density is zero in the liquid by definition.) $\bar{\rho}_v$ is thus the vapor mass, m_v , divided by the sample volume, V , in which the measurement is made.

$\bar{\rho}_l$ = density of the liquid averaged over A. (The liquid density is zero in the vapor.) $\bar{\rho}_l$ is thus the liquid mass, m_l , divided by the sample volume, V .

s_v and s_l are velocities (speeds) of the vapor and the liquid parallel to the tube axis, again averaged over the cross section A.

For future reference, define

ρ_l = liquid density--the usual definition averaged only over region where liquid is present, e. g., $\rho_l = 1.14 \text{ gm/cm}^3$ for LOX

ρ_v = vapor density--usual definition.

Equation (2-1) is the ratio of the vapor mass flow to the total mass flow. An equivalent form of Equation (2-1) is based on the following equality:

$$\bar{\rho}_l A s_l = \sum_i \rho_l v_i s_i = \sum_i m_i s_i \quad (2-2)$$

where v_i , s_i , and m_i are the volume, speed along the tube axis, and the mass of the i^{th} drop or incremental volume of fuel. The sum is over all v_i per unit length of tube at the point of measurement.

The important point of these formulae is that the vented liquid and vapor elements contribute to the quality in proportion to their speed as well as their masses. A series of large drops of fuel which have not accelerated as rapidly as the vapor carrying it, or a liquid film on the wall moving more slowly than the vapor, will not contribute to the ejected quality as much as if they were at the vapor speed. This is physically obvious because, for example, a fluid film will contribute to the rate of loss of liquid fuel both in proportion to the thickness of the film and in proportion to the film speed.

If the liquid is broken up and well mixed in the vented vapor, it is reasonable to assume, in such a case, that the liquid droplets are moving at the same speed as the vapor--i. e., $s_v = s_l$. Then the speeds may be cancelled from Equation (2-1) yielding

$$Q = \frac{\bar{\rho}_v}{\bar{\rho}_v + \bar{\rho}_l} = \frac{m_v}{m_v + m_l} \quad (2-3)$$

which is a ratio of the masses present at the cross section where the measurement is made. (m_v and m_l are the vapor and liquid masses, respectively, in the region where the measurement is made.) No velocity measurement is called for and a considerable simplification in the instrument is possible.

A further point to consider in the definition of quality is the location, along the length of the vent tube, of the quality meter. In order that the energy-mass ratio of the vented fluid be representative of the efficiency of venting, the measurement should be made where the heat transfer of the stored fuel with the vented fluid is essentially complete and the heat transfer from the ambient has not become significant. This is somewhere in the vicinity of the point where the vent tube pierces the tank wall. The heat transfer to the fluid in the vent pipe is to be neglected in this study. Thus, to within the specified accuracy of 5% quality, the location of the quality meter is not critical. Fortunately, the section of vent pipe just outside the tank is suitable as a practical location for an instrument and

as a fundamentally meaningful point at which to make a measurement.

2.2 Selected Physical Properties of Hydrogen and Oxygen

A knowledge of the physical properties of hydrogen and oxygen is essential to the design of a quality gauge. Rather exact values of some physical properties utilized in the recommended system are necessary; others need to be known only approximately (one or two significant figures) since their exact value is automatically taken into account by an empirical calibration curve. Approximate physical properties are essential in determining the practicality of various theoretically plausible systems.

The following table and three figures are selected on the basis of relevance to this study. Whenever needed, constants will be drawn from this section without explicit reference. The number of significant figures used in calculations is based on consistency with an ultimate error of less than 5% quality, rather than on the basis of a uniform number of significant figures.

Selected Physical Constants of Hydrogen and Oxygen³⁻¹²

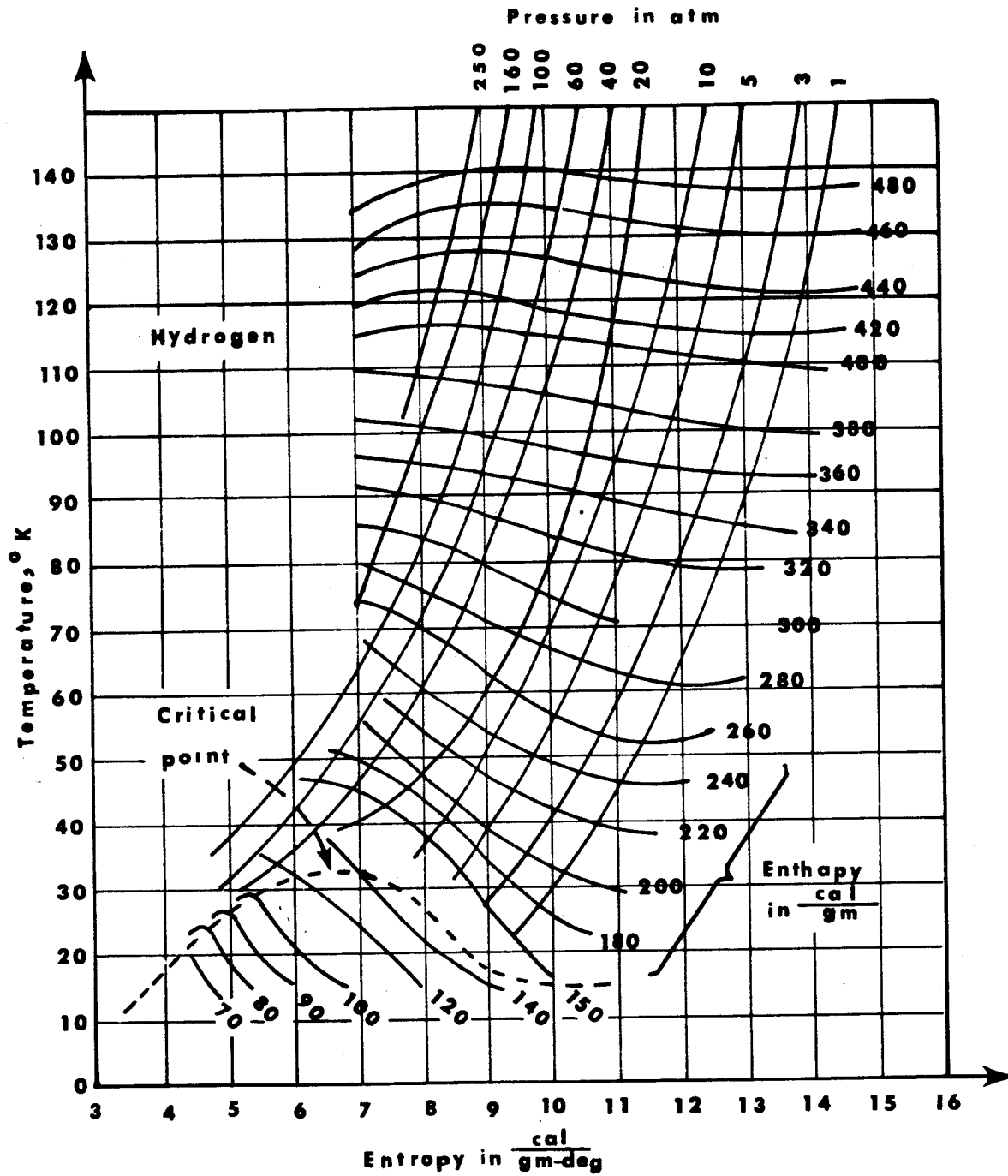
<u>Parameters</u>	<u>Hydrogen</u>	<u>Oxygen</u>
Normal Boiling Point (NBP) at 1 atm	-252.7°C 20.4°K	-183.0°C 90.19°K
Melting Point	-259.14°C	-218.4°C
Critical Gas Constants (Triple Point)	t _c = -239.9°C p _c = 12.8 (atm) V _c = 0.0310 gm/cm ³	t _c = 118.8°C p _c = 49.7 (atm) V _c = 0.430 gm/cm ³
Specific Heat of Vapor, C _p cal/gm-K°	2.5 at 20°K (0 atm)	0.22 at 80-140°K (1 atm)
Specific Heat of Liquid cal/gm-K°	0.231 at -252°C	0.394 at -200°C
Vapor (or Gas) Density, ρ _v gm/liter (at 1 atm)	0.08987 at STP 1.33 at -252.7°C (8.32 x 10 ⁻² lb-m/ft ³)	1.4290 at STP 4.74 at -183.0°C
Liquid Density, ρ _l gm/cm ³ at NBP	0.0709	1.14
Liquid/Vapor Density Ratio, ρ _l /ρ _v , at 1 atm NBP	53	241
Saturated Vapor Pressure, ^a p in mm of mercury, Temperature in °K	A = -849.48 B = 4.5331 C = 0.0324 D = -0.0004189 E = -0.00000484 (Range: above -254.73°C)	A = -8028.1 B = 8.1173 C = -0.0064 (Range: -182 to 211°C)
Saturated Vapor Density, ^b ρ = $\frac{\rho_v}{\rho_{vo}}$, ρ _{vo} = STP density p in atm	$\frac{a}{2\beta}$ $\frac{\beta}{2\beta}$.06094 .000527 at 16.65°K .06647 .000505 at 18.16°K .07518 .000470 at 20.55°K	

a. $\log_{10} p = \frac{0.05223}{T} A + B + \frac{CT + DT^2}{T} + ET^3$ (Equation 2-4).

b. $p/\rho = a - \beta\rho$; $\rho = \frac{a - \sqrt{a^2 - 4\beta p}}{2\beta}$ (Equation 2-5).

<u>Parameters</u>	<u>Hydrogen</u>	<u>Oxygen</u>
Heat of Vaporization cal/gm at NBP	105.5 at 20.5°K (1 atm) 102.0 at 23.0°K (2 atm)	50.9
Viscosity of Vapor Micropoises (Air = 180 at STP)	83.5 at 0°C 33.6 at -198.4°C 8.5 at -252.5°C 5.7 at -257.7°C	189 at 0°C ≈ 109 at -183°C
Viscosity of Liquid Micropoises	110	
Surface Tension (liquid against its vapor dyne/cm) (water is 73 at 20°C)	1.91 at 20.4°K	13.2 at 90.0°K
Speed of Sound, (liquid) m/sec at 44 mcps	1187 at 17°K	952 at 87°K
Speed of Sound, (vapor) m/sec	1270 at 0°C	317 at 0°C
Index of Refraction of Liquid at NBP	1.0974 at 579 mμ	1.221 at 590 mμ
Dielectric Constant - Liquid ϵ/ϵ_0	1.228 at 20.4°K	1.507 at -193°C
Molecular Weight	2.016	32.00
Typical Purity in Space Vehicles	95% + parahydrogen (99.79% equilibrium fraction at NBP)	99.75% O ₂
Relative Abundance	H ¹ 99.9844% H ² 0.0156 H ³ 1 part in 10 ¹⁷	O ¹⁶ 99.52% O ¹⁷ 0.07 O ¹⁸ 0.41
Electronic Magnetic Moment Effective number of Bohr magnetons (9.274 x 10 ⁻²¹ erg/gauss) per molecule	0	2.80
Nuclear Magnetic Moment Magnetic moment in Bohr magnetons (9.274 x 10 ⁻²¹ erg/gauss) per nucleus	1.52 x 10 ⁻³ (H ¹) .462 x 10 ⁻³ (H ²)	0 (O ¹⁶) -1.03 x 10 ⁻³ (O ¹⁷) 0 (O ¹⁸)

<u>Parameters</u>	<u>Hydrogen</u>	<u>Oxygen</u>
Relative Permeability, μ Liquid at NBP	$1 - 1.5 \times 10^{-6}$	$1 + 4 \times 10^{-3}$
Gamma Ray Attenuation		
1. Cross Section, σ cm^2/gm	0.160 at 600 keV 0.326 at 60 keV	0.0806 at 600 keV 0.180 at 60 keV
2. Half Thickness of Liquid, cm	61 at 600 keV 30 at 60 keV	7.5 at 600 keV 3.4 at 60 keV
Beta Ray Attenuation "Half Thickness" at $E_{\text{max}} = 2.24 \text{ meV}$		
1. Liquid (mm)	~ 6.5	$\sim .81$
2. Vapor (cm)(NBP)	~ 35	~ 20
Alpha Particle Attenuation Liquid penetration in <i>mm</i> for 5 meV alphas	$\sim 0.1 \text{ mm}$	$\sim 0.1 \text{ mm}$
Thermal Neutron Cross Section, σ		
1. Absorption, millibarns/atom	332 for, $\text{H}^1 (n, \gamma) \text{H}^2$ 5 for $\text{H}^2 (n, \gamma) \text{H}^3$	< 0.2 for ${}_8\text{O}^{16}$ 21 for ${}_8\text{O}^{18} (n, \gamma) {}_8\text{O}^{19}$
2. Scattering, millibarns/atom	38,000	4,200
Fast Neutron Cross Sections, σ ; 14-15 meV, millibarns/ atom (absorption)	200 for ${}_1\text{H}^2 (n, 2n) {}_1\text{H}^1$	42 for ${}_8\text{O}^{16} (n, p) {}_7\text{N}^{16}$ 300 for ${}_8\text{O}^{16} (n, \alpha) {}_6\text{C}^{13}$
Molecular Dissociation Energy, electron volts	4.48	5.08
Principle Spectral Lines A°	1215.7 4861.327 6562.79	1302.27 1304.96 1306.12 7771.928 (principle line) 7774.138 7775.433



TEMPERATURE-ENTROPY DIAGRAM FOR HYDROGEN

Figure 1

CONTINUOUS VENT ORBITAL COAST
PRESSURE HISTORY FOR SATURN 5/S-IVB

60 lb. Minimum Thrust

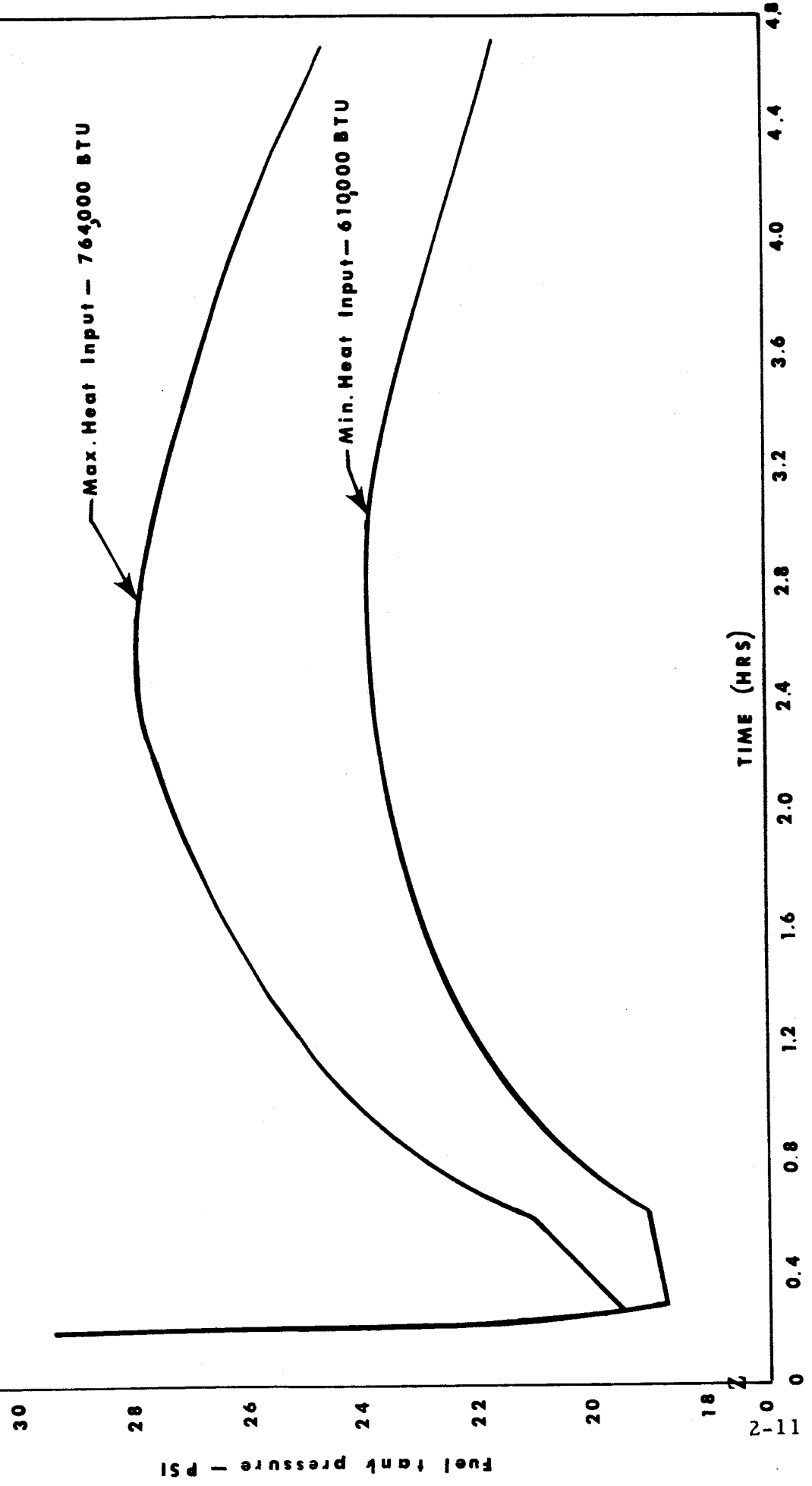


Figure 2

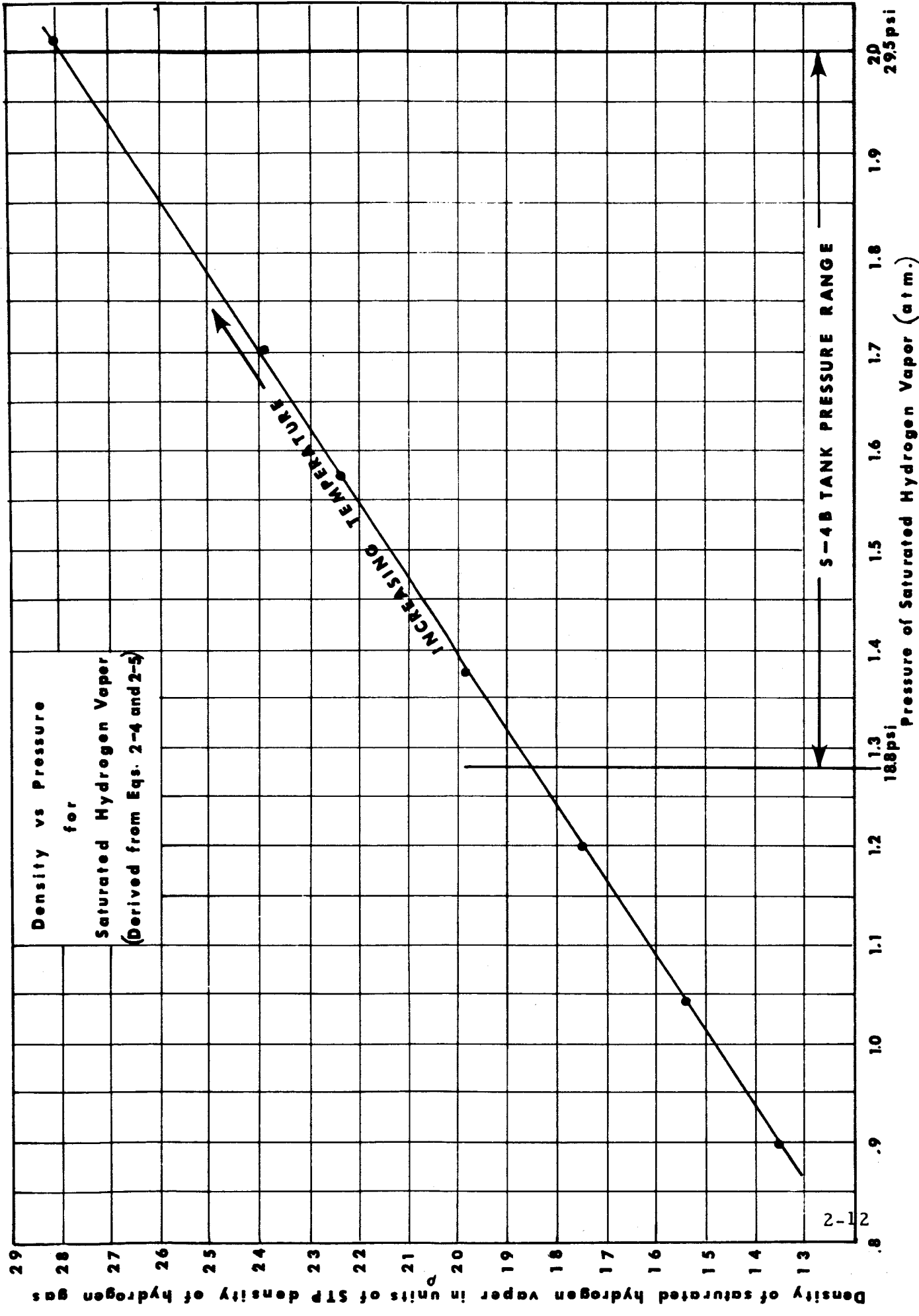


Figure 3

2.3 Explicit Specifications

The following specifications are taken from NASA Contract No. NAS8-11736 and from subsequent handouts and conferences. Hydrogen is the cryogenic of particular interest and a number of the specifications apply to hydrogen only.

Propellants

Hydrogen

Oxygen

Meter Inlet Pressure (psi): Maximum = 100

Discharge Pressure (psi) = 0-15

Maximum Vent Flow Through Meter (ft^3/sec) = 0.5

Meter Accuracy

Above 50% Quality $\pm 5\%$

Below Q = 50%, Sense Only

Continuous Operation Time

Maximum of 5 Hours

Electrical Power Supply

Maximum of 25 volts, 5 amps

Vehicle Acceleration

During Operation - 0 to 0.01 ft/sec^2

Vibrational Maximum - 30 $\text{g}'\text{s}$

Response Time

100 milliseconds for Vent Quality Meter

10 milliseconds for Suction Duct

Output

The output and final function of the quality meter is to produce a 0-5 volt analog signal which is uniquely correlated with quality. Any pressure or temperature measurements required are included as a part of the meter.

Altitude:

185 kilometers

Temperature

Maximum 500°R with a maximum rate of change of 50°R per second inside tube.

Helium Concentration During Orbital Period

Probably negligible; a maximum of 9.1% by weight in hydrogen vent and 4.8% in oxygen vent.

The design principle should be applicable to the above range of specifications. The explicit design which is included in the final report should be engineered for the S-IVB hydrogen vent application as shown in the drawings and graphs handed out. Also, study the following possible extensions of the quality meter:

1. Bubble concentration in the S-IVB suction duct during powered flight.
2. Adaptability to vent or suction lines ranging from 1 to 10 inches in diameter.
3. Flow measurement.

2.4 Implicit Specifications

The physical properties of oxygen and hydrogen coupled with the explicit specifications of this study lead directly to some important conclusions which are reviewed in this section.

The quality range of particular interest is 100 to 50%. Equation (2-3), which defines quality for a well mixed fluid, shows that 100% quality is equivalent to no liquid in the vapor while at 50% quality the liquid mass just equals the vapor mass. Figure 3 shows that vapor density increases by about 50% (29.5 psi is 57% greater than 18.8) over the pressure range of interest. Thus, depending upon the pressure, the liquid mass or volume may vary significantly without changing the quality. Quality is a ratio; any system which merely measures the liquid present can seriously misjudge the quality.

As an example of the preceding point, refer to Figure 3 and suppose the quality is 50% at 29.5 psi. Since quality is a ratio, the vapor and liquid masses may be taken in arbitrary units. The dimensionless density unit of the vertical scale is a convenient choice. Equation (2-3) for quality becomes

$$Q = \frac{27.9}{27.9 + 27.9} = 50\% \quad (2-6)$$

Consider that at some later time an equal mass of liquid is escaping through the vent tube. However, the pressure is only 18.8 psi. Then,

$$Q = \frac{18.6}{18.6 + 27.9} = 40\% \quad (2-7)$$

which is a 10% change in quality with no change in the amount of liquid in the vent. This example was chosen at random and does not maximize the error. However, it clearly shows that measuring the liquid alone will not satisfy the specifications. Both the liquid and the vapor densities must contribute to the response of the quality meter.

The importance of measuring the vapor mass can also be seen from a simple example. Fifty percent quality means the liquid mass equals the vapor mass. The vapor mass is quite variable depending upon the pressure. Hence, it is not possible to know when equality of the masses occurs unless both the liquid and vapor masses are known. (They may, of course, be known only implicitly.)

The ratio of the liquid density to the vapor density at NBP is 53 for hydrogen and 241 for oxygen. Correcting these ratios to a pressure of approximately 22 psi yields typical ratios of

$$\begin{aligned} \frac{\rho_l}{\rho_v} &= 35 \text{ for hydrogen, and} & (2-8) \\ \frac{\rho_l}{\rho_v} &= 160 \text{ for oxygen.} \end{aligned}$$

At 50% quality, the vapor volume is 35 times that of the liquid for hydrogen.

The 100% to 50% quality range is thus 0 to 3%^a LH₂ by volume. The permissible

a. $\frac{1}{35 + 1} = 2.78\% \approx 3\%$.

$\pm 5\%$ error is 1/10 of the range or $\pm 0.3\%$ hydrogen by volume. If one-third of the overall $\pm 5\%$ error is allowed for this one source of error, then no increment of liquid hydrogen greater than 1/10 of 1% by volume may be erroneously measured. Similar considerations for LOX show that 100% to 50% quality corresponds to 0 to 0.6% LOX by volume and the one-third of the permissible $\pm 5\%$ error in quality is $\pm 0.02\%$ or 1/50 of 1% LOX by volume.

These calculations are very important for they give a physical indication of the amount of liquid which must be observed. In particular, they show that any meter which measures quality to $\pm 1\%$ by volume (rather than the standard definition by mass) is much too inaccurate for this NASA application. Plus or minus 1% by volume covers two-thirds of the whole quality range of interest for hydrogen and more than covers the whole range for oxygen.

There is, of course, a very good reason for defining quality by mass and for being interested in very small volumes of liquids. Even though, at 50%, the liquid volume is only three percent or less of the vapor volume, nevertheless, the rate of fuel loss is twice as great as would occur at 100% quality for the same amount of cooling.

According to the specifications, there is a maximum flow rate of 0.5 ft^3 per second which corresponds to a speed of

$$s = \frac{0.5}{A} = 2.55 \text{ ft/sec} \quad (2-9)$$

through a six inch line ($A = \pi/16 \text{ ft}^2$). (For hydrogen, a typical flow is

shown in a handout graph as 0.14 lb-m/sec or roughly one cubic foot per second at 100% quality.) During the 1/10 second response time, a 2.5 ft/sec flow will move about three or four inches. Thus, in order to meet specifications, the readout of the quality meter should represent the average quality over a volume equal to the cross sectional area of the pipe, times, at most, four inches in the flow direction. At any one time the readout is to correspond to the average quality of the flow which has passed the measurement or reference point during the last 1/10 second.

The sample volume is equal to

$$V = 4A = 113 \text{ in.}^3 \quad (2-10)$$

For hydrogen, the maximum liquid volume is approximately $.03 V = 3.4 \text{ in.}^3$ which corresponds to a droplet with diameter D

$$\frac{4}{3} \pi \left(\frac{D}{2}\right)^3 = 3.4 \text{ in.}^3; D = 2.7 \text{ in.} \quad (2-11)$$

Thus, a single blob of fuel up to 2.7 inches in "diameter" should not cause the quality meter to go off scale--i. e., below 50% quality. Such a blob might result if the continuous acceleration technique failed to keep LH_2 from reaching the vent tube inlet.

At the other extreme, the turbine is not able to separate the very small-sized droplet from the vapor. In such a case, the 3.4 in.^3 of hydrogen

could consist of trillions of micron-sized droplets. Both of these possibilities fall within the specifications.

2.5 Mixing of Vented Fluid

If the vent fluid is not well mixed, the entire cross section of the vent tube should be monitored. This is a consequence of the fact that very small volumes of liquid can contribute 5% or more to the quality. Such small droplets could easily slip by a sample volume which did not cover the entire cross section.

There is an obvious advantage for the instrument designer if the vented fluid is well mixed--say by the insertion of a screen or other device in the flow. Only a reasonable-sized sample volume need be monitored. It is not necessary to include every square millimeter of the vent tube cross section in the field of the quality meter. This not only reduces the size of the instrument, but, more importantly, it avoids edge-effect problems near the inner tube wall.

There is a much more basic reason, however, for mixing the flow. As shown in Equation (2-1), the elements of the vented fluid contribute to quality proportional to their speeds as well as their masses. Thus, it is necessary to detect the masses and speeds of any droplets, blobs, or films of liquid as well as to determine the density and speed of the vapor. Relative velocity is just as important as mass in determining quality and is by no means a small correction.

The low density of LH_2 would normally suggest it is relatively easy to accelerate droplets and that large velocity gradients are thus not likely to occur. On the other hand, the viscosity of LH_2 at NBP is only about 8 micropoises or less than 5% that of air at STP. In a Stokes law estimate of the viscous acceleration, the low viscosity more than outweighs the advantage of the low density. (For a drop of fixed mass, the viscous acceleration is proportional¹³ to $\mu\rho^{-1/3}$ showing that the viscous factor, μ , dominates the density factor.) In particular, the turbine separator works on the principle that the liquid and vapor phases will acquire dissimilar velocities when the mixed fluid is accelerated.

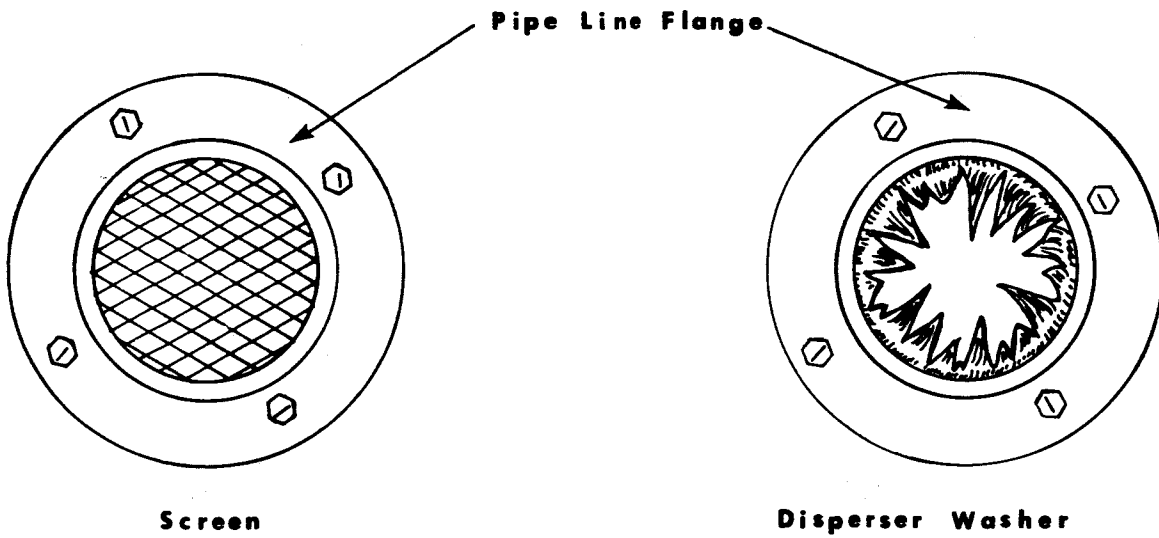
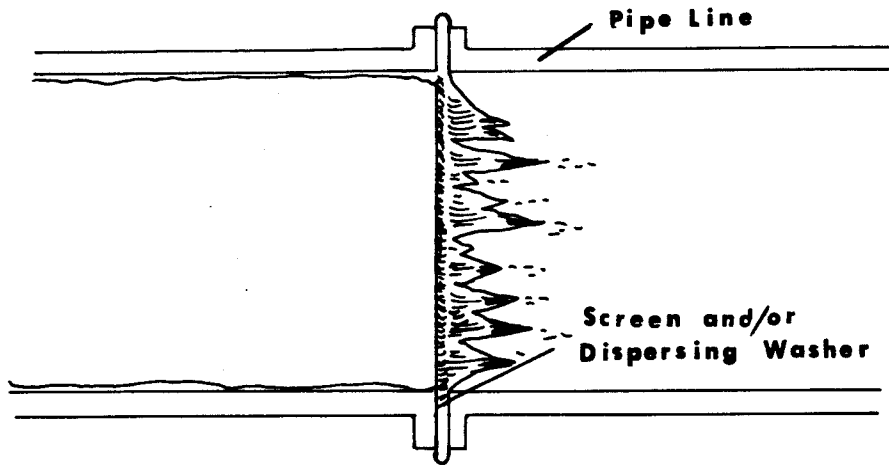
The viscosity of LH_2 is about 13 times that of hydrogen vapor at NBP. Any film on the inner vent tube wall can be expected to travel much more slowly than the vapor. Since the cryogenics considered are wetting fluids and since there is negligible heat flow into the vent fluid from the ambient, such a film will undoubtedly exist. The amount of liquid in such a film may be small in some sense of the word, but it is a questionable assumption to presume it small in comparison to the volume of 1/10 of 1% (H_2) or 1/50 of 1% (O_2) involved in this application.

Most approaches to the quality measurement are much simpler if they can measure the liquid and vapor densities present in a sample section in the vent line. Measuring and taking into account the various velocities can be an extremely complex undertaking. Therefore, it is recommended that steps be taken to produce a mixture of liquid and vapor which is fairly homogenous

on a scale of one cubic inch or so. It is probably not practical to produce such a fine and even dispersal of the liquid that a sample volume of a few cubic millimeters will have a quality representative of the whole. On the other hand, recommendations will be made for a device which should produce good mixing on a larger scale. Then a sample volume covering half of the cross section or more would give an accurate indication of quality.

In Section 2.4, it was shown that the maximum velocity of the vented hydrogen is about 2.5 ft/sec. This flow rate is something less than turbulent. Therefore, in applications where good mixing may not be presumed, it is recommended that a screen or dispersing washer be inserted in the line ahead of the quality meter as shown in Figure 4. The screen will break up any blobs or large drops of liquid and also pick up and disperse film from the pipe wall (by adhesive flow from wall onto screen). Essentially complete dispersal of the film can be produced by a dispersing washer with tapered points bent back in the flow direction. Film will crawl out these points and break away into the flow.

By this dispersal technique, a great simplification results. Equation (2-3) becomes valid and no velocity measurements need be made of the various fluid components. Sampling becomes justified and it is only necessary to determine quality over a reasonably large mid-stream volume. Finally, the problem of accurate measurement of blobs two inches or more in thickness is avoided. Except where otherwise stated, this report will assume good mixing. Obviously, in an application where mixing is known to be good, the dispersing screen may be omitted.



LIQUID DISPERSER

Figure 4

2.6 General Measurement Principles

The desired output of the quality meter is a voltage. The quality, Q , is to be a single valued function of this voltage. As given by Equation (2-3), quality is

$$Q = \frac{m_v}{m_l + m_v} \quad (2-12)$$

where

m_v = mass of vapor in the sample volume, and

m_l = mass of liquid in the sample volume.

Ideally, a single sensor in the quality meter should have an output A , which is a unique function of Q (i. e., a single sensor responds directly to the quality). The next best approach is a quality meter made up of two sensors with outputs A and B , plus a simple electronic computer. For example, A may respond to the total mass in the sample volume, while B responds only to liquid mass, the functional relations being

$$A = k(m_l + m_v) \quad (2-13)$$

$$B = cm_l^2$$

where k and c are known calibration constants. Then

$$Q = \frac{A - \frac{k}{\sqrt{c}} \sqrt{B}}{A} \quad (2-14)$$

and the function (2-14) is computed from A and B by the electronic circuit. If A were also influenced by the temperature, T, then a third sensor C is required. If C is a thermometer, then

$$\begin{aligned} A &= A(m_v, m_l, T) & (2-15) \\ B &= cm_l^2 \\ C &= C(T) \end{aligned}$$

and

$$Q = Q(A, B, C) . \quad (2-16)$$

The function (2-16) is then computed electronically. Four or more sensors are theoretically possible; however, the more sensors required, the less attractive is the approach.

Frequently, the function to be computed implies a rather involved electronic circuit. Then, it is often possible to replace the exact function with an approximate function. The approximate function is chosen for electronic convenience but is subject to the restriction that it differ from the exact function by less than the allowable error.

There are some rather simple ways to determine the vapor mass in the sample volume. Chief among these is from a pressure measurement (see Figure 3) which gives the vapor density, ρ_v , immediately. The vapor mass is then

$$m_v = V\rho_v \quad (2-17)$$

at 100% quality (V , the sample volume need not be precisely known since it cancels out when the quality ratio is taken). At 50% quality, the LH_2 occupies 3% of the volume and

$$m_v = .97 V \rho_v . \quad (2-18)$$

Thus, the assumption that

$$m_v = .985 V \rho_v \quad (2-19)$$

is good to $\pm 1-1/2\%$ over the 100% to 50% quality range without even taking into account the liquid mass. For oxygen, the error is much smaller because the liquid volume is less than 1% at 50% quality. Any rough determination of the liquid mass can reduce the error even further. For this reason, in screening the various possible approaches, the principle emphasis will be on sensors which derive a significant signal from the liquid component--the more elusive and important component of the fluid mixture.

Two general pitfalls should be mentioned before considering specific approaches. In Equation (2-3), m_l is the total liquid mass in the sample volume. Normally, the liquid will be dispersed in many drops, and m_l is thus the sum of the masses of the drops. Over the pressure and narrow temperature range involved, the liquid density is constant to a high degree of accuracy. Thus, to within a known constant multiplier, measuring the liquid mass is equivalent to measuring the liquid volume.

Any system which measures m_1 as a sum of contributions from the separate droplets must be so designed that the contribution to the signal from each droplet is proportional to the mass, or equivalently the volume, of that droplet. As a counter example, the scattering of long wavelength light from small droplets is proportional to the square of the volume of the droplet, not proportional to droplet volume. In this case, the quality cannot be determined unless the droplet size is known. In theory, it is possible to make multiple measurements and thereby determine the approximate distribution by the size of the droplets. In practice, such an approach is impractically cumbersome. Furthermore, the sensitivity is adequate over a rather limited range of droplet sizes.

The second pitfall occurs when the liquid volume is inferred from a measurement of the vapor volume--for example, by dynamic compressibility. It is certainly true that any liquid present in the vent tube will reduce the volume available for the vapor. However, as shown in Section 2.4, it is necessary to know the fuel volume to 1/10 of 1% or better. Thus, any vapor volume measurement must be good to one part in a thousand. This extreme accuracy is difficult to realize in a practical measurement of this type.

This last pitfall is an example of the general problem of signals produced with a very weak dependence on the amount of liquid. A better approach measures the total mass in the sample volume in the tube--i. e., $m_1 + m_v$. In this case, the liquid produces 50% of the signal at 50% quality rather than 3% as in the case of vapor volume measurement.

3.0 APPROACHES STUDIED AND METHOD OF SCREENING

3.1 Approaches Studied

The instruments and principles of measurement studied in this report are summarized in the following list:

Mechanical

Pressure
Force
Viscosity
Turbine
Vibratory Reactance

Acoustical - Resonance Scattering Attenuation, and Speed of Sound

Ultrasonic
Audio
Low Frequency

Electromagnetic - Static and Resonant Effects, Absorption and Scattering

Capacitance
Microwave
Electron Magnetism
Nuclear Magnetism
Light
Infrared
Ultraviolet
Fluorescence
Spectroscopy

Thermal

Heat Flow

Temperature Change

Thermodynamic*

Nuclear - Attenuation, Scattering, and Activation

Using Alpha Particles

Using Beta Particles*

Using Gamma Rays*

Using Neutrons

3.2 Basis of Selection of Approaches Studied

An extensive literature search was conducted in the hope of finding practical devices which could be modified, combined, or improved in such a manner as to effect the quality measurement required in this study.¹⁻¹⁴⁸ Considerable literature exists in the general area of flow measurement. There do not appear to be many devices specifically designed for quality measurement, however. In particular, none of the instruments were even represented as being capable of quality measurement with the accuracy and range required by NASA.

The literature search uncovered a large number of physical phenomena which might form the basis for a quality meter. An effort was made to study any approach which could conceivably be utilized. Certain phenomena such as Raman scattering, electric quadrupole coupling with an external field, conductivity of the fluid, and others were dismissed as being obviously impractical

*A recommended approach.

effects without making an extensive explicit evaluation.

3.3 Method of Screening Approaches

The preliminary screening of any approach follows three steps:

1. Identification and explanation of the physical principle utilized in the measurement.
2. Determination of whether or not this principle is inherently capable of being correlated with quality. As was extensively discussed in Section 2.0, the most difficult part of the quality measurement is obtaining a measurement of the liquid mass. Thus, this step will usually center around the possibility of obtaining a signal which has a strong dependence on the liquid mass but not, for example, upon such unknown factors as the liquid shape or droplet size distribution. If a negative result is found at this point, the approach is rejected forthwith. A positive result justifies proceeding to the third step.
3. An assessment is made of the practicality of building and flying a gauge which will meet NASA requirements of accuracy, reliability, weight, etc.

This three-step procedure should eliminate unworkable gauges, particularly those designs which are practical to build but which are inherently incapable of meeting the accuracy and other requirements of the application specifications.

Methods which rate poorly in one of these aspects are grouped in Section 4, "Less Promising Approaches." The three recommended methods are treated more extensively in Section 5.

4. LESS PROMISING APPROACHES

4.1 Mechanical Techniques ¹⁴⁻⁶¹

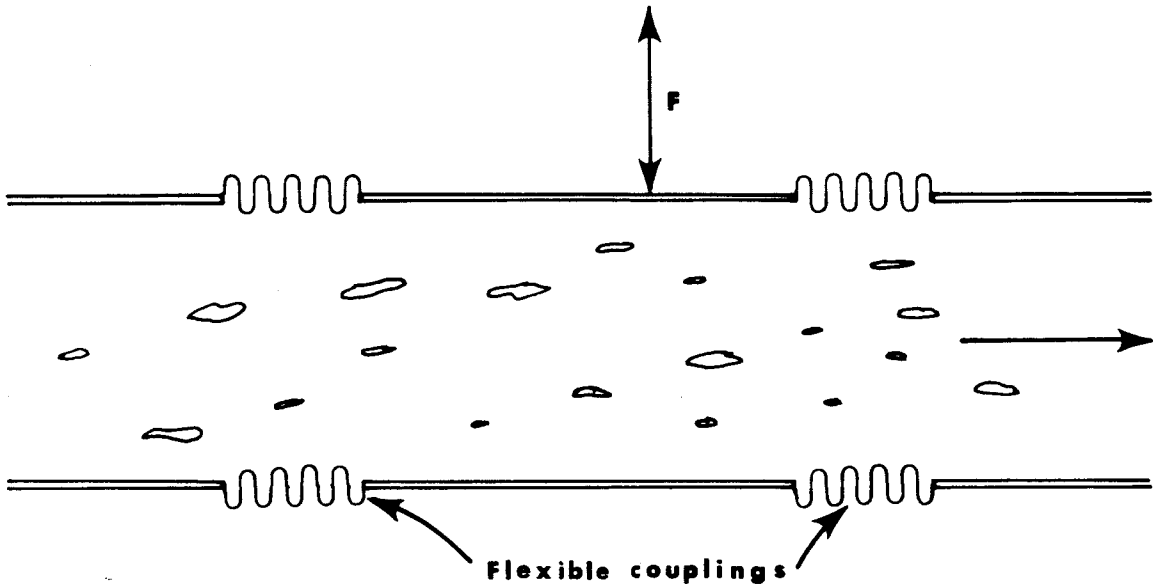
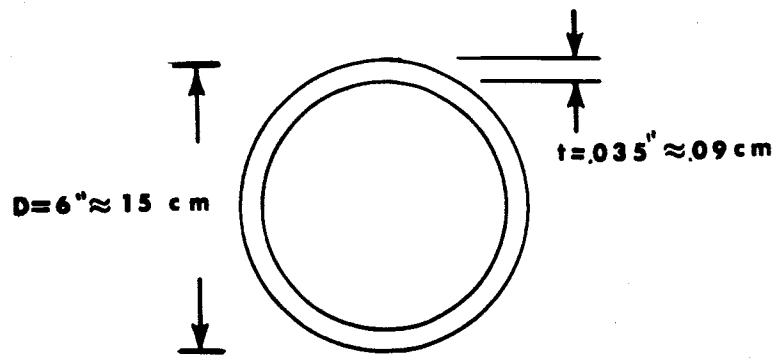
Included under this heading are techniques, other than acoustical, in which a mechanical force measurement plays a critical role. Examples are single point pressure measurements, pressure differentials across impedances in the flow, forces on bodies immersed in the stream, torques on turbines, reaction forces on the tube when there is a change in tube diameter or direction, and vibratory reactance (inertial resistance) to oscillations of sections of the pipe. Many of these techniques are utilized in flow measurements and, hence, are extensively covered in the literature.

4.1.1 Simple Pressure Measurement

As discussed in Section 2.6, a single point pressure measurement is related to the vapor mass but is essentially unrelated to the liquid mass. Thus, in its simple form, a direct pressure measurement seems to have no promise. When certain obstructions are placed in the flow, it can become significant. This possibility is covered under the thermodynamic approach.

4.1.2 Mechanical Reactance

As shown in Figure 5, flexible couplings permit a section of the pipe to be driven by a sinusoidal force F perpendicular to the flow direction. When the liquid is in the form of tiny droplets, it vibrates, along with the vapor, as if it were rigidly fixed relative to the pipe.⁷¹ The inertial mass of the pipe thus appears to be increased over its empty value by an amount equal to the sum of the liquid plus vapor masses, $m_l + m_v$. This is a direct measurement



MECHANICAL REACTANCE

Figure 5

of $m_1 + m_v$ and, hence, if practical, would solve the critical step in the quality measurement.

Some practical factors are serious problems in this case. A centimeter length of six-inch pipe has a mass of

$$7.5\pi Dt = 7.5\pi 15 \times .09 = 28 \text{ gm} \quad (4-1)$$

where 7.5 is the approximate density of steel⁵ in gm/cm³. At 100% quality, the mass of the enclosed hydrogen vapor is

$$1.33 \times 10^{-3} \times \frac{\pi}{4} D^2 = .23 \text{ gm} \quad (4-2)$$

therefore, about one percent of the signal comes from m_1 , the quantity of interest. This percentage is, of course, independent of the length of pipe considered. The flexible couplings and the mass of the driving arm will considerably impair the measurement as would reducing the cross sectional area of the tube. Significant reduction of the pipe thickness destroys the required rigidity. This provides a good basic reason for rejecting a system which is clearly undesirable from the practical implementation standpoint. Further limitations are discussed in Section 4.2 on acoustical techniques.

Attention is directed to a convenient method of estimation used in this section and elsewhere in this report. Due to the fact that $m_1 = m_v$ at 50% quality, and m_v changes very little from 100% to 50% quality, any sensor which responds to $m_1 + m_v$ will receive a signal from the vapor mass m_v at 100% which is essentially equal to the change in signal from

the liquid mass, m_l , from 100% to 50% quality. Normally, the second quantity is the one of interest, while the first is easier to evaluate.

4. 1. 3 Quality from Flow Measurements

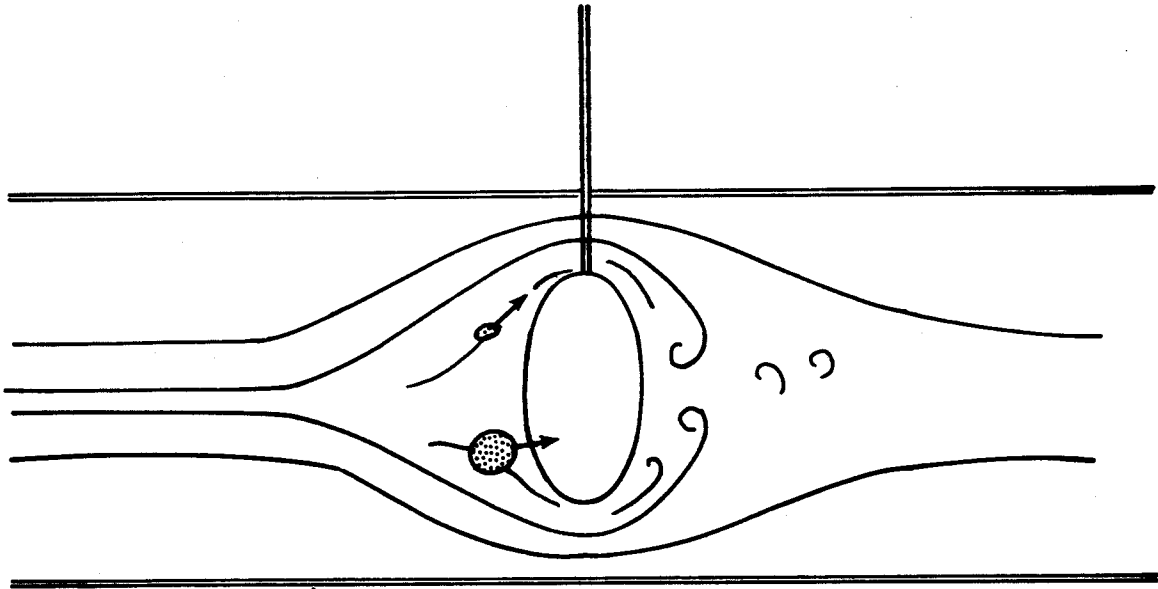
Innumerable devices ¹⁴⁻⁶¹ measure mass flow. In the case of this study, the flow is given by

$$\text{Flow} = (m_l + m_v)s \quad (4-3)$$

where $m_l + m_v$ is the total mass, liquid plus vapor, in a suitably chosen volume and s is the speed of that volume. A knowledge of flow plus an independent determination of the speed leads directly to $m_l + m_v$, thus solving the difficult step in quality determination.

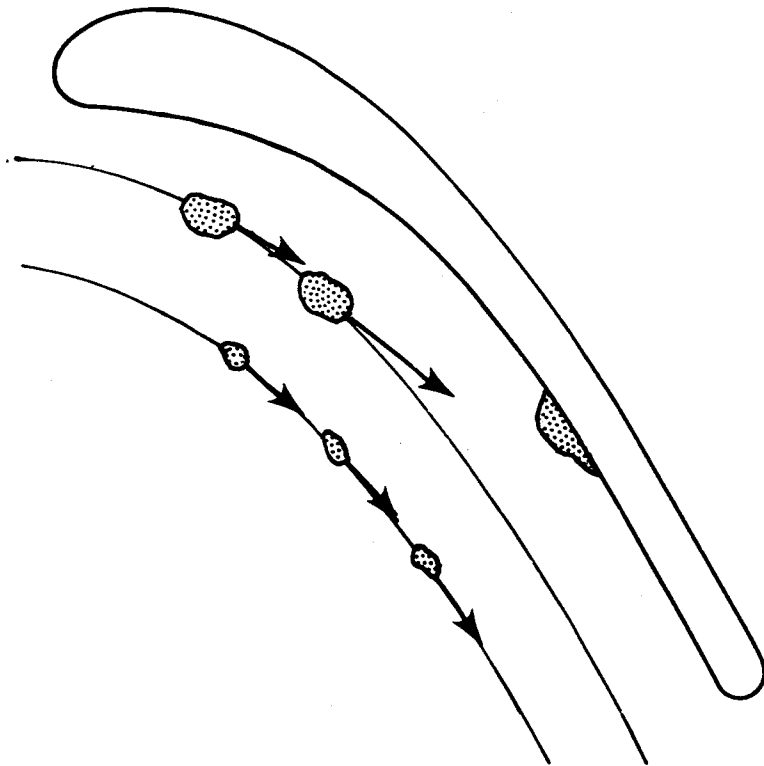
Many flow meters measure flow for single phase fluids only. In Figure 6, the viscous drag on a body immersed in the fluid is influenced by the presence of the droplets in the flow. However, the very small droplets follow the streamlines and contribute very little (i. e., much less than an equal mass of vapor) to the drag since they interfere very little with the viscous shear forces. When the body is very poorly streamlined, the small droplets begin to contribute more due to their momentum change when entering the turbulent region. The large droplets cannot follow the acceleration of the streamlines and, thus, they hit the face of the immersed body, imparting their full momentum to it and produce in it a disproportionately large force. This force is largely independent of the viscosity in contrast to the contribution from the vapor flow.

Figure 7 shows a two-phase flow passing a turbine blade. The flow



VISCOUS DRAG
(Two Phase Flow)

Figure 6



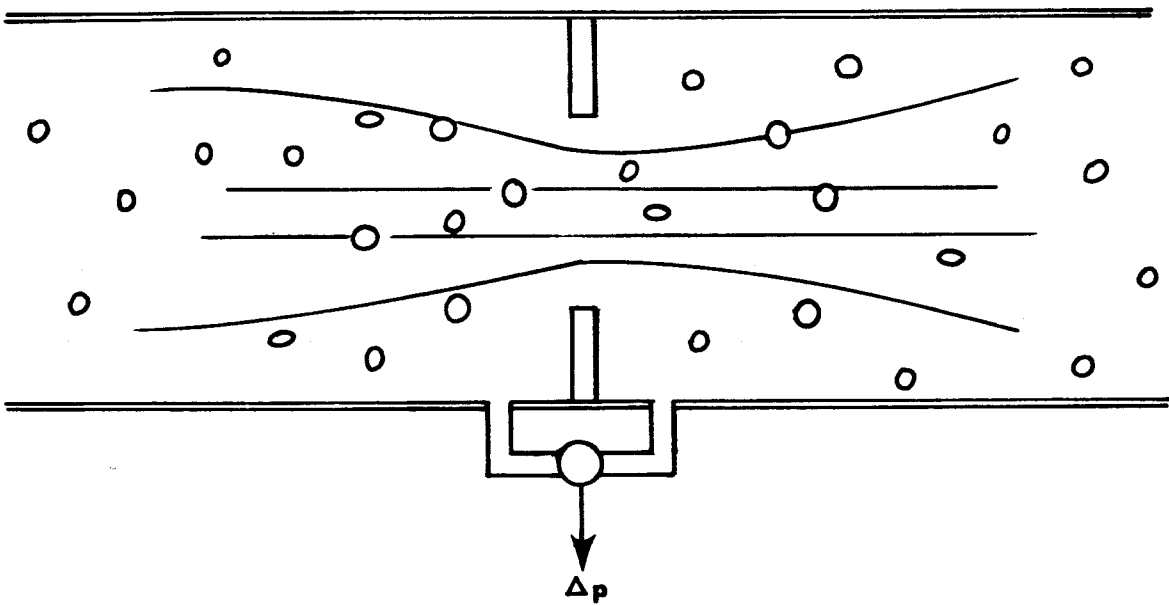
TURBINE BLADE
(Two Phase Flow)
SEPARATION OF PHASES

Figure 7

drives the turbine against a restoring torque. As in Figure 6, the small droplets are carried along with the flow while the larger droplets are apt to hit the blade. Assuming the turbine is not rotating but has assumed an angular position (and associated counter torque due to a restoring spring) proportional to the mass flow, then the torque imparted to the turbine from the large droplets is virtually zero--i.e., they are not counted. In contrast, however, to the viscous drag device, the turbine does read correctly the mass flow contribution of the small droplets carried along with the stream since they are presumed to undergo the same velocity change as the vapor. Intermediate-sized droplets cannot completely follow the acceleration of the streamlines. Hence, they undergo reduced momentum change and are only partially counted. This limitation is characteristic of a large class of reaction devices. The degree of coupling between liquid and vapor is treated in more detail in Section 4.2 on acoustical techniques.

Other objections to the turbine method include obstruction to flow and a response time considerably greater than 0.1 second in a vapor.

The pressure drop across an orifice (Figure 8) is very weakly dependent upon the liquid volume for the small liquid volumes of interest in this study. To a good approximation, the immediate entropy change in the vapor does not result from any energy transfer with the droplets. In other words, the thermodynamic state of the droplets undergoes little change and their volume is not great enough to make a significant reduction in the effective



**FLOW THROUGH AN ORIFICE
(Two Phase Flow)**

Figure 8

orifice diameter. This assumes that the orifice cannot be a large obstruction to flow but must be a sizable fraction of the tube diameter.

On the other hand, if the quality is known and if the orifice is calibrated for flow at 100% quality, then the above conclusions indicate that an accurate mass flow measurement is implicit in the knowledge of quality, the pressure difference Δp and p .

The problems of Figures 6, 7, and 8 are typical of many techniques. For any of these mass flow measurements, there is the additional minimum error associated with the determination of the stream speed--for example, by the speed of an ionized region or from the RPM of a free-wheeling turbine. Accurate calculations of the performance of these mass flow techniques in a quality measurement are lengthy and difficult at best. Extensive experimentation is required to measure many of these effects. (The many mass flow references in this section of the report deal almost exclusively with turbines in single-phase flow. This is the optimum environment for turbines, but little insight is given into the conditions which are of interest here.)

The foregoing discussion strongly indicates that good correlation with quality, if it occurs at all, will probably be limited to an empirical calibration curve valid for a rather narrow range of vapor density, flow rate, and droplet size distribution. This approach is not recommended.

4.2 Acoustical Techniques

The technology of acoustics has been extensively developed for many years. Authoritative and comprehensive references⁶²⁻⁶⁶ are available which quantitatively describe the capabilities and limitations of such techniques.

From the standpoint of hardware required to generate the signal, the frequency spectrum may be divided into three ranges:

- (1) Ultrasonic (15 kcps and up),
- (2) Audio (16 cps - 20 kcps), and
- (3) Very low frequency (0 - 25 cps).

Ultrasonic sound is usually generated by a vibrating piezoelectric crystal energized by high voltage AC power or by magnetostriction. Piezoelectric detectors operate in the reverse manner. Frequencies up into the megacycles per second range are commonly generated. Audio sources typically use a moving magnetic diaphragm or coil in a magnetic field. Similar devices or piezoelectric crystals are used as detectors. A piston-type transducer (probably driven by a motor and cam) produces very low frequency sound which can be detected by a pressure sensor with a compatible frequency response.

The theoretical upper limit for sound is of the order of 10^{12} cps corresponding to a wavelength equal to typical atomic spacing in solids. The mean free path of 10^{-5} cm in air at STP implies a limit frequency of approximately 10^9 cps. Modern research, such as on parametric amplifiers, is pushing ever closer to these limits. Frequencies of 100 Mc. are commonly

produced. However, the generation of sound above 1 Mc. becomes increasingly complex. Piezoelectric generators are inefficiently coupled with gases at such frequencies. For these reasons, 1 Mc. can be taken as a representative upper limit in frequency for the purpose of practical quality measurement.

The speed of low energy sound in a gas is accurately given by⁷

$$s = \sqrt{\frac{\gamma' RT}{M}} \quad (4-4)$$

where

R = the gas constant,

T = the absolute temperature,

M = the molecular weight, and

γ' = a complex factor⁷ approximately equal to the ratio of specific heats γ .

Thus, the speed of sound in hydrogen and oxygen, corrected to the normal boiling points of the gases, is given approximately below:

Approximate Speed of Sound meters/sec at NBP		
	<u>Vapor</u>	<u>Liquid</u>
H ₂	350	1200
O ₂	180	950

At 1 Mc., these speeds correspond to wavelengths of the order of a millimeter. Sprays, by definition,¹³⁸ are characterized by droplet diameters of

millimeters down to 10 microns, and mists fall below that. Turbine separators are expected to function down to the one to ten micron region which implies droplets of that size might be present. It is obvious that ultrasonic waves available for quality measurement can never be presumed to be short compared to particle size. At best, they can be comparable to the larger drops.

For more practical frequencies, the kilocycle region and below, wavelengths are of the order of inches or longer and can be presumed to be long compared to the droplet size.

4. 2. 1 Attenuation and Scattering

Except at frequencies of the order of 1 cps, the pressure variations associated with passage of a sound wave occur so rapidly that there is no time for vaporization or condensation at the droplet surface. The principal loss mechanism associated with the liquid is scattering of the acoustical wave by the droplets and viscous flow of the vapor as it oscillates relative to the more inertial liquid droplets. These effects are much more easily observed at high frequencies than at low. At low frequencies, the droplets tend to oscillate with the fluid and thus minimize the viscous loss. Also, the scattering is greatly minimized because the longer the wavelength compared to the obstruction, the more easily can the wave diffract past it. This point is consistent with experience. A pencil, for example, can be damaged by absorbing a large amount of ultrasonic energy. Yet, placing a pencil along the line of sight between two people in conversation has no noticeable effect on their sound wave.

Deformation of the droplets can also produce losses. The very low surface tension of hydrogen (2.6% of the 20°C value for water) suggests that small droplets are relatively easily deformed by pressure waves. Droplets of the order of millimeters or larger in diameter cannot be assumed to be spherical if the flow is even somewhat turbulent. The low surface tension coupled with low viscosity (the viscosity of LH₂ is 1% of that of 20°C water) suggests that deformations and oscillations of the droplets are easily produced and persist for some time before damping out.

Analytic treatments^{67, 68} have been made of the scattering of sound from spheres, cylinders, and other ideal shapes. For a plane wave scattered by a sphere, the fraction of the incident power per unit area which is scattered is given by⁶⁸

$$W = 4\pi a^2 \sum_{n=0}^{\infty} \frac{2n+1}{(ka)^2} \sin^2 \left[\theta_n(ka) \right] \quad (4-5)$$

where

a = radius of sphere,

$$k = \frac{2\pi}{\lambda}$$

λ = wavelength of the sound wave in vapor.

θ_n is given by

$$\theta_n(z) = -\frac{j_n(z)}{\eta_n(z)} \quad (4-6)$$

where j_n and η_n are spherical Bessel functions. Values of these functions are available in tabular form.⁶⁹

For the first case of possible interest, the wavelength of the sound is assumed to be in the range of possible droplet diameters. There may be droplets equal to, greater than, or less than the wavelength. In such a case, W may be numerically computed from Equation (4-5) and plotted as a function of the droplet radius, a . Such a plot has been made.⁶⁸ Its exact shape, however, is not important. More important is the fact that, from Equation (4-5), the scattered intensity is a very irregular function of the radius of the droplet. Unless the scattered intensity is proportional to the radius cubed, the scattered intensity will not be a measure of the amount of liquid present. Such a relation does not exist even approximately over the wide range of droplet sizes that might be encountered. A proof of this conclusion is also implicit in the following statements since droplets can always exist which are small compared to the wavelength.

At audio frequencies and below, the wavelength is large compared to droplet diameters ($\lambda \gg 2a$) and a good approximation exists for Equation (4-5).

$$W \rightarrow W_o = \frac{2\pi}{k} \sum_{n=0}^{ka} (2n+1) = 2\pi a^2, \quad ka \gg 1. \quad (4-7)$$

The scattered energy is proportional to the projected area of the droplet.

The volume of a sphere is given by

$$V = \frac{4}{3} \pi a^3 \quad (4-8)$$

thus

$$W_o = \text{const. } V^{2/3} \quad (4-9)$$

and the signal is not proportional to the volume of the droplet.

The fact that the signal should be proportional to the volume of the droplet can be shown again by a simple example. Suppose there are n droplets all the same size, where n is not so great that the signals from separate droplets interfere significantly with each other. Then the total scattered signal is proportional to

$$S = nV^{2/3} . \quad (4-10)$$

Then, consider the signal at some later time when the amount (total volume) of the liquid is the same but all the droplets have ten times as large diameters. From Equation (4-8), each droplet has one thousand times the volume of the small droplets and, therefore, there are a less number of droplets by a factor of one thousand for the same quality. Using primed variables to describe the new situation, we find

$$S' = n'V'^{2/3} = \left(\frac{n}{1000}\right) (1000V)^{2/3} = \frac{1}{10}S . \quad (4-11)$$

The signal has changed by a factor of ten with no change in quality. This is not a small error which may be corrected easily; this is an order of magnitude error.

In the actual case, however, the droplets will not all be the same size. Regardless of this, any shift in droplet size with no change in quality would produce a large change in signal. (The preceding analysis is still applicable

since any collection of assorted size droplets may be thought of as made up of subgroups, each group consisting of droplets of approximately equal size.) Thus, either the droplet size distribution must be accurately known or the scattering approach is not satisfactory. Extensive work has been done on particle size measurement,⁷⁰ confirming the conclusion that a determination of droplet size to at least two significant figures would be very difficult in this application.

Statistical treatments of droplet size have been made⁷⁰ based on assumptions of probable values for the average and the extreme size of the droplets. Such assumptions are clearly not valid to one significant figure. For example, micron-size droplets may be produced in the tank by vibration and acceleration and then pass through the separator and diffusing screen. Large blobs could hit the diffusing screen and become millimeter or larger droplets. Even these droplets would depend in size upon the flow rate and upon the original blob size.

Furthermore, as the droplet size changes from micron to millimeters, the signal decreases by a factor of 1,000 with no change in quality. This is an enormous dynamic range. The sensor in this case would need to be good to about 5% of the measured value over several orders of magnitude. Thus, even if the droplet distribution were exactly known, accurate compensation would not be very practical.

This one aspect of acoustical sensing has been pursued to a considerable length to exemplify the importance of finding a sensing technique which

actually responds to the quantity of interest, not to some other quantity which is related in some inaccurately known and variable manner.

More careful studies^{70,71} have been made of the passage of sound through a gaseous medium containing liquid droplets. One mathematical analysis⁷¹ included all of the following effects: deformation of the droplet, translation of the droplet due to coupling with the sound wave, viscosity of the liquid and the gas, and thermal conduction. As might be expected, the results are complex and lengthy relations. In particular, they do not evidence any linear dependence upon droplet volume or mass over the range of droplet sizes of interest. Thus, there does not appear to be any way to relate the attenuation of the acoustical wave or the intensity of a scattered wave to the quality without detailed measurements of factors such as particle size which are more difficult to measure than quality.

Even if the above analysis had lead to acoustical phenomena directly related to liquid volume, there would be serious implementation problems. Any measured acoustical signal will be influenced by attenuation within the vapor, by multiple reflections with the tube, by waves passing through the metal tube, etc. This could easily result in a noisy and inconclusive signal. Laboratory studies of scattering by experts have produced results in which the desired signal was completely unobservable⁷² above the hash of other acoustical effects. This is, unfortunately, often a problem in quantitative acoustical measurements.

The technology of sound in liquids has also been studied extensively. However, for this quality measurement, the small liquid volume infers there is likely not to be any all-liquid path between source and detector. The liquid will appear as a perturbation in the vaporous acoustical path.

It is worth mentioning that high frequency sound may be used to disperse the liquid into small droplets. However, the power level falls in the hundreds of watts range and is thus inconsistent with the specifications.

4.2.2 Speed of Sound

Equation (4-4) for the speed of sound in a gas takes the form of a square root of a fraction. This function appears frequently in physics and is typical of a large class of phenomena in which a medium exerts a restoring force proportional to the distortion of the medium from an equilibrium position. Under this general condition, the speed of a disturbance is characteristically proportional to the square root of a fraction. The numerator of the fraction is proportional to the elastic constant of the restoring force while the denominator is proportional to the mass or density of the substance.

The passage of a sound wave through a gas is a process in which there is a small adiabatic compression and expansion over each wavelength. The same is true of a vapor (very low frequencies of the order of one cycle per second may be excluded when there is time for condensation and evaporation to occur during each cycle). The relation between the pressure and volume of an ideal gas undergoing adiabatic compression is²

$$pV^\gamma = \text{const.} \quad (4-12)$$

Differentiation of this equation leads directly to

$$\frac{dp}{p} = -\gamma \frac{dV}{V} \quad (4-13)$$

showing that γ is the ratio between a fractional change in pressure and the corresponding fractional change in volume--i. e., an elastic constant.

Clearly, M is an inertia term since it is the mass of a molecule. This confirms the applicability of linear elastic theory to cryogenic vapor.

Although the vapor is not perfectly represented by the ideal gas law, the low pressure variations along the sound wave in the gas and the limited temperature range of the vapor do justify linear elastic theory with, at most, a small correction in the value of γ .

Consider the addition of 3% LH_2 by volume to the vapor. The liquid mass in this case equals the vapor mass and hence the quality is 50%. To a good approximation, the liquid is incompressible. Thus, the volume available to the vapor is only 97% of its former self and a slight reduction in the compressibility occurs. Much more important, however, is the apparent increase in the inertial mass of the vapor if the liquid is well dispersed in tiny droplets which oscillate with the vapor. This liquid doubles the average density of the gas and reduces the speed by approximately the square root of two as can be seen from Equation (4-4). Or,

$$\text{at 100\% Quality, } s_{100} = K \sqrt{\frac{\gamma' RT}{m_v}} ; \quad (4-14)$$

$$\text{at 50-100\% Quality, } s = K \sqrt{\frac{\gamma^* RT}{m_1 + m_v}} ; \text{ and}$$

$$\text{at 50\% Quality, } s_{50} = \frac{K}{\sqrt{2}} \sqrt{\frac{\gamma^* RT}{m_v}} \approx \frac{1}{\sqrt{2}} s_{100} ,$$

where K is a constant which relates the molecular mass to the total mass in the sample volume, and γ^* differs slightly from γ' due to the small change in compressibility resulting from the liquid. The difference between γ' and γ^* can be neglected during feasibility considerations but must be reintroduced as a correction if a precise calibration curve is to be determined.

This phenomena is truly related to the mass of the liquid and is independent of the droplet size or shape, and subject only to the restriction that the droplets be small and well dispersed. A correction for temperature is, of course, required since T enters Equation (4-14).

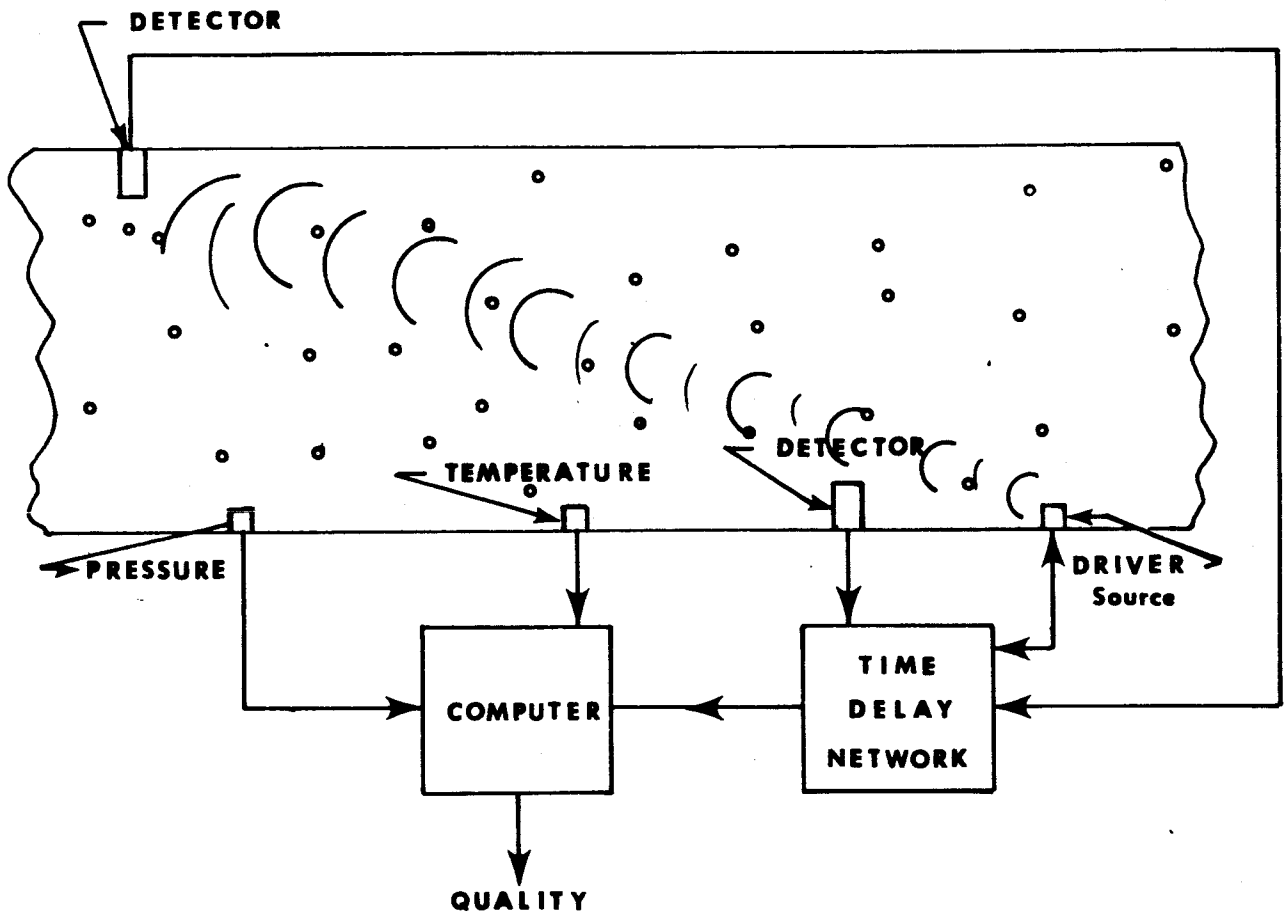
Both T and $(m_1 + m_v)$ enter the fraction to the same power and, thus, T must be measured at least as accurately as the mass, or one to two percent or 0.2 to 0.4 K^o for LH₂. This is a fairly stringent demand.

The 100 to 50% quality range corresponds to about a 30% range in values of s as shown by Equation (4-14). Allocating 2% of the 5% permissible source of error to this measurement demands the speed of sound be measured to roughly 1/2 of 1%. A path length of 6" across the tube or a foot or so along the tube is available for the sound measurement. For measurements along

the tube, the flow speed of 2.5 ft/sec and less corresponds to 1/4 of 1% of the speed of sound in hydrogen vapor. Thus, the doppler-type velocity shift may be neglected. Figure 9 shows a typical embodiment with an optional second detector. A pressure sensor is shown since pressure is a more sensitive indicator of the vapor density than temperature, and a measure of m_v is needed in addition to $m_l + m_v$.

A path length of one foot is probably as large as is practical. At 350 meters/sec, sound will travel this distance in about one millisecond. A 1/2 of 1% measurement of the sound velocity thus corresponds to a time error of five microseconds. Electronically, this is no problem. The principal difficulty arises as follows: Either the sound can be emitted continuously or in pulses. For the continuous case, the phase difference between the source and detector or between two physically separated detectors may be measured. At 350 meters/sec, five microseconds corresponds to a path length of less than two millimeters. At audio frequencies, a phase shift of 1/10 degree is good resolution for a clear signal. Due to the multiple paths, diffraction of the beam, and reflection from the walls, etc., a phase angle measurement of 1° would be a difficult goal to achieve. However, assuming 1° to be a practical limit of resolution (which corresponds to the minimum two millimeters of path length cited above), the maximum wavelength is $2 \times 360 = 0.7 \times 10^3 \text{ mm} = 0.7 \text{ meters}$.

$$\lambda \leq 0.7 \text{ m} \quad (4-15)$$



ACOUSTICAL QUALITY METER
 (Speed of Sound)

Figure 9

A frequency of 500 cps produces a 7/10 meter wave at 350 m/sec. So far, these numbers have fallen within the range of practicality, but some estimate is now needed of the degree of coupling between the droplets and the vapor.

Reference 71 gives a general treatment of the passage of sound through a two phase medium of liquid droplets in a gas. Numerical results are given for water droplets in air at STP. When coupling between the liquid and the vapor is good, there is a driving force on the droplet proportional to the viscosity of the gas plus an inertial term due to the mass of the droplet. The NBP viscosity of hydrogen is nearly 5% (i. e., $\frac{8.5}{180}$) of the STP value for air and the density of LH₂ is 7% that of water. The driving force and the inertial term are both scaled down by approximately the same factor, and thus for droplets of equal size, the viscous coupling between water and air at STP is rather close to that for LH₂ droplets in hydrogen vapor. Figure 1 of Reference 71 shows that coupling is essentially complete, that is, no relative motion between the liquid droplets and the vapor, at

$$\frac{fa^2 \rho_v}{4\pi \mu_v} = 5 \times 10^{-2} \quad (4-16)$$

where

- f = frequency of sound,
- a = droplet radius,
- ρ_v = vapor density, and
- μ_v = vapor viscosity.

Solving (4-16) for the particle diameter ($d = 2a$) shows that droplets less than roughly one millimeter in diameter will be tightly coupled with the vapor. A more accurate calculation must, of course, be made should this method ever be utilized. The previous calculation is just an order of magnitude estimate.

Droplets larger than one millimeter do not vibrate as much as the vapor and, hence, are not measured in proportion to their mass. In general, the larger the particle, the worse the error. Any droplet which has a radius as much as ten times the tightly coupled limit will be almost entirely neglected. (The small contribution it will make will be considered in another velocity technique discussed in the last part of this subsection.) Obviously, the large droplets cannot be neglected if there is to be any accuracy to the quality measurement. Therefore, either such an acoustical meter must be limited to applications where there are only small droplets or else the liquid must be dispersed into submillimeter droplets.

Another alternative, more commonly used in acoustical techniques, is pulsed sound. The detector measures the time of arrival of the wave front coming from the source. As shown in the preceding paragraphs, the frequency should be taken as low as possible to get good coupling with the droplets. Thus, the wavelength is fairly long, being of the order of the source-detector spacing or greater. This, in turn, implies that the pulse sent from the source to the detector cannot have a well defined frequency and, at the same time, be localized in space over a distance comparable to

the two millimeter uncertainty derived earlier.⁷³ In short, the pulse must be more of a square wave than a sinusoidal wave. A square wave can be represented by a Fourier series⁶⁸ and is, thus, equivalent to a mixture of waves of different frequencies including many which are much greater than the basic frequency of the source. The high frequency waves couple with the smallest droplets only (reference, Equation (4-16)) and thus do not feel the inertia of the majority of the liquid. Hence, these waves reach the detector first and do it in a time which is largely insensitive to the liquid present, a most unsatisfactory result. The result is no quality measurement.

Finally, consider very high frequencies where the viscosity of the vapor has a negligible effect on the droplet motion. There still exists, even with no viscosity at all, a force on the droplets due to the reaction of the mass of the vapor as it rushes back and forth around the drop. The rushing is, of course, the passing of a compression wave. This reaction to the vapor flow has been fully treated in the literature.⁷⁴ For a spherical droplet, the ratio of the droplet displacement to the vapor displacement is given by

$$\frac{3}{1 + 2 \frac{\rho_l}{\rho_v}} = \begin{array}{l} 4\% \text{ for LH}_2 \\ 1\% \text{ for LOX} \end{array} \quad (4-17)$$

Equation (4-14) shows that with 100% coupling between vapor and liquid, there is up to a 30% change in the velocity of sound. This was sufficient for a marginal system at best. Reducing the coupling by a factor of 25 or more thus produces a signal with an intolerably small dependence on the

liquid mass. Hence, any system based on (4-17) seems hopelessly impractical.

The majority of the sample calculations in this subsection are based on hydrogen data. From the standpoint of instrumentation, the results for oxygen are of the same order of magnitude or worse. This is to be expected because the NBP viscosity of oxygen vapor and the density of LOX are within a factor of two of the 20°C values for air and water. Also, the volume of the LOX at 50% quality is considerably smaller than the comparable value for LH₂.

In general, it has been shown that theoretically it is possible to design a speed of sound sensor which responds to the liquid mass in the vapor. It is necessary that the liquid be dispersed in droplets which are smaller than a well-defined upper limit. This upper limit was previously roughly estimated to be one millimeter in diameter.

On the other hand, the practicality of a speed of sound system is in considerable question. Almost every favorable result is marginal. In practical acoustical systems in a closed container, there is an enormously complex signal resulting from multiple reflections and multiple paths of the sound and possibly from resonances of the system at audio frequencies and below. Thus, unless there is a good order of magnitude more sensitivity than is theoretically required, practical development can be presumed to be difficult or even impossible.

A continuous wave from the source to the detector is particularly apt to be garbled by the various extraneous signals. The optimum wavelength is of the order of pipe dimensions which is an invitation for unwanted resonances. Sensitivity calculations showed that it is not possible to increase the wavelength (Equation 4-15). Thus, it might have to be shortened by a factor of ten or more to avoid resonance. The wavelength of the sound is shortened by increasing the frequency and, hence, from Equation (4-16), the maximum allowable droplet size is reduced even further.

Insuring that the droplets will all be sufficiently small is a significant problem in itself. It is further necessary that they be rather uniformly dispersed so as not to diffract and disperse the sound wave. A nonuniform spatial distribution of droplet sizes is equivalent to a spatial variation in the speed of sound. Such a medium is dispersive.

As one last attempt to circumvent these difficulties in the measurement of the speed of sound, note that the resonant frequency of an organ pipe or Helmholtz resonator is directly proportional to the speed of sound.⁷⁵ A suitably resonant structure might be inserted in the vent tube or a section of the tube itself might be redesigned to resonate.

In order to have good coupling with the larger droplets, the frequency should be low. Since the frequency is directly proportional to the speed of sound, the percent accuracy requirements derived for the speed measurements are directly applicable to the measurement of the resonant frequency. The allowable errors were quite small; therefore, small shifts in the resonant

frequency must be accurately determined. The resonant structure must be sharply resonant--that is, frequencies slightly off resonance must suffer considerable destructive interference. This last requirement is at odds with the need for low frequencies and low impedance to flow. The probability of uncovering a practical structure which can meet all these requirements is not great.

In summary, it should be said that speed of sound techniques are theoretically capable of a quality measurement. The marginal sensitivity, however, raises serious questions about the practicality of such an approach in a nonlaboratory environment. Since other more promising techniques exist, sound-speed methods are not recommended.

Speed of sound techniques do have one interesting possibility in mass flow measurement. If there are two detectors, one upstream and one downstream from the sound source, then there is a difference in the apparent speed of sound as determined from the upstream detector compared to the downstream one. This difference depends on the quality but, more importantly, it is proportional to the speed of flow. The average of the two speed measurements is a measure of quality. Thus, both quality and mass flow may be computed from the two speed signals. In the particular application of interest to NASA, the flow velocity is small compared to the speed of sound (0.2% and less for hydrogen). Thus, again sensitivity is the problem.

4.2.3 Dynamic Compressibility

Equation (4-13) may be rewritten as

$$dp = - \frac{\gamma p}{V'} dV . \quad (4-18)$$

A small change in volume, dV , produces a corresponding change in pressure, dp , which depends on the pressure, p , and the volume, V' , occupied by the vapor. A known small change, dV , in V' can be produced by a driven piston or diaphragm. The pressure and the change in pressure can be measured by a pressure sensor. Finally, γ is a known property of the gas or vapor. Thus, V' is the only unknown, and it may be determined from the other parameters using Equation (4-18).

In a practical sense, the liquid is incompressible. Thus, the volume available to the vapor is given by

$$V' = V - V_1 \quad (4-19)$$

where V is the sample volume (Total volume in which the measurement is made) and V_1 is the liquid volume. Equation (4-18) becomes

$$dp = - \frac{\gamma p}{V - V_1} dV \quad (4-20)$$

showing that the measured pressure rise depends upon the liquid volume, V_1 , the other variables being known or measured.

Equation (4-20) represents a direct measurement of the liquid volume (and hence, mass) without extensive assumptions about the size, shape and location of the liquid. This is, of course, desirable. However, as briefly indicated in Section 2.6, the problem is one of sensitivity. The 100 - 50% quality range corresponds to $V_1 = 0$ to $V_1 = .03V$ for hydrogen. There is only a three percent change in the pressure rise over the whole range of interest. The required sensitivity is 1/10% of one percent of the pressure rise and the rise cannot practically be greater than roughly 1/10 of the actual pressure at most. Thus, pressure changes must be measured to an accuracy of the order of 1/100 of one percent of the ambient pressure or roughly $\pm .0025$ psi. This sensitivity is clearly impractical; furthermore, extraneous pressure variations will completely dominate the signal.

As an example of the sort of extraneous signal which will occur, consider the problem of defining a sample volume. The pressure rise should not be measured concurrently with compression. It is preferable to wait until the pressure fluctuations associated with sound waves travel around and damp out. For a closed container, this is no problem since equilibrium is established in a fraction of a second or slightly longer and there is a well defined pressure everywhere in the sample volume. However, with fluid passing through an open system, acoustical filters must be used. Filters are of limited efficiency, especially at low frequencies. In particular, they cannot contain a static pressure rise. Thus, the pressure measurement must be made somewhat prematurely before all damping has occurred. If the

useful signal is a very small part of the pressure rise, it will be dominated by the undamped fluctuations and, hence, cannot be seen regardless of the sensitivity of the pressure sensor.

A very low frequencies, of the order of one cycle per second, the expected pressure rise is reduced by the condensation of the vapor on the surface of existing drops. The rate of condensation is thus related to the presence of liquid. Such a measurement is not very practical and, worse yet, it is dependent on the surface area of the liquid which cannot be directly related to the volume of the liquid even if the liquid is assumed to be in the form of spherical droplets (large spheres have less surface area per unit volume than do small ones).

In summary, acoustical methods are not recommended for the quality measurement required by NASA.

4.3 Electromagnetic Techniques

The table of physical properties of hydrogen and oxygen reveals a number of electrical and magnetic properties which might form the basis of a quality measurement. Various basic texts and applied articles⁸¹⁻¹¹⁵ are helpful in determining the suitability of these approaches for the NASA quality measurement. In two cases,^{82, 83} actual quality meters were built and tested. A systematic discussion follows.

4.3.1 Capacitance

The relative dielectric constant ϵ of hydrogen and oxygen differ noticeably from unity. It is thus possible to sense the presence of either of those liquids

by means of their response to an applied electric field.

Let C_o be the capacitance of a condenser when there is nothing between the plates. If the space between the plates is filled with liquid, the capacitance will be

$$C_f = \epsilon C_o \quad (4-21)$$

where ϵ is the relative dielectric constant of the liquid. Partial filling of the space with liquid will result in a capacitance, C , intermediate between C_f and C_o --i. e.,

$$C_o \leq C \leq C_f \quad (4-22)$$

It is natural to hope that the additional capacitance is directly proportional to the volume of liquid present, that is

$$C - C_o = (C_f - C_o) \frac{V_1}{V} = (C_f - C_o) \delta \quad (4-23)$$

where,

V_1 = the liquid volume,

V = the total volume between plates
(the sample volume), and

δ = the filling fraction $\frac{V_1}{V}$.

Unfortunately, Equation (4-23) is false. In fact, there does not exist a unique relation between the capacitance and the amount of liquid present.

The proof follows from Figures 10A and B. The region between the plates is half full of liquid. Figure 10A represents a large bubble passing between the plates. This is idealized on the right hand side of the page by liquid and vapor paths in parallel between the plates. In Figure 10B, the fluid sticks to the plate and is idealized as the same amount of fluid but now in series with the vapor. The capacitance of Figure 10A is

$$C_a = \frac{1}{2} C_o + \frac{1}{2} \epsilon C_o = C_o \frac{1 + \epsilon}{2} \quad (4-24)$$

since it is a case of the two halves of the initial capacitor in parallel. For Figure 10B, the series capacitance is

$$C_b = C_o \frac{2\epsilon}{1 + \epsilon} \quad (4-25)$$

The useful relative signal is

$$S = \frac{C - C_o}{C_o} \quad (4-26)$$

hence,

$$S_a = \frac{\epsilon - 1}{2} \quad (4-27)$$

$$S_b = \frac{\epsilon - 1}{\epsilon + 1} \quad (4-28)$$

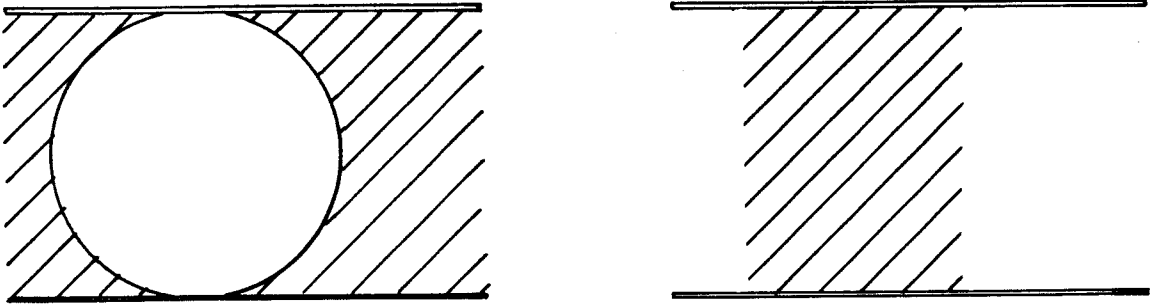
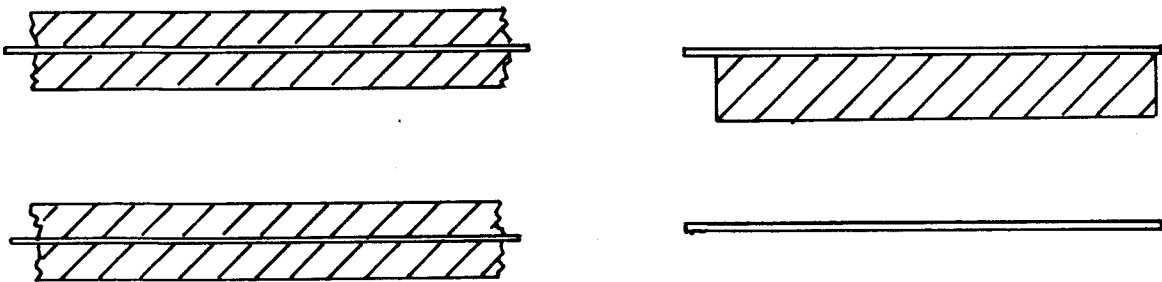


Figure 10 a



LIQUID DISTRIBUTION IN A CAPACITOR

Figure 10 b

The ratio of the two signals is

$$\frac{S_a}{S_b} = \frac{\epsilon + 1}{2} . \quad (4-29)$$

Evaluating this ratio for LH₂ and LOX yields

$$\frac{S_a}{S_b} = \begin{array}{l} 1.11 \text{ for LH}_2 \\ 1.25 \text{ for LOX} \end{array} . \quad (4-30)$$

Changing from configuration b to configuration a, gives a signal corresponding to an 11% change in the amount of LH₂ or a 25% change in the amount of LOX when there was actually no change at all. This error cannot be corrected by some sort of signal processing. The only possible correction is based on a determination of, or a knowledge of, the fuel location.

In the limit $\epsilon \rightarrow 1$, the error becomes a negligible part of the signal (see Appendix I). The signal, unfortunately, also becomes negligible. For LH₂ and LOX, the dielectric constants are considerably greater than unity, hence the large errors calculated in Equation (4-30).

From the foregoing remarks, it is clear why a capacitance fuel quantity gauge may show good results when "tested" in the laboratory. If the "test" is performed by partial immersion of the capacitor, the designer can presume the liquid distribution and calibrate accordingly, regardless of the value of

the dielectric constant. Unfortunately, the test fuel distribution will probably be quite unlike the actual distribution under operating conditions. If a low dielectric constant liquid is used, the special factors mentioned in the last paragraph and in Appendix A apply, but the results are not valid for liquids of higher dielectric constant.

In the NASA quality measurement, the liquid volume is 3% or less-- that is, $0 \leq \delta \leq 3\%$. In Appendix A, Section 2, a calculation is made for small values of δ . The result (Equation A-1-7) shows the error in signal due to the position of the fuel is

$$\frac{S_a - S_b}{S} = \frac{\epsilon - 1}{\epsilon} \text{ for small } \delta \quad (4-31)$$

where

S_a corresponds to well mixed (dispersed) liquid, and

S_b corresponds to liquid in a layer on the electrode plates.

Evaluating Equation (4-31) for LH_2 and LOX yields

$$\frac{S_a - S_b}{S} = \begin{array}{l} 19\% \text{ for } LH_2 \\ 34\% \text{ for LOX} \end{array} \quad (4-32)$$

which shows the amount of liquid may be misjudged by as much as 19% (LH_2) or 34% (LOX) of its value, depending on where it is located between the plates.

All of these calculations have been made for an ideal parallel plate capacitor which produces a perfectly uniform field. The significant point is that even at this ideal limit, there is position sensitivity capable of producing errors much greater than allowed by the NASA requirement. For reasons which will now be discussed, any practical capacitor will fall far short of even this imperfect ideal.

First, there is the simple problem of having an adequate signal. The parallel plate capacitor should include a sufficiently large sample volume so that the reading is representative of the whole flow, for instance, in a four-inch cube. The formula⁸¹ for the capacitance of a parallel plate condenser is given in any introductory book on electrostatics. Neglecting fringe effects

$$C_o = \frac{\epsilon_o A}{d} \quad (4-33)$$

where

A = the plate area,

d = the plate spacing,

ϵ_o = the vacuum dielectric constant

= 8.85×10^{-12} farads/meter (mks units)

= 1 (relative units).

For a 4 inch x 4 inch x 4 inch sample volume, the empty capacitance is approximately

$$C_o = 10^{-12} \text{ farads} = 1 \text{ picofarad.} \quad (4-34)$$

Filled with LH_2 , the capacitance is

$$C_f = \epsilon C_o = 1.228 \text{ picofarad} \quad (4-35)$$

or a .228 picofarads capacitance change due to sample volume full of LH_2 .

As has been shown earlier, 1/10 of 1% by volume of LH_2 must be detected.

Thus, it is necessary to sense capacitance changes of

$$\Delta C = 2 \times 10^{-4} \text{ picofarads.} \quad (4-36)$$

For LOX, the corresponding value is

$$C = 10^{-4} \text{ picofarads.} \quad (4-37)$$

From the standpoint of a practical, nonlaboratory instrument, these values are ridiculously small. Furthermore, they are changes of about one or two parts in ten thousand of the capacitance being measured which is an unacceptable relative measurement as well as an unacceptable absolute one. Constructing more and closer electrodes will increase the minimum absolute value of ΔC which must be detected. Unfortunately, nothing can be done to improve the minimum relative increment in the capacitance.

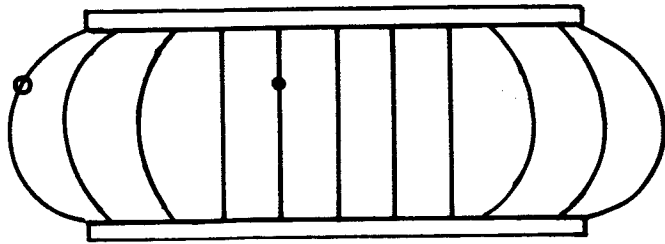
Measuring a capacitance to one part in 10^4 is not only difficult in itself, but it also requires that every extraneous influence (temperature, mechanical distortion, etc.) on the capacitance be known or controlled to better than one part in 10^4 .

By considering the simple parallel plate capacitor, two large sources of error are uncovered, namely:

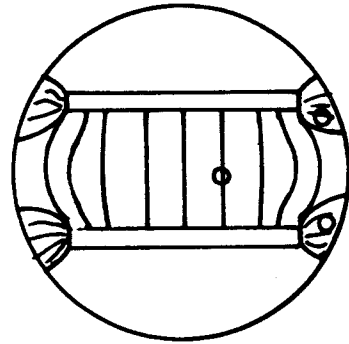
- (1) Sensitivity to the fuel location, and
- (2) The very small maximum relative error allowable in the capacitance measurement.

Assuming any other size, shape, or type of capacitor can aggravate these errors. These errors cannot be improved since they are a minimum for the ideal parallel plate.

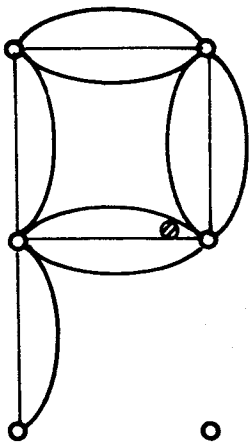
Other sources of error include nonuniform averaging due to the fringe field. This is shown in Figure 11A. The sampling error can be great if a small capacitor is used. If a large fraction of the cross section is included within the capacitor, then edge effects are serious with a metal-walled tube, (see Figure 11B). In particular, a high field intensity will exist in the region between the plates and the wall and give a disproportionately large weight to any film on the wall. If many parallel plates are used to raise the capacitance change to a measurably large value, there will be obstruction to the flow, particularly to the liquid flow, producing a greater drag between the plates and, hence, a higher liquid concentration in the measured volume than is representative of the flow. The large increase in surface area due to the



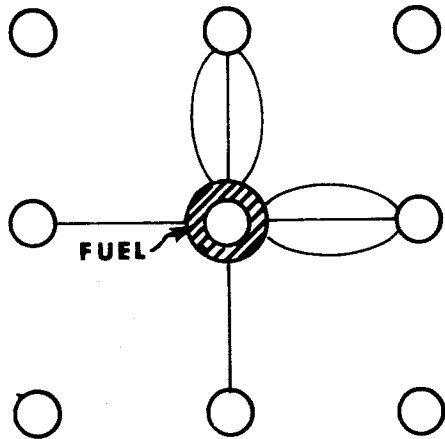
a



b



c



d

FUEL

CAPACITOR ELECTRIC FIELD STRUCTURE

Figure 11

additional plates increases the amount of surface film which contributes to the signal without actually being a part of the flow. For the small volumes of liquid of interest to NASA, this could be a 50% error or more in the quality measurement.

A matrix of rod shaped electrodes may be used. The proximity and number of the rods increases the capacitance to a measurable level, minimizes the relative contribution of edge effects and provides a certain amount of mixing. Another result is a highly nonuniform field structure. If the electrodes have very small diameters compared to their spacing, the electric field is much stronger at the electrode surface than in the middle of the void between electrodes. See Figure 11C. Thus, the electrodes not only provide a large total surface area for film collection, but they also respond to any collected film far out of proportion to the response to an equal amount of liquid in the void region.

If the matrix rods have large diameters which are a sizable fraction of the spacing as in Figure 11D, the nonuniformities of the field are somewhat reduced although still important. The surface area for film accumulation is considerably increased, thus defeating the purpose.

The flow over the electrodes performs some mixing. However, for typical electrode spacing and for the moderate flow speeds expected, this is not a strong effect. Furthermore, mixing due to flow past obstructions tends to slow down the liquid component relative to the vapor component while in the mixer. The errors discussed in going from Equation (2-1)

to Equation (2-3) could thus be important. Mixing should be performed ahead of, not within, the sample volume.

The most expedient "solution" to the majority of these serious problems lies in a different definition of quality and in a carefully designed performance "test." If quality is defined by volume, then, $\pm 1\text{-}1/2\%$ quality covers the whole 100% to 50% range of quality by mass for hydrogen. Similarly, an apparently small error of $\pm 0.3\%$ quality (volume) covers the whole 100 to 50% quality (mass) range for LOX. By defining quality by volume, one may speak in terms of small percent errors even though these errors greatly exceed the NASA 5% tolerance.

Similarly, immersion tests and many other procedures create a situation in which most of the cells between adjacent electrodes are either completely full or completely empty. Only in the partially filled cavities is there any uncertainty in the fuel location and gravity helps to minimize even this ambiguity. In actual application, however, the flow is through the matrix; therefore, every cell can contribute to the error. Film attachment at zero g's is a prime example of such an error.

In contrast to the other approaches discussed, there is some experimental performance data available on existing capacitance quality meters.^{82, 83} The best claim made for either of these, even by their own manufacturers, is only $\pm 1\%$ by volume. In Section 2.4, the volume errors corresponding to $\pm 5\%$ quality by weight were derived. The result is that $\pm 1\%$ by volume is many times the allowable error either for LH_2 or LOX.

The preceding arguments seem sufficient to eliminate the capacitance approach. The various problems of temperature compensation, circuit stabilization, etc. are in addition to the other problems discussed, but are not so critical as to eliminate the approach by themselves.

In this analysis, the contribution of the vapor phase to the signal was not explicitly discussed. Actually, of course, the sum of the vapor plus liquid masses, $m_v + m_l$, is sensed. The vapor mass m_v is of the same order of magnitude as the liquid mass and is essentially constant over the 100 to 50% quality range. Thus, although the signal from the vapor would influence the calibration curve, it has an entirely negligible effect on the feasibility estimates made. In this connection, it is interesting to note that capacitance gauges are often advertised as being insensitive to the gaseous phase. For 100 to 50% quality by weight, the signal from the liquid phase is less than or equal to the signal from the vapor phase.

In conclusion, a capacitance gauge is not recommended for measurements of the accuracy required by the NASA application. The practical sensitivity of a capacitor is much too small and there are too many other sources of error which make a calibration curve unreliable and even different in space than on the earth. This conclusion is supported by basic arguments and by reference to optimistic experimental results which are themselves many times greater than NASA tolerances.

4.3.2 Susceptibility (Atomic)

The capacitive approach to fuel measurement is based on the electrical response of the liquid to an applied electric field. Similarly, a magnetic field may be applied either by a permanent or electromagnet, and an attempt made to measure a change in this field due to the magnetic response of any liquid present. Hopefully, the amount of such a change would be a measure of the quantity of fluid present. In complete analogy to the relative dielectric constant, ϵ , is the relative permeability, μ , which is the ratio of the magnetic fields with and without the liquid present.

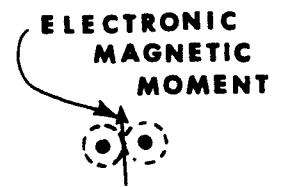
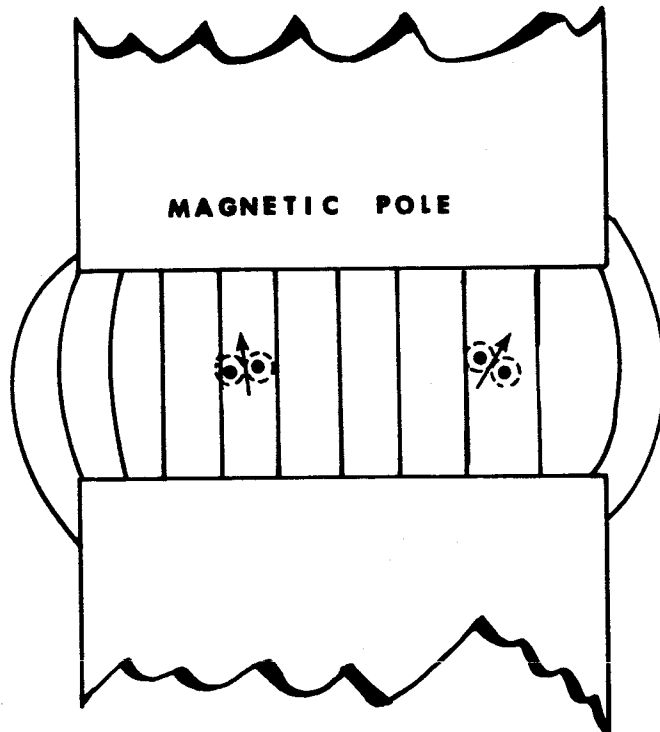
The oxygen molecule is something of an anomaly in nature. In the ground state, its electronic structure has a permanent magnetic moment. The application of a magnetic field tends to line up the magnetic moments of the various oxygen molecules present, and when aligned, they produce a detectable macroscopic field. (See Figure 12.) The alignment is opposed by thermal agitation and is thus only partially complete at any finite temperature and applied magnetic field strength. The degree of alignment is given by the Brillouin function.⁸⁷ At the NBP and for magnetic fields of practical magnitudes, the Brillouin function implies that the susceptibility is linear in the field strength. The value is

$$\mu = 1 + 4.0 \times 10^{-3} \text{ for 100\% LOX} \quad (4-38)$$

compared to

$$\mu_o = 1 \text{ for vacuum.}$$

It is the difference between the liquid and vacuum values which is a measure



**ALIGNMENT OF O_2 ELECTRIC MOMENT
BY AN EXTERNAL FIELD**

Figure 12

of the liquid present. For LOX, the following comparison may be made

$$\frac{\epsilon - \epsilon_0}{\epsilon_0} = 0.5 \quad (4-39)$$

$$\frac{\mu - \mu_0}{\mu_0} = 0.4 \times 10^{-2}$$

Oxygen is two orders of magnitude less sensitive to magnetic fields than it is to electric fields. Almost all of the relative error analyses made in the capacitance section of this report are directly applicable to the magnetic approach. Only one correction need be made--the required sensitivities remain the same, but the obtainable sensitivities drop by two orders of magnitude. For example, the required sensitivity is now one part in 10^6 . Since the capacitance approach was not sufficiently sensitive, the magnetic approach must be rated as hopelessly insensitive for oxygen.

Hydrogen is typical of most diatomic molecules. The magnetic moments of the electrons are so aligned that the net magnetic moment of any molecule is zero in the ground state. All H_2 or O_2 molecules can be assumed to be in this state at cryogenic temperatures.

Even though H_2 has no permanent atomic moment, a small moment can be induced by an applied magnetic field. The field distorts the paths of the electrons around the nuclei. Since the moving electrons are in effect small currents, they can produce a magnetic field. The effect as described is diamagnetism and it opposes the applied field. As a result, H_2 has a susceptibility which is slightly less than unity.

$$\mu = 1 - 1.5 \times 10^{-6} \text{ for } 100\% \text{ LH}_2 . \quad (4-40)$$

Thus,

$$\frac{\mu - \mu_0}{\mu_0} = - 1.5 \times 10^{-6} \quad (4-41)$$

The remarks following Equation (4-39) are applicable here except that they are several more orders of magnitude more pessimistic. Clearly, this approach may be rejected without further consideration.

There are, of course, numerous other practical problems associated with a susceptibility measurement. Producing an adequately strong and uniform field over a reasonably large sample volume is quite difficult. Permanent magnets are heavy and rather limited in field strength. Electromagnets are heavy and draw considerable power. Superconducting electromagnets are lighter and require less power, but they must have special cooling apparatus. At this time, there are no known superconductors which will operate at temperatures as high as the boiling point of hydrogen.¹⁰⁷

Almost every problem encountered by the capacitance approach is present in the susceptibility method and usually it is considerably more severe in the latter case. Capacitance, while not recommended, is still much the better approach. One possible way to obtain the extreme sensitivity required for a magnetic measurement is through a resonance measurement. This is covered in Section 4.3.4.

4.3.3 Susceptibility (Nuclear)

Some nuclei have permanent magnetic moments. An external field

could be used to align these nuclei. It might then be possible to detect the incremental field due to the aligned nuclei. The strength of the incremental field would be proportional to the number of nuclei present and hence a measure of the fluid mass. This situation is completely analogous to the alignment of the atomic O_2 moment, and the Brillouin function still applies. Figure 12 is still appropriate except that now the magnetic moment is associated with each nucleus rather than with the electronic structure of the molecule.

For 1_1H , the nuclear proton has a magnetic moment which is approximately 1/1000 of the electronic moment of the oxygen molecule. In parahydrogen, the two nuclei of each molecule are so arranged that they cancel each other's moments and cannot be detected by an external field. In orthohydrogen, the nuclear moments are aligned; they reinforce each other and thus respond to an applied magnetic field. The factor of 1/1000 means that the sensitivity is down three orders of magnitude from Equation (4-39) plus a further correction for thermal agitation. The small nuclear moment is much more easily agitated thermally and thus the sensitivity is reduced by even more than three orders of magnitude unless the sample is cooled well below the NBP of hydrogen.

The nuclear susceptibility effect is so small that it was unobservable for many years even in a laboratory. It was finally detected in a famous experiment¹⁰⁹ by cooling to 2°K (solid hydrogen) to reduce thermal agitation. Other conditions of the experiment included a large orthohydrogen concentration,

100% solid hydrogen (0% quality), and a very small sample volume. Detecting the nuclear susceptibility of 1/10 of 1% liquid at 20.4°K in a largely parahydrogen sample is completely unreasonable.

Oxygen is 99.9% O^{16} and O^{18} which have no nuclear moment. The nuclear moment of O^{17} is comparable to that of hydrogen. The high boiling temperature, low O^{17} concentration, and the smallness of nuclear moments imply that the nuclear susceptibility of oxygen could not be detected and would be dominated by atomic paramagnetism. See, however, Section 4.3.4 on resonance techniques.

4. 3. 4 Nuclear Paramagnetic Resonance and Electron Paramagnetic Resonance

The preceding three sections considered the detection of hydrogen vapor and liquid through the susceptibility of their atomic and nuclear moments-- a magnetic analogy of dielectric capacitance. There is a possible alternative way of detecting these magnetic moments which has no electrical analogy for LH₂ and LOX.

The electronic magnetic moment of O₂ and the nuclear magnetic moment of hydrogen exist independently of the strength of the magnetic field applied; the field serves merely to align the moments. A classical analysis of certain aspects of this alignment leads to false conclusions and, thus, it is necessary to use quantum mechanics¹⁰⁹ to arrive at correct conclusions. For example, classical mechanics allows the nuclear magnetic moment of an orthohydrogen molecule to be pointed in any direction. It can be shown,¹¹⁰ quantum mechanically, that a measurement of the degree of alignment of an orthonuclear moment with an applied field can lead to only three possible outcomes. Classically, there are no such restrictions in the direction of the nuclear moment which is continuously variable through 180° from parallel to antiparallel with the applied field. In a classical sense, quantum mechanics dictates that the ortho moment must be with, perpendicular to, or against the field; no intermediate values are possible.

An external magnetic field applies a torque on the nuclear moment, tending to align the moment with the field. To disalign the moment requires

the application of a counter torque and, more particularly, requires the expenditure of energy. Since there are only three possible degrees of alignment, the amount of energy that a given molecule can accept just equals the difference in energy associated with changing from one degree of alignment to another.

A quantum mechanical treatment of the electromagnetic field⁹⁰ shows that any radiation is made up of discrete units of energy called photons. The energy of a discrete unit is

$$E = hf$$

where f is the frequency of the electromagnetic wave and h is Planck's constant.⁷

Based on the foregoing preliminaries, a resonance measurement can be described. In the manner of Figure 12, a static external field is applied. All moments can be found in one of the three possible states of alignment. A dynamic external field of frequency f is also applied. The frequency (or alternatively, the static field strength) is varied until the energy of the photons just equals the energy required to change the state of alignment of individual molecules. At just this correct frequency, the sample, for example, hydrogen, can absorb energy. This is a basic example of nuclear magnetic resonance (NMR). The amount of energy absorbed is proportional to the number of ortho molecules present and is thus a measure of the amount of mass ($m_l + m_v$) present in the sample volume.

Typically, this frequency falls in the kilo or megacycles per second portion (RF) of the electromagnetic spectrum.

Nuclear magnetic resonance is a very highly developed and sensitive measurement technique and is extremely well reviewed in a basic treatise.⁸⁸ Many subtle conclusions can be reached using this technique, such as differentiating between the molecules in the gaseous and those in the liquid phase. This is equivalent to separate measurements of m_v and m_1 and, hence, of quality.

While NMR techniques are certainly very sensitive, the practical problems of making a flyable NMR quality meter are enormous. The sensitivity is so great that very small nonuniformities in the static magnetic field cause variations in the frequency of resonance absorption with position in the sample volume. The amount of absorption may be influenced by nonuniformities as much as by the presence of the LH_2 unless great care is taken. Producing an adequately strong and highly uniform magnetic field over a sample volume of several cubic inches or more is very difficult and requires a very large magnet. Only the very center of the field between poles attains the required uniformity. This is disadvantageous in two ways. First, the magnet poles must be much larger than the sample volume and, hence, tend to be heavy. Laboratory magnets commonly move about on tracks and weigh from hundreds of pounds up to many tons. Alternatively, superconducting magnets require supercooling systems (below the NBP of LH_2). Secondly, the short length of time spent by the flow in the field could

interfere with the determination of the relaxation time which is about 30 milliseconds for 5% orthohydrogen at 20° K.⁸⁸ The relaxation time refers to the period required for the alignment to return to its equilibrium value after an RF pulse.

Even a minimal discussion of the many possible NMR techniques⁸⁸ would probably fill one hundred pages. Many of these systems are theoretically capable of determining quality. By far, the most significant point, however, is the enormous complexity and delicate sensitivity of the apparatus. Careful adjustments are frequently made for weeks in preparation for a measurement of a sample less than one cubic centimeter in size. Questions of magnet size and weight are really somewhat beside the point, and, in fact, NMR measurements have been performed using the earth's magnetic field as the static field.⁸⁸ In general, any single isolated objection can usually be avoided by switching to some other range or technique within the NMR domain. However, to design a reasonably compact and reliable NMR quality meter which can operate on a variable speed flow is a major research undertaking with no guarantee of success. Other approaches are much more promising.

Electron paramagnetic resonance⁸⁷ is in many ways analogous to NMR. The greater strength of the electronic moment means EPR experiments are usually done with microwaves rather than low frequency RF electromagnetic waves.

The general principle of operation, however, is the same as for NMR. In particular, the remarks about the complexity and precision required of the apparatus is applicable to EPR. Furthermore, the method is not applicable to H₂ or most other molecules. Hence, this approach is not recommended.

4.3.5 Microwave Techniques

Microwaves form another extensively developed technology with many variations and alternatives too numerous to review.¹¹¹ A selection was, therefore, made of what appears to be the best microwave approach to quality measurement. The following analysis applies to that selection.

Microwaves refer to electromagnetic radiation in the frequency range of 10⁸ to 10¹¹ cps. The corresponding wavelengths are of the order of centimeters which is a convenient mechanical size. In fact, microwaves are commonly utilized in metallic cavities or wave guides which have dimensions equal to simple multiples of the wavelength. Resonance and standing waves can be maintained in a closed cavity. The size of the cavity determines the resonant wavelength. The resonant frequency is thus given by

$$f = \frac{c}{\lambda} \quad (4-42)$$

where,

c = the speed of light in the medium enclosed by the cavity, and

λ = the resonant wavelength.

In a nonmagnetic material such as hydrogen, the speed of light is given by

$$c = \frac{c_0}{\sqrt{\epsilon}} \quad (4-43)$$

where

- ϵ = the relative dielectric constant, and
 c_0 = the velocity of light where the cavity is empty.

Thus, from Equations (4-42) and (4-43),

$$\epsilon = \frac{c_0^2}{\lambda^2 f^2} \quad (4-44)$$

which shows that the dielectric constant of the medium may be determined from a knowledge of the resonant wavelength and frequency. The resonant wavelength may be determined from the dimensions of the cavity. These cavity dimensions are temperature dependent because of thermal expansion coefficients of the material of construction. The temperature, however, may be measured and used as a correction. A typical coefficient of expansion of 10 ppm per $^{\circ}\text{C}$ implies a temperature measurement accurate to $\pm 2^{\circ}\text{C}$ should be sufficient.

More importantly, the dielectric constant depends upon the resonant frequency, f , which can be directly measured. As discussed at some length in Section 4.3.1 on capacitance meters, the dielectric constant can be a

direct measure of the total mass present in the sample volume, $m_l + m_v$. If the liquid and vapor phases are well mixed and flowing at the same average speed, then the critical step in the quality measurement is accomplished.

The capacitance device introduced a large electrode area into the flow where film might accumulate. Also, as a mechanical obstruction, it tended to slow the liquid phase relative to the vapor phase. Both of these factors have been shown to be capable of producing large errors. In contrast to this, a cylindrical resonant cavity could be constructed using the vent tube itself as the cylindrical wall and two metal screens as the ends. Within the cavity, where the measurement occurs, there would be nothing to obstruct the flow except possibly a small driving element.

The electric field is by no means uniform within the cavity, and in this respect, the microwave technique is similar to the matrix capacitor. However, there is a very significant difference. In the matrix capacitor, the flow streamlines have a definite relation to the mechanical structure and, hence, to the nonuniformities of the field. In the microwave cavity, the field structure has cylindrical symmetry, but is otherwise fairly complex. Any one of a number of structures is possible depending on how the cavity is driven. Accurate charts of the field structure are available.¹¹³ As the flow passes through the cavity, each drop moves unobstructed through the field. Good averaging will take place if the averaging time is long compared to the time of passage of a drop through a wavelength of the field. During the one-tenth second response time, the flow moves three inches or so.

Thus, using a wavelength of the order of a centimeter and a cavity three or four inches long will result in resonant frequency that is accurately averaged over the contents of the cavity. All of the flow passes through the sample volume and, hence, is measured.

Another advantage results from the designer's freedom in choosing the field structure. The electric component of some field structures goes to zero at the walls of the cavity. Thus, any film adhering there would not contribute very much to the signal. This is desirable since film will travel much more slowly than the rest of the flow, and, hence, not contribute nearly as much to the ejected quality as its mass would imply. Similarly, driving the cavity with a magnetic dipole antenna would virtually eliminate any signal from a thin fluid film attached to the driver. These desirable field structures are, of course, not obtainable in a capacitance-type probe.

At 50% quality $m_v = m_l$. Since the liquid volume is very small, m_v at 50% is approximately equal to m_v at 100%. Thus, we may determine the maximum signal from the liquid by simply calculating the signal from the vapor. The dielectric constant of LH_2 is 1.228. The vapor is about 40 times less dense. Thus,

$$\epsilon_v = 1 + \frac{.228}{40} = 1.0057 \quad \sqrt{\epsilon} = 1.0028. \quad (4-45)$$

From Equation (4-43), the speed of light is decreased by 0.28% in changing from 100% to 50% quality. Allocating the speed of light measurement to

account for 2% of the total permissible 5% error demands the speed be measured to plus or minus a relative error of

$$\frac{\Delta c}{c_0} = \frac{2}{50} 0.28 = .01\% . \quad (4-46)$$

From Equation (4-42), the resonant frequency is directly proportional to the speed of light and, hence, the .01% accuracy applies to the sensitivity of detecting the resonant frequency shift.

At a microwave frequency of 3,000 mc (ten centimeter wavelength), preceeding calculations indicate that a 100 to 50% quality change will cause a resonance frequency shift of

$$\Delta f = (0.28 \times 10^{-2})(3,000) = 8.4 \text{ mcps} = 8,400 \text{ kc} , \quad (4-47)$$

and the required sensitivity is

$$\Delta f = (10^{-4})(3,000) = 300 \text{ kc} . \quad (4-48)$$

Although this resolution is not impossible, it is not particularly easy either. ¹¹¹

Microwave sources for this purpose are the Klystron or a high-frequency (up to 3,000 mc/sec) triode. Twenty watts or less input power can produce sufficient power for such a measurement. Detection is usually

accomplished by solid-state diodes and ordinary electronic amplifiers. Frequency modulation is ordinarily used to lock an oscillator to the resonant cavity. Coupling of microwave power to and from the cavity may be accomplished by means of electric dipole or magnetic dipole antennas, the latter being preferable in this application.

For LOX, similar calculations may be made:

$$\epsilon_v = 1 + \frac{.507}{160} = 1.0032, \sqrt{\epsilon} = 1.0016 \quad (4-49)$$

$$\frac{\Delta c}{c} = \frac{2}{50} 0.16 = .0064 \quad (4-50)$$

The sensitivity requirements are about one-third more difficult.

In summary, the microwave measurement appears capable of a quality measurement. Due, however, to rather stringent sensitivity requirements and due to the fairly complex system involved, it is not recommended as a preferred approach.

4.3.6 Scattering of Light

Surface tension is a relatively strong factor in determining the shape of small liquid bodies. Thus, if the liquid in the vented fluid was broken into many small droplets, these droplets would be rather spherical in shape.

Small dielectric spheres are known to scatter light and the amount of scattering has been accurately calculated¹¹² as a function of the wavelength

of the light, the diameter of the sphere, and the change in dielectric constant across the vapor-liquid interface. For a given wavelength of light and a given dielectric constant, this calculation shows that the scattering is a very complex and irregular function of the drop size. An accurate plot of this function is available.¹¹² In particular, it can be seen that the functional dependence on the drop size changes radically for droplets larger than the wavelength to droplets smaller than the wavelength. Therefore, if any reasonable sort of averaging of the droplets is to take place, one of two conditions must be met. Either the wavelength of the light is shorter than all the droplets of interest, or else it is longer. This necessity of choosing one of two possibilities will be apparent from the following discussion.

First, there is the possibility of choosing the wavelength of the light so short that 98% or more of the liquid will certainly be in droplets larger than the wavelength. Then the scattered light intensity is to a fairly good approximation, proportional to W where W is defined as

$$W = a^2 \tag{4-51}$$

and a is the radius of the spherical droplet. Using Equation (4-8) for the volume, V , of a sphere implies

$$W = \text{const } V^{2/3} \tag{4-52}$$

which is the same as Equation (4-9). The remarks associated with Equations (4-9) to (4-11) are applicable here and show that high frequency light does not produce an appropriate signal.

There is a further problem in determining suitable shorter wavelengths than any droplet of interest. Micron size droplets could well appear in quantity. Submicron light is in the range of optical frequencies and the assumption that a liquid is a homogeneous sphere breaks down. This light is in a suitable energy range to interact directly with individual atoms causing electronic transitions. Spectroscopic techniques are covered in the next subsection.

If the wavelength is taken long compared to the droplet diameter, it can be shown¹¹⁴ that the scattering intensity is directly proportional to the square of the droplet volume (Rayleigh scattering)

$$W = \text{const } V^2. \quad (4-53)$$

The argument following Equation (4-9) may be repeated here showing that an analogous error occurs for long wavelength light, the error being much more for light than for sound. Orders of magnitude error are easily produced. This problem is recognized in texts on the measurement of droplet sizes by optical techniques.⁷⁰

An intermediate wavelength light will mix the $V^{2/3}$ and the V^2 responses which will certainly produce no correlation with quality.

Since there does not appear to be any relation between the scattering of light and the mass of liquid, m_1 , present, this approach will not be pursued further.

4. 3. 7 Spectroscopic Techniques

The atomic structures of H_2 and O_2 have been studied rather thoroughly.¹² Comparisons of theory and experiment indicate that their atomic structure is well understood. The possibility arises of irradiating the fluid flow with light of a wavelength corresponding to a principal absorption line of the cryogenic fluid. The amount of absorption would be proportional to the fluid mass present. For good resolution, a laser might be used as a source.

A direct pass of the light through the fluid may yield an ambiguous signal. There must be ports or windows of sort, and there is the possibility that film collecting on them could decrease the signal by an amount which is comparable to the rather small signal attenuation by the fluid.

The absorption may also be measured by making the inside walls of the tube good reflectors and noting the rate at which a light pulse decays. The decay may be measured either in time or space along the tube. A section of the tube is really not a very good absorbing cavity, however, since it must be open at the ends. The loss in light intensity is more due to the open ends than the presence of the fluid.

Absorption measurements are intensity measurements requiring accurately calibrated power levels and quantitatively accurate intensity

detectors. The advantage of laser light sources and spectroscopic interactions occurs when frequency rather than intensity is the critical parameter of measurement. Some compounds have atomic levels from which they decay by spontaneous emission of a photon. When this decay is only part of the way down to the ground state, the photon frequency differs from the wavelength of the light which first raised the molecule to the excited state. Thus, the detection of the emitted photon may be easily accomplished without interference from the light source. For most molecules, decay is nonradiative and it would be very fortuitous to find a radiative process for LOX and LH₂. An exhaustive search was not made, however, due to the other limitations of the method discussed in this section.

It is reasonable to hope that when H₂ and O₂ molecules pass from the gaseous to the liquid state, the effect of close contact will distort the spectroscopic levels. Thus, the characteristic spectra of the liquid state would be noticeably different from the gaseous state. Choice of the proper wavelengths of light would permit separate and simultaneous measurement of the vapor mass, m_v , and the liquid mass, m_l . From these two values, the quality may be directly computed without any further probes. This would also solve most of the problem of accurate intensity measurement if one detector and light supply were used for both frequencies. Quality is a ratio and any gain errors would cancel. Unfortunately, the desired shift in the spectra does not occur when going from vapor to gas.¹² Hence, one of the principal attractions of this method is lost. Only the sum, $m_l + m_v$, can be measured and an independent determination of m_l or m_v is still necessary.

The mechanical coupling problem is difficult when light must be introduced into a system through optical windows. High thermal shock and wide temperature ranges do not mix well with tightly mated combinations of dissimilar and fragile materials.

Finally, spectroscopic techniques involve a good deal of precision and normally find their best application in a laboratory-type environment. Similarly, lasers are less reliable, rugged, and compact than would be desirable in this quality measurement. For all these reasons, spectroscopic techniques are not recommended.

4.4 Thermal and Thermodynamic Techniques

A number of instruments are based on heat flow and/or the associated temperature change between a probe and the process variable being measured.^{117-127, 14, 15} Almost invariably, the medium sensed is a single phase (either gas or liquid). Various relations can then be deduced relating the heat flow to the density, flow, etc., of the medium. There is little reason to think any of these results are relevant to a two-phase cryogenic vent flow.

4.4.1 Heat Flow (Hot Wire Technology)

A small heater element can be inserted into the gas stream and the rate of heat loss monitored. In the usual application, no phase change takes place--only slight heating of a gas or liquid. In the NASA application, the vapor pressure is virtually equal to the equilibrium value. Thus, a droplet impinging on a heated element may immediately vaporize at the

liquid-heater interface as shown in Figure 13, probably causing the droplet to appear to bounce off the heater. The amount of heat transfer will be influenced by an inertial term due to the mass of the drop and, more particularly, a term due to the surface area of contact. The inertia tends to prolong the time of contact. The rate of heat transfer is proportional to the contact area.

In general, it is expected that tiny droplets will be completely vaporized while large droplets will only lose little of their surface liquid before bouncing away. The heat transfer, then, attributes a disproportionately large mass to small droplets and, hence, simply fails to sense quality.

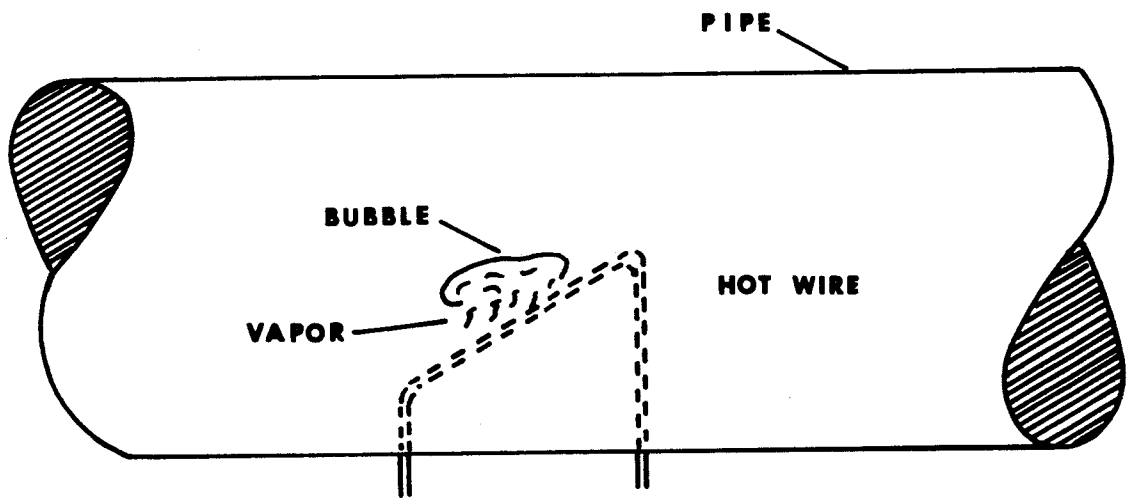
Other limitations include the very small part of the flow which can be sampled with reasonable heater power. Further corrections are required for temperature and velocity of the gas stream which also influence the heat transfer. Because the response is not proportional to the total droplet mass or volume, the heat transfer element cannot be calibrated for mass flow or quality. The approach appears to have little promise.

4.4.2 Vaporization of Liquid

This approach is discussed in the section on promising techniques.

4.5 Nuclear Techniques

An enormously wide range of nuclear particle and energies is produced in laboratories today. Nevertheless, this section should be limited to the application of those particles and energies which are available from light,



HEAT TANSFER QUALITY METER

FIGURE 13

convenient and reliable sources. This virtually limits the discussion to radioactive nuclei although X-ray tubes will be considered since they produce the same radiation as that from low energy gamma ray sources.

The four useful types of particles available are:

1. Gamma ray photons, γ . Electromagnetic energy is in units of energy called photons. Whether or not these photons are called particles is largely a matter of semantics. Photons in the few hundred to million electron volt energy range are referred to as either gamma rays or X rays.
2. Beta particles, β . High energy electrons.
3. Alpha particles, α . Helium nuclei.
4. Neutrons, n .

4.5.1 Gamma Ray Transmission

Gamma rays will penetrate a .035" pipe wall very easily. Thus, it seems quite appropriate to place a radioactive gamma ray source and a gamma ray detector opposing each other across the vent tube and measure the attenuation of the signal due to the presence of the fluid inside. Such measurements are commonly made in industry. See Figure 14. The attenuation is a function of the total mass, m_v and m_l , in the sample volume. Such a measurement is actually not practical for the NASA quality measurement as the following analysis will show.

When a gamma ray system is designed, there will be some average number, N , of photons counted during the measurement interval (empty pipe). Filling the pipe with hydrogen vapor will produce a change ΔN given by¹⁰

$$\frac{\Delta N}{N} = 1 - e^{-\mu \rho D} \quad (4-55)$$

where

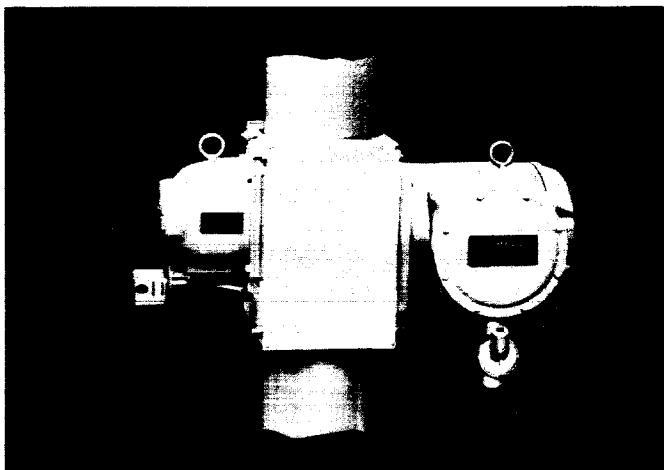
μ = cross section of hydrogen

ρ = density of hydrogen vapor

D = pipe diameter.

In order to get a good signal, μ should be as large as possible to offset the low density of hydrogen. This is done by using low energy gamma rays. The order of 60 kev is the lowest gamma energy which will penetrate the pipe wall. Also, energies well below 60 kev are not practically available. For LH_2 , at 60 kev and 22 psi,

DENSITY MEASURING GAUGES



$$I = I_0 \epsilon^{-\mu \rho x}$$

- x IS FIXED

- μ IS CONSTANT

- ρ IS MEASURED

Applications . .

- PETROLEUM
- CHEMICALS
- MINING
- GAS TRANSMISSION
- CRYOGENICS
- PROPELLANTS
- FOOD & BEVERAGES

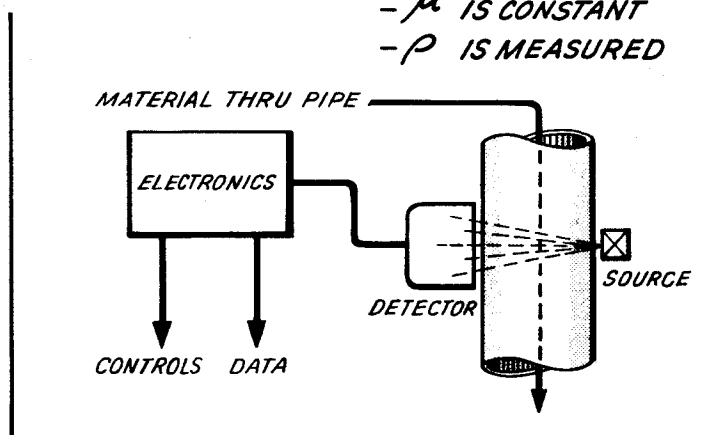


Figure 14

$$\begin{aligned}\mu &= .326 \text{ cm}^2/\text{gm}, \\ \rho_v &= 2.1 \times 10^{-3} \text{ gm/cm}^3 \\ D &= 6'' = 15 \text{ cm, and} \\ \mu\rho D &= 10^{-2}.\end{aligned}$$

Thus,

$$\frac{\Delta N}{N} = 10^{-2}. \quad (4-56)$$

This is the signal which results from a quality change from 100% to 50%. Allocating 2% of the permissible 5% error for this source alone dictates a minimum detectable change in ΔN , given by,

$$\frac{\Delta N}{N} = \frac{2}{50} 10^{-2} = 4 \times 10^{-4} = \frac{1}{2500}. \quad (4-57)$$

As shown in Appendix B, when the average count is N , there will be an unavoidable statistical error having a root mean square value of \sqrt{N} .

This is set equal to the allowable error, ΔN . Thus,

$$\frac{\Delta N}{N} = \frac{\sqrt{N}}{N} = \frac{1}{\sqrt{N}} = 4 \times 10^{-4} \quad N = 6.2 \times 10^6 \quad (4-58)$$

or the device must be so designed that 6×10^6 counts per one-tenth second averaging time or 6×10^7 counts/sec. is the average count rate at the detector. This presents an electronic design state-of-the-art problem.

A large source and detector are also required. By Equation (4-57), every other source of error in the count rate, such as distortion of the vent tube (vibration) thermal contraction of the source detector distance, temperature coefficient of detector, etc., must be held stable or corrected to better

than one part in 2500. This does not appear practical for the NASA application.

The measurement of scattered gamma rays is considerably more promising and is treated extensively in Section 5 of this report.

4.5.2 Beta Rays

Beta rays are widely used in instrumentation.¹⁰ Beta rays are high-speed electrons in the kev-mev energy range. Conventionally, they are produced by the decay of radioactive nuclei. In contrast to most nuclear gamma ray sources, beta rays are produced with a broad spectrum of energies from a single source. The two main techniques in their utilization are transmission and backscatter measurements.

In backscatter technology, both the source and the detector are on the same side of the specimen. For a given source, the intensity and spectral distribution of the beta particles scattered back to the detector are characteristic of the atomic numbers of the atoms in the specimen. Most of the signal comes from atoms at or near the surface of the specimen. Thus, this technique is used for thickness control of thin materials and for thickness and composition control of coatings, particularly on backing materials too thick for beta particle transmission. Backscatter measurements are considerably more sensitive to samples near the source and detector than to distant ones. For thin films and coatings, this causes no serious problem. The material to be measured is planar rather than distributed over a volume. Compensation for possible motion of the

sample relative to the source and detector is customarily a part of beta ray measurement systems. For a six-inch diameter pipe, much better averaging over the sample volume may be had by a transmission method. Also, a transmission measurement has greater sensitivity since the back-scattered intensity is relatively weak. For these reasons, a beta ray transmission gauge is preferred.

It is, of course, possible to measure the scattered radiation at any angle relative to the incident beam. Where the attenuation is of the order of a half thickness (50%), measurement of the transmitted beam is preferred. If the attenuation is very small, much less than a half thickness, then a transmission measurement is inaccurate due to the relatively large statistical noise and relatively small change in the signal with changes in the measured quantity. This is analogous to the gamma ray example treated in Section 4.5.1.

The total cross section of the vented hydrogen is in the right range for a good beta ray transmission measurement. Thus, beta scattering techniques are not recommended. A transmission gauge is described in considerable detail in Section 5 on promising approaches.

4.5.3 Alpha Particles

Alpha particles are helium nuclei--that is, two neutrons and two protons. In contrast to gamma rays which undergo arbitrarily large changes in directions due to a single scattering, alpha particles collide with many electrons successively. Each collision causes only a small energy loss

by the alpha particles, and due to the relatively light mass of the electrons, the alpha particle continues to move in nearly the same direction. Repe-
tition of this ionizing process eventually dissipates all the alpha particle
energy. Thus, alpha particle penetration is characterized by a range
rather than by a half thickness. Within moderate limits of statistical
variations, all alpha particles are brought to rest in a range which depends
upon their energy and the attenuating material.¹⁰

Five mev alpha particles are the highest energy available from
practical radioisotope sources. Even at this energy, the range is only
approximately 1/2 cm (hydrogen vapor) or .1 cm (oxygen vapor).¹⁰ This is
objectionably short for a six-inch vent line and disqualifies the method.
Furthermore, the range in liquids is only about 0.1 millimeter for LH₂
or LOX. Therefore, very small blobs of fuel will saturate
the response. Finally, a direct correlation between quality and alpha
particle flux does not exist. For example, many small droplets of liquid
will reduce the energy of a large percent of the alpha particles while per-
mitting essentially all of them to reach the detector. A few larger droplets
containing the same total liquid mass will stop those alphas which hit the
liquid droplet while permitting other alpha particles to reach the detector.
Hence, the same quality can produce different detected alpha particle
fluxes. (An analogous point is considered in some detail in the design of
the recommended beta particle quality meter.) If the detected alpha parti-
cles are to reveal the quality of the fluid, a pulse height analysis must be

made of their energy distribution. This requires, of course, a more complex electronic system. In summary, alpha particles are not recommended.

4.5.4 Neutrons

Neutrons can be produced in a number of ways including generators which occupy only a few cubic feet. However, for the purpose of this NASA application, only compact (cubic inches) radioactive sources²⁵ are considered practical.

The neutrons do not come directly from a radioactive nuclei. Instead, a radioactive source emits an alpha particle which penetrates into a target material knocking out a neutron. This is referred to as an (α , n) reaction in the target material. The inefficiency of this process limits the neutron source strength to about 10^7 neutrons sec, which is comparable to millicuries of a gamma or alpha emitter. Popular (α , n) sources are Po-Be and Ra-Be which emit neutrons in a broad energy range around 5 mev. A moderator can be added to reduce this energy to thermal values, if desired.

The total mass, $m_1 + m_v$, in the vent tube will scatter and absorb neutrons. This phenomenon permits a quality measurement in theory. However, some practical limitations should be considered. As shown in Appendix B (Section 2) and Section 4.5.1, detection of a few half thicknesses of mass results in maximum sensitivity and minimum required count rate. Alternatively, when the fluid density is low and the pipe diameter is well under a half thickness, high count rates and, hence, high source strengths are required.

The half thickness for absorption or scattering of neutrons in the energy range between thermal energy and five mev is considerably greater than six inches for hydrogen vapor.^{11, 116} For oxygen, the situation worsens. Thus, the contradictory requirements of small available source strength and large required source strength are present. The low efficiency of neutron detectors²⁵ must also be compensated by a corresponding increase in source size. Even if large neutron source strengths were available, shielding presents a weight problem. Neutron techniques are thus not recommended.

It is a rather general rule that bulk mass measurement by neutron absorption and scattering is less desirable compared to the appropriate choice among alpha, beta, and gamma rays. Production, detection, and shielding of neutrons are each more inconvenient than the corresponding process for the other particles. The utility of neutrons occurs when some special property such as a characteristic neutron reaction is involved.

4.6 Other Techniques

An effort has been made to consider any approach to quality measurement which might appear reasonable. Nevertheless, some preliminary screening is desirable. Many phenomena are rejected as being undesirable in a practical sense, or too complex for airborne applications, or inapplicable to hydrogen and oxygen, or as not relevant to measuring quality. Random examples include nuclear spectroscopy, quadrapole coupling with an external field, the Mossbauer effect, power thermally radiated by the fluid, activation analysis, magnetohydrodynamics, and the Auger effect.

5. PROMISING APPROACHES

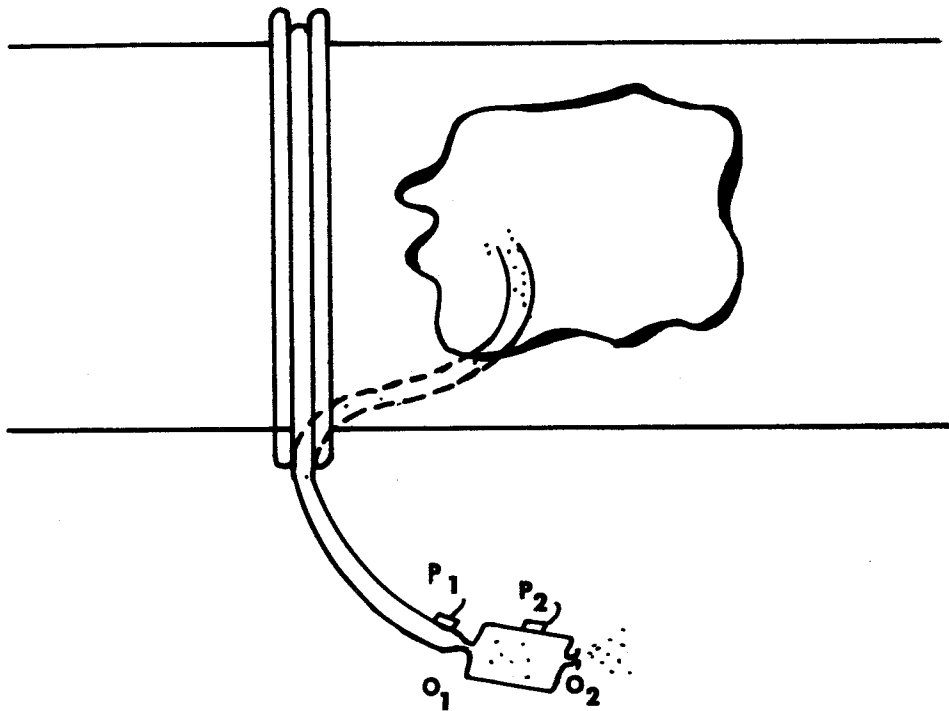
Three approaches have been selected as being promising. They have been selected on the basis of simplicity and accuracy in the measurement of quality and should easily meet NASA specifications of $\pm 5\%$ over the 100% to 50% quality range. Each approach has certain advantages and disadvantages unique in its use and not possessed by other approaches. A unique characteristic may be, for example, performance outside of the specified quality range. The choice of a best system is rather subjective. The choice depends upon the importance of these unique peripheral features to NASA. These three approaches are described below.

5.1 Vaporization

At 50% quality, the liquid volume is less than 3% (hydrogen) or 1% (oxygen). Since the mass of the liquid equals the mass of the vapor at 50% quality, conversion of the liquid to vapor doubles the amount of vapor, and hence at a fixed pressure nearly doubles the volume flow.

If the vented fluid is well mixed, for instance, by a diffusing screen, a sample of the fluid may be extracted and measured, the result being representative of the whole. The liquid in the extracted sample can be forced to vaporize by means of a pressure reduction or a heat transfer technique. The resulting increase in the quantity of vapor indicates the quality. Probably, the most convenient way of detecting the vapor increase is through pressure drop across an orifice.

As an explicit example, consider Figure 15. A small tube is inserted



EXPANSION TECHNIQUE QUALITY METER

FIGURE 15

in the mixed flow. The small tube vents to vacuum ambient. The amount of flow extracted by the tube is controlled by the series impedance of two expansion orifices, one at each end of an expansion and vaporization chamber (which may actually be just a short length of tube).

At 100% quality, there is an equal mass flow of vapor through both orifices and the pressure in the expansion chamber is determined by the relative size of the two orifices. At 50% quality, there are many small droplets passing through the first orifice. However, the volume of the droplets is less than 3% of the flow and thus the increase in pressure drop for a given value of the vapor mass flow rate is slight. In the expansion chamber, the lower vapor pressure causes the liquid to vaporize and thus doubles the vapor flow and pressure drop across the second orifice for a given flow rate. As a result, the effect of the vaporizing liquid is to decrease the flow velocity approaching the first orifice. More importantly, the effect is to increase the pressure in the expansion chamber since a relatively larger share of the pressure drop occurs across the second orifice.

Suppose at 100% quality the orifices are of such a relative size that the pressure in the expansion chamber is 50% of the vent pressure. Typically, this might be a vent pressure of 24 psi and an expansion chamber pressure of 12 psi. (The absolute size of the orifices is determined by the size of the sample which is required to be representative of the flow.) The pressure drop is the same across each orifice. Assume the quality changes to 50%. The mass flow rate of vapor through the second orifice will be twice that

through the first orifice. To a first approximation, neglect the contribution of the liquid to the pressure drop across the first nozzle. The pressure drop across the second orifice will then be about twice that across the first, resulting in a chamber pressure of 16 psi. If the 4 psi chamber pressure change is monitored to $\pm 1/5$ psi, then the sensitivity is approximately $\pm \frac{1/5}{4} 50 = \pm 2.5\%$ quality over the 100-50% quality range. Although this gives a rough estimate of obtainable sensitivities, determination of calibration and sensitivity should be made empirically. It is difficult to make an exact calculation of the pressure loss in two-phase flow.

In the actual implementation of this technique, it is necessary to consider the heat flow through the expansion chamber wall. The first possibility is an adiabatic expansion. In this case, the chamber is insulated. This reduces sensitivity since the presence of vaporizing liquid tends to cool the vapor and, hence, reduces the volume flow through the second orifice. Furthermore, there is the limited quality range over which the technique is applicable. Reducing pressure from 22 psi to 12 or 16 psi reduces the corresponding saturated vapor pressure of hydrogen by only about 1 K^o. The heat of vaporization of LH₂ is 105 cal/gm. The specific heat of the vapor is roughly 2.5 cal/gm K^o. Thus, a 1 K^o temperature reduction would permit the vaporization of a liquid mass of about 1/40 the vapor mass. (The Joule Thomson coefficient and other smaller effects are neglected here.) At this point, thermal equilibrium is re-established and

no further vaporization occurs. Any additional liquid would not be detected. The quality range is thus of the order of 100% to 97.5% which is too narrow for the application. Adjusting the ratio of the orifice dimensions will change the pressure level in the expansion chamber and thus increase the quality range. The increase is slight, however, because the pressure drop across the two orifices must be comparable if there is to be any sensitivity to the measurement.

The other alternative is to introduce heat into the flow and thereby induce further vaporization. Methods of partial vaporization do not appear attractive. The heat flow must be controlled within suitable limits. This is not easily accomplished. Unknown variations in droplet size and distribution may influence the heat transfer rate. Driving the vaporization to completion isothermally is a more prudent choice. These sources of uncertainty are thereby removed.

A practical embodiment would extract vapor from the flow using a tube with an orifice at each end as shown in Figure 16. The tube then passes through the flow or perhaps back through the tank in order to contact the LH_2 . In order to insure good thermal contact, the tube may be designed to have internal screens or fins. To prevent pressure losses due to frictional flow from dominating the signal, the pipe diameter should be large compared to the orifice diameters, although not necessarily large in the absolute sense. With this isothermal arrangement, the vaporization quality meter should approximate the performance levels calculated earlier in this section.

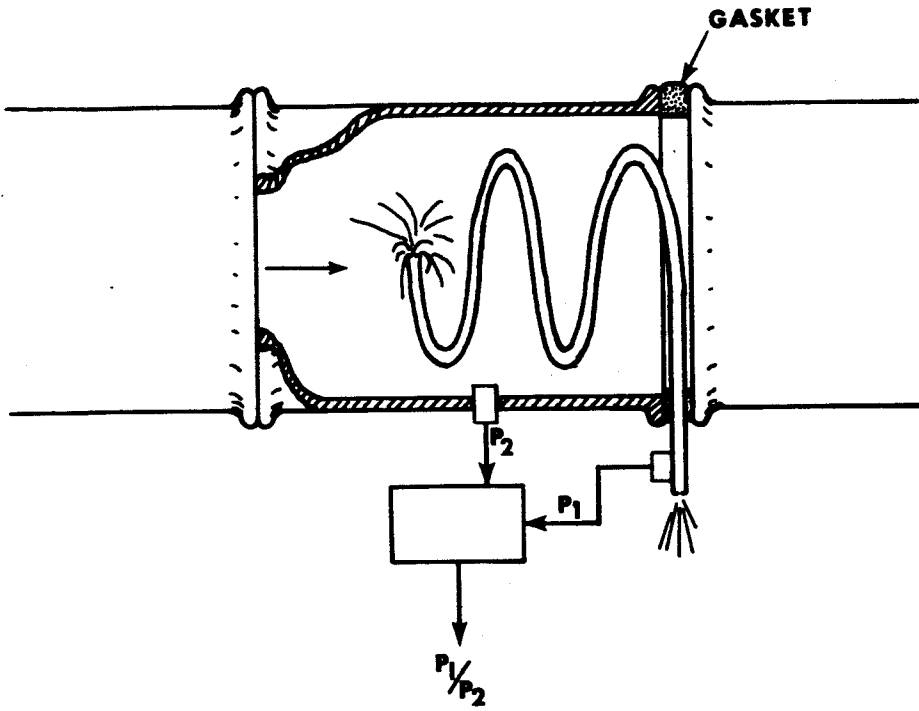
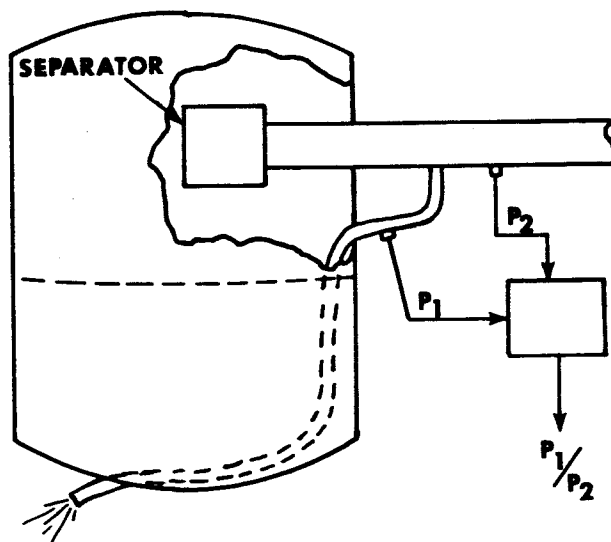


FIGURE 16a



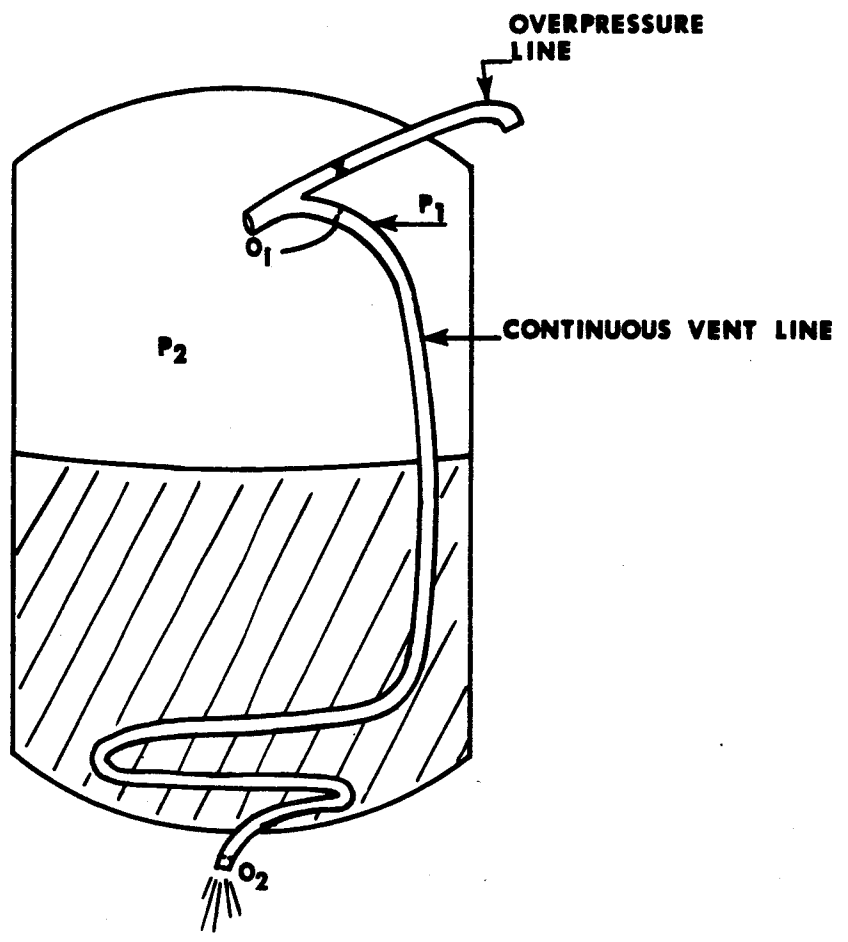
VAPORIZATION QUALITY METER

FIGURE 16b

Good correlation probably exists between quality and the ratio of p_1 and p_2 , the chamber and tank pressures. Quality can be expressed in terms of the ratio over a fairly wide tank pressure range. The small temperature range probably will not introduce a significant error but could be monitored as a correction. Since, however, temperature is implicit in the vapor pressure, p_2 , such a measurement is not necessary. Temperature correction could be implicitly included by using p_2 as a small correction to $\frac{p_1}{p_2}$.

Finally, there is the possibility of running the entire continuous vent line flow back through the fluid. Such a technique permits starting up from rest even when fluid covers the vent aperture. An example embodiment is shown in Figure 17. The first orifice, O_1 , is variable and is driven by a pressure sensor, p_1 , in the vent line. The second orifice, O_2 , has a fixed aperture of appropriate design to achieve the thrust of continuous venting. The command signal drives O_1 , maintaining p_1 at a fixed number of pounds per square inch less than p_2 , for example, 4 psi less.

Based on the control system just described, an operational sequence may be described. Start with the adverse initial conditions of O_1 fully open, the inlet of the vent tube immersed in fluid, and the vent tube full of fluid. Since $p_1 \approx p_2$ (the principal pressure drop is mostly across O_2 with O_1 open), the logic will immediately close O_1 . The fuel in the vent line past O_1 will vaporize and escape out O_2 , thus accelerating the missile and settling the fuel away from the orifice. When p_1 drops, O_1 opens to



QUALITY CONTROL AND MEASUREMENT SYSTEM

FIGURE 17

maintain p_1 four psi below p_2 . The standard rate of venting is determined by the orifice size of O_2 which is variable if desired. Any overpressures which occur in the tank will be passed along to O_2 for venting since O_1 is driven to keep a constant difference between p_1 and p_2 . The position of O_1 is a measure of the quality passing O_1 since at low quality O_1 closes more due to a lower volume flow at O_1 than at O_2 . The system also corrects poor quality by vaporization. Alternatively, the logic of the venting can be based on controlling O_2 with or without a variable O_1 .

This system is suitable for pipes of almost any diameter. Mass flow can be directly computed from p_2 and O_2 .

The simplicity and reliability of the system shown in Figure 16 is its special advantage. Response to a step change in quality will probably be nearer to one second than 1/10 second due to the inertia of heat flow. Although a 1/10 second burst of poor quality would not pass unnoticed, the response time is not within the 1/10 second specification.

5.2 Beta Transmission

Beta ray transmission is one of the most widely used techniques in nucleonic process control instruments. Its general characteristics and dependence on material properties are treated in nuclear instrumentation books.¹⁰ The attenuation of beta particles by matter is a fairly complex process on an atomic scale.¹²⁶ For materials of the order of six half thicknesses or more, beta particle attenuation is characterized by a "range" (a penetration depth). For material thickness of up to about three half

thicknesses, an exponential attenuation law applies to a collimated beam

$$I = I_0 e^{-\mu \rho t} \quad (5-1)$$

where

I_0 = unattenuated flux of beta rays,

I = transmitted flux,

μ = atomic cross section,

ρ = density of absorber, and

t = thickness of absorber.

Commercially available radioactive nuclei emanate beta rays with energies up into the kev and low mev range. The beta rays emitted by a given isotope are not monoenergetic. However, there is a well-defined maximum energy, E_m , for each isotope. A continuous spectrum of energies extends from E_m down to zero. Formulas are conventionally written in terms of E_m , although the average beta particle energy is roughly one-third of E_m .

The atomic cross section is given by¹⁰

$$\mu = 22 E_m^{-4/3} \quad (5-2)$$

where E_m is in mev and μ in cm^2/gm . This equation is independent of the chemical composition of the absorber and hence is limited in accuracy to about one significant figure. This is sufficiently accurate for design purposes. The exact value of attenuation is implicitly utilized when an empirical calibration curve is determined. Using Equations (5-1) and (5-2)

and making an approximate correction for the chemical composition of the fluid absorber yields half thickness values of approximately

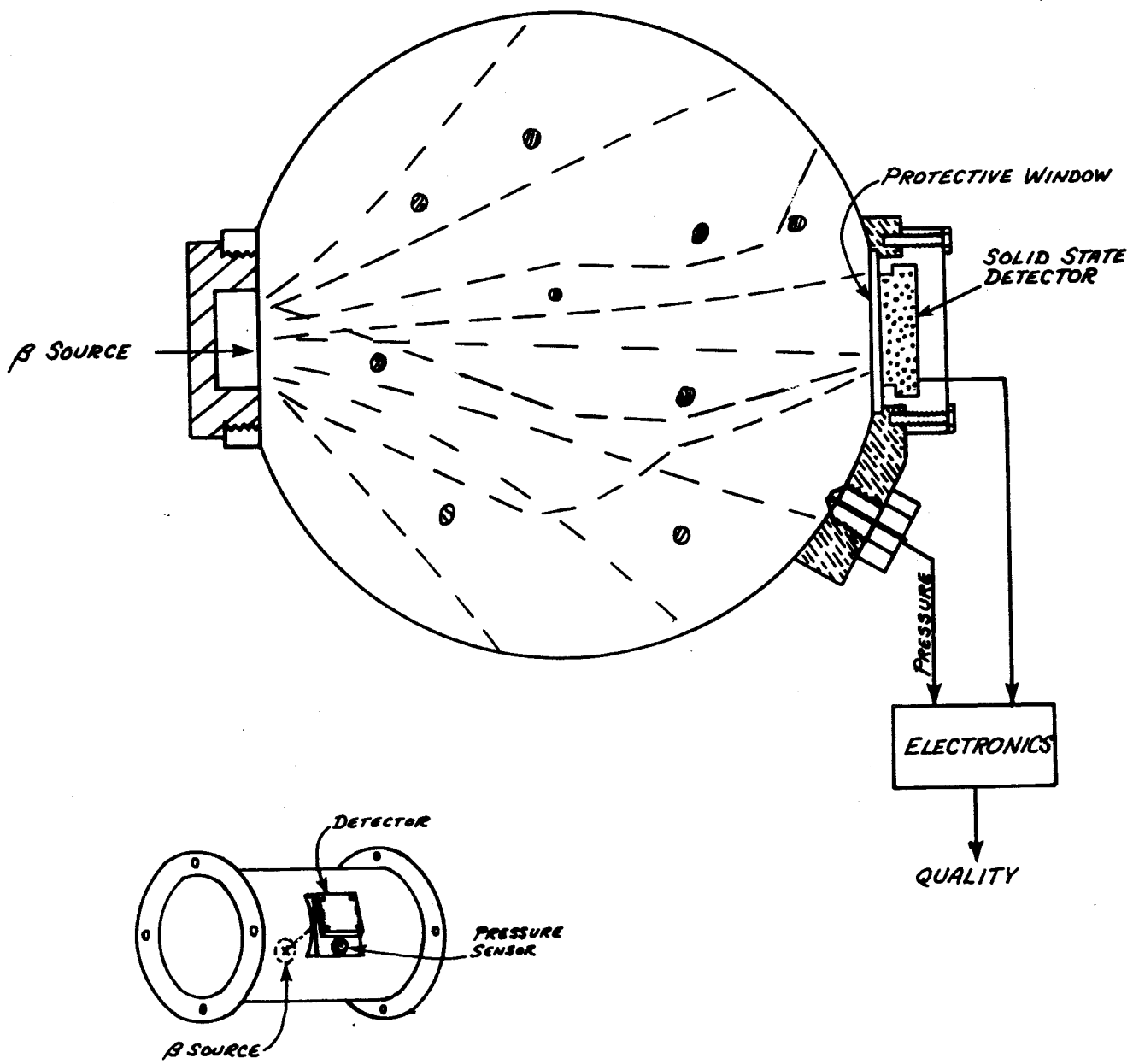
$$\begin{aligned} T_2 &= 6.5 \text{ mm, LH}_2; 28 \text{ cm, hydrogen vapor at 22 psi} \\ &= .8 \text{ mm, LOX; 13 cm, oxygen vapor at 22 psi} \end{aligned} \quad (5-3)$$

where E_m was taken as 2.2 mev which is the value for the commonly used strontium-yttrium source (20 yr. half-life).

The half thickness (amount of material to attenuate flux by a factor of two) values of Equation (5-3) are just about a perfect compromise. On the one hand, droplets in the centimeter-millimeter size range may be handled without saturating the response. On the other hand, the vapor itself in a six-inch diameter (15 cm) tube causes roughly a half thickness of attenuation in a beam sent across the tube. As has been shown in Section 4.1.2 and elsewhere, the 100% to 50% quality range corresponds to adding a liquid mass equal to the vapor mass. In this case, changing from 100% to 50% quality adds an additional half thickness and hence changes the signal by a factor of two, which is good sensitivity.

A typical embodiment might look as shown in Figure 18. Due to the moderate penetrating power of beta particles, the pipe wall acts as a good shield and it is probably unnecessary to collimate the beam or to make the pipe wall any thicker than is required for mechanical strength.

This is a particularly attractive application for a lithium-drifted, solid-state detector. The properties of these detectors are extensively discussed in the literature.^{128, 136} At cryogenic temperatures, many



BETA TRANSMISSION QUALITY METER

FIGURE 18

of their objectionable features disappear. By counting betas in a digital mode, it is possible to be relatively insensitive to any changes in detector characteristics. Section 5.4 on electronics is partially devoted to a suitable circuit for this beta transmission quality meter.

The attenuation of the beta particles is a measure of $m_v + m_l$, the sum of vapor and liquid masses in the measured volume. An independent measure of m_v comes from a pressure transducer. The general philosophy of this pressure measurement is included in Section 5.3 on gamma ray scatter. Other questions such as the probability of a given beta ray hitting a droplet are implicitly answered in Appendix C.

An estimate of the required source strength is of interest. Since the 100% to 50% quality range corresponds to roughly a factor of two in the received signal (100% change in signal), an allowable 2% change or error in quality means a $\frac{2}{50} \cdot 100 = 4\%$ change in the count rate N (the signal). By Appendix B, the statistical error in N is \sqrt{N} . Thus,

$$.04 = \frac{\Delta N}{N} = \frac{\sqrt{N}}{N} = \frac{1}{\sqrt{N}}, \quad N = 625. \quad (5-4)$$

That is, a minimum count rate of 625 counts per 1/10 second response time or 6250 counts/sec. is required. Without attenuation, the number of particles falling on the detector per 1/10 sec. is given by Equation (5-5). This is also the number of counts since solid-state beta particle detectors are nearly 100% efficient in their response.

$$625 = N = \frac{3.7 \times 10^{10} \text{ C A}}{4\pi D^2} \quad (5-5)$$

where

3.7×10^{10} = the number of nuclear disintegrations per second per curie,

C = the number of effective curies, defined as the product of the actual curies (which refers to the number of disintegrations) times the probability of producing a beta particle per disintegration. This probability is of the order of unity for most radionuclei,

A = sensitive area of detector (say 4 cm^2), and

D = pipe diameter (15 cm).

Solving for C yields,

$$C = 10 \text{ microcuries.} \quad (5-6)$$

Increasing C to compensate for the two half thicknesses of vapor and the loss through metal covers for the source and detector still yields a source strength in the submillicurie range which is very tiny from a shielding and handling standpoint.

This device can span the 1 to 10" pipe diameter range while still using a very small source strength. It will, however, saturate at qualities well below 50%. Its principal attraction includes being lightweight. The principal weight is due to the mechanical structure rather than the functional elements of the meter. The device has a very high sensitivity (and thus a very low required source strength) over the 100% to 50% quality range. Radiation levels are so low that quite likely no shielding will be necessary except the actual housing around the source.

5.3 Gamma Ray Scatter

Section 4.5.1 concluded that gamma ray transmission has very low sensitivity in the NASA quality meter application. Thus, the transmission quality meter was not recommended. In contrast, however, a gamma ray scatter quality meter gives a much more sensitive response over the whole range from 100% to 50% quality.

It is a good approximation to assume for high gamma ray transmission that the fluid is irradiated with a spatially uniform, intense flux. (The small change in intensity due to attenuation by the fluid is implicitly incorporated in an empirical calibration curve - Appendix C.) Every fluid atom thus has an equal chance to scatter a gamma ray. The number of scattered gamma rays is then directly proportional to the number of fluid atoms in the field. The count rate at the detector is directly proportional to the total fluid mass, $m_l + m_v$. The facts that this system responds directly to total fluid mass and that the signal is a linear function of this mass are desirable advantages and facilitate electronic signal processing.

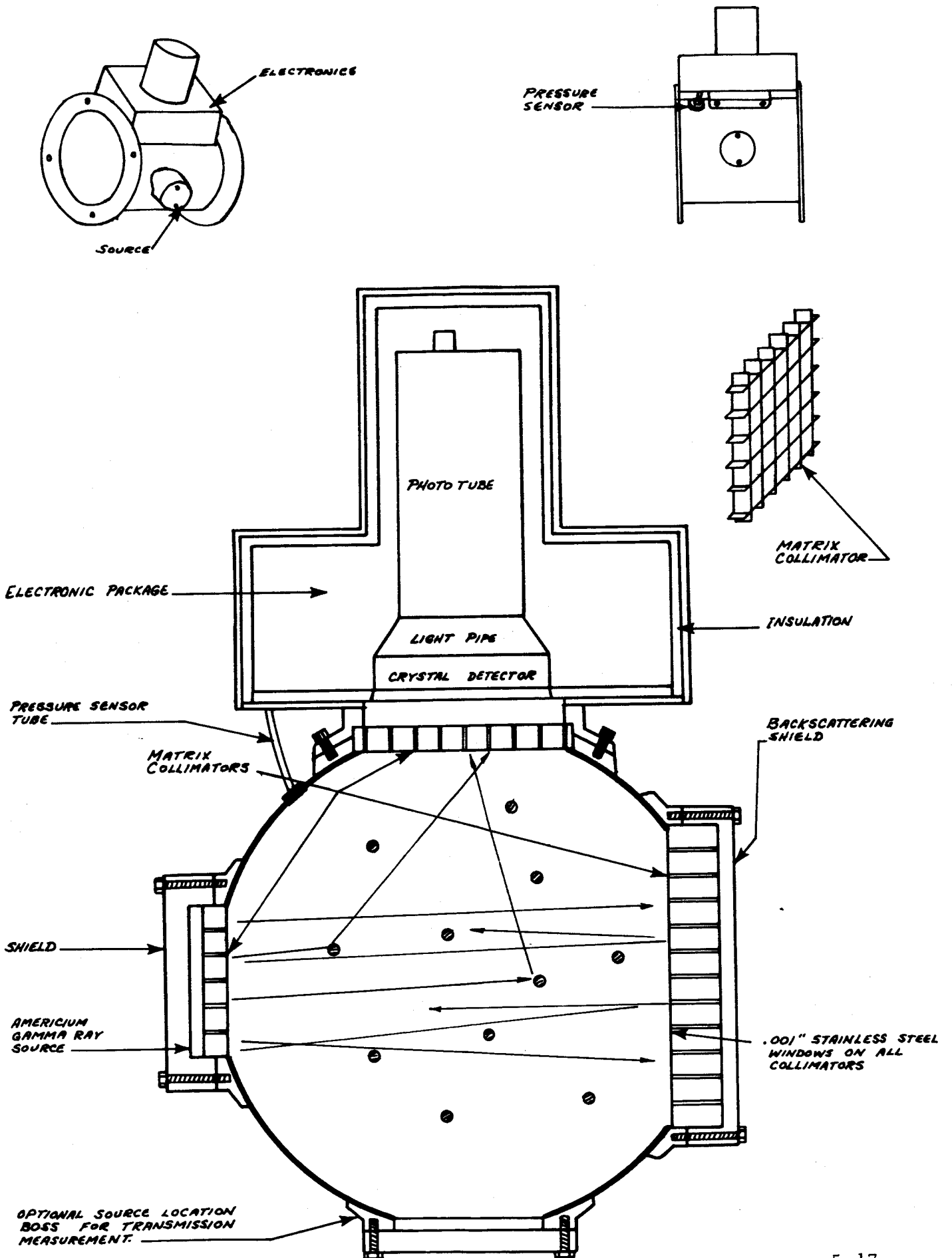
Transmission measurement of very low density substances results in a large unattenuated flux with a small superimposed scattered signal. The scatter signal is difficult to distinguish from statistical fluctuations in the large unattenuated flux. The signal-to-noise ratio is greatly improved if the system is so designed that the detector responds only to the scattered radiation. In this manner, the system responds only to pulses

which have been directly influenced by the measured fluid. However, a large scattered signal is desirable for adequate measurement sensitivity.

An embodiment of the gamma scatter quality meter is shown in Figure 19. The detector responds to gamma rays scattered by the fluid at 90° from the incident radiation. The collimator prevents incident gamma rays from entering the detector or from being scattered by pipe areas normally outside the incident collimated area. Therefore, unwanted direct or scattered gamma rays do not add undesirably to the basic response. The detector is also collimated to limit its field of view to the central region of the fluid flow and from viewing stray gamma rays. Even those gamma rays that scatter from the source collimator (or collimator window) have no direct path to the detector.

A suitable cover on the collimator (window) to prevent fuel collection in the collimator matrices may be desirable. Typically, stainless diaphragms, circumferentially supported, 0.001" in thickness, restrain pressures of 50 psi. The collimator matrix support will increase the cover's pressure restraint capabilities.

It may also be necessary to shield the pipe wall area illuminated by direct gamma rays for best signal-to-noise ratio. Figure 18 shows this accomplished by another collimator in front of this area. Gamma rays scattered by this collimator shield will be highly attenuated by the detector collimator. Those scattered back toward the source will enhance the useful gamma ray flux in the measured volume.



GAMMA RAY SCATTER QUALITY METER

FIGURE 19

The design of Figure 18 produces a signal proportional to the total mass, $m_1 + m_v$. Low energy gamma rays are recommended to enhance sensitivity and absolute signal level. Use of a 60 keV gamma ray source (americium-241) rather than a 600 keV source (cesium-137) doubles the effective scattering cross section of cryogenic fluid. From the standpoint of size, weight, simplicity, reliability, and particularly stability, there is little question about the superiority of an isotopic source over an X-ray tube.

Further safety may be built into the gamma ray source with a simple on-off switching arrangement. The soft (low energy) gamma rays may be produced by beta particles decelerated in a high atomic number target (bremsstrahlung). This type of source may be turned on or off by simply inserting a low atomic number (Z) absorber between the beta particle source and the high atomic number target. A gaseous beta absorber, such as krypton-85, might be substituted for a solid radioisotope source. Then should an accident occur, the gaseous source is dissipated and lost to the atmosphere or space, eliminating any personnel hazard.

Low energy gamma radiation offers further advantage in lightweight shielding and collimation. For comparison, a lead sheet thick enough to attenuate 600 keV gamma rays by a factor of two (a half thickness) will attenuate a 60 keV beam of gamma rays by a factor of 200,000,000 (~28 half thicknesses).⁹ A one curie americium-241 source (60 keV) with complete shielding can be held in a closed fist.

The higher attenuation of low energy gamma rays in materials simplifies signal detection components. A one-inch deep sodium iodide or cesium iodide crystal is adequate to produce a detectable response to a vast majority of the 60 kev incident gamma rays. The space ruggedized multiplier phototube and associated electronic data processing system are described in Section 5. 4.

The accuracy of this gauge is computed in reverse. An allowable statistical error ($\pm 2\%$ quality) is selected and the source size and detector requirements are determined to keep the error within this limit. Other design errors are estimated and added to the originally selected statistical error to obtain overall design requirements.

Appendix D shows each effective curie of source strength in the meter (Figure 19) produces a 1/10 second count, N, at the detector, of

$$N = 3 \times 10^4 C \quad (5-7)$$

at 100% quality. At 50% quality, the small liquid volume has increased, almost doubling the average fluid density. Thus,

$$N_{50} = 6 \times 10^4 C \quad (5-8)$$

and

$$N_{50} - N_{100} = 3 \times 10^4 C. \quad (5-9)$$

ΔN for a 2% error in quality is given by

$$\Delta N = \left(\frac{2.0}{50} \right) 3 \times 10^4 C = 1.2 \times 10^3 C. \quad (5-10)$$

At 50% quality (point of lowest accuracy), the relative error in count

rate corresponding to a 2% quality error is

$$\frac{\Delta N}{N_{100}} = \frac{1.2 \times 10^3}{6.0 \times 10^4} = \frac{1}{50} \quad (5-11)$$

Allowing statistical fluctuation to account for the maximum 2% error,

$$\frac{\Delta N}{N} = \frac{\sqrt{N}}{N} = \frac{1}{\sqrt{N}} \quad (5-12)$$

as shown in Appendix B. Comparing the last two equations,

$$\frac{1}{\sqrt{N}} = \frac{1}{50}, \quad N = 2500 \text{ (per 1/10 sec.)} \quad (5-13)$$

Finally, from Equation (5-7), the number of effective curies required is

$$C = \frac{N}{3 \times 10^4} = \frac{2500}{3 \times 10^4} = 83 \times 10^{-3} = 83 \text{ millicuries,} \quad (5-14)$$

a very moderate requirement indeed! This size of source is easily shielded. A one-mil steel window attenuates 2% of the gamma rays. To overcome this attenuation error, selecting a slightly larger source does not jeopardize these simple shielding requirements.

Background count may be comprised of natural gamma ray background and multiple-path scatter of gamma rays between source and detector with vacuum in the pipe. The natural radioactive background is very small compared to 25,000 counts per second. Due to the low density of vapor, the multiple-path scatter will be virtually constant even at 100% or 50% quality. Thus the output count rate, N' , is

$$N' = N_o + N \quad (5-15)$$

where N_o is almost constant and

$$N = K (m_1 + m_v). \quad (5-16)$$

K is a calibration constant. N_0 depends slightly on the amount of fluid in the vent tube. This is not a source of error, however; it just changes the value of K slightly. The natural background count is small compared to N. Hence, the average value of the background may be included in N_0 . In case of operation in very high background areas, N_0 may still be kept to low levels by pulse height selection or shielding. In extreme cases of large and variable natural background, a second detector can monitor the natural background and subtract it from N'. Such conditions are not anticipated in the NASA application. The principal contribution to N_0 is from internal scatter and this may be easily corrected as indicated previously.

The presence of N_0 does increase the statistical error slightly. Thus, a source of approximately 120 effective millicuries is advisable to stay well within the 2% statistical error limit. Americium-241 is recommended as the gamma emitter. Its half-life of 460 years is most attractive. The probability of emission of a 60 keV gamma ray is 0.4 per disintegration. Thus, on the basis of disintegrations, 300 millicuries are required, although from a shielding or detection standpoint, the number of effective millicuries is only 120. The collimator and self-absorption also increase the difference between the number of disintegrations and the number of gamma photons which are available. One-half a curie (actual, not effective) is thus suggested as an appropriate source to be utilized to insure good

response and statistical error within 2%. This amount of radiative material can be encapsulated and fully shielded to below any personnel radiation tolerances in a container much smaller than a golf ball.

The vapor density can be determined from either the temperature or pressure because of the saturated conditions in the tank. Small changes in temperature cause large changes in vapor pressure and density. For this reason and also because of the ease of measuring pressure compared to measuring temperature, it is recommended that the pressure rather than the temperature be monitored.

Figure 3 shows the dependence of density on pressure for saturated hydrogen vapor. It is very linear, although not directly proportional. This is much preferred in data processing as compared to the exponential dependence of density on temperature. The graph of Figure 3, over the S-IVB pressure range, can be summarized by

$$\rho_v = K \left(\frac{P}{30} + 0.06 \right) \quad (5-17)$$

where K is some constant, p is in psi, and 0.06 is an offset due to the non-ideal behavior of the gas. Since the mass of the vapor, m_v , in the sample volume is proportional to the density, to a very good approximation

$$m_v = K \left(\frac{P}{30} + 0.06 \right) \quad (5-18)$$

where K is another constant. The error in assuming that m_v is directly proportional to ρ_v was shown in Equation (2-19) to be less than $\pm 1.5\%$ quality and a best fit calibration curve will reduce the error to $\pm .75\%$ quality.

Even this .75% error can be removed electronically, since N' is measured. However, this does not seem justified because the error is so small.

Combining Equations (2-3), (5-18) and (5-16) results in

$$Q = K \left(\frac{N - N_o}{\frac{p}{30} + 0.06} \right)^{-1} = f^{-1} \quad (5-19)$$

where f is defined as the term in the parenthesis and K is a constant. N is the output count of the detector in 1/10 second. N_o is the empty tube count rate which is determined during calibration. The pressure, p , in the vent tube is measured.

The calibration factor, K , may be estimated theoretically, but for best accuracy, an experimental verification is necessary. The scattering cross section of the elements are known to very good accuracy⁹ and thus the calibration may be accurately simulated using a solid foam plastic material of appropriately adjusted density. This technique is also very helpful during the development of the quality meter as cryogenics are not required. A final verification using hydrogen should, of course, be performed, but any calibration adjustments which result would be small.

The pressure, p , can be measured with sufficient accuracy by a standard Bourns Model 441 absolute pressure transducer with a zero to 30 psi range. Manufacturer's brochures indicate an accuracy of $\pm 1.2\%$ of full scale with some temperature stabilization. Due to the -320°F limit of the pressure transducer, it is shown in an insulated and thermally stabilized compartment. Electrical heating similar to that used on the electronics (see Section 5.4)

is used. A tube from the vent pipe cuts down direct contact heat transfer from the vent pipe to the pressure sensor. Finally, it is shown in a separate compartment from the electronics since it need not be kept at so high a temperature.

Adding together the principal errors of statistics ($\pm 2\%$), electronics ($\pm 1\%$, refer to Section 5.4), the pressure sensor ($\pm 2\%$), and the approximation of Equation (5-18) ($\pm .75\%$) yields a total error of

$$\sigma = \sqrt{2^2 + 1^2 + 2^2 + (.75)^2} = 3.1\%.$$

Each of these errors is taken equal to or greater than its expected value and each is evaluated at its maximum point over the 100% to 50% quality range.

Another point which might appear to be a source of error is that of adding mass in the liquid form. This does not always produce the same scattered response as when it is added as vapor. However, as shown in Appendix C, they are the same over the 100%-50% quality range.

If the gas is at its saturated vapor pressure and then expands slightly, no liquid would be present to return the fluid to equilibrium saturated vapor pressure. The response would thus indicate greater than 100% quality. This is a desirable result, however, for it contains useful information and leads to no ambiguity. It simply means that the quality is still 100%, but some expansion has occurred.

The preceding analysis has been for hydrogen. However, entirely similar calculations apply to oxygen. In fact, an almost identical calibration

curve would result using a smaller source (or the same source partially covered). The principal change is in the nonideal gas offset factor of 0.06 in Equation (5-17). Therefore, this factor appears as a variable resistor in Section 5.4.

The dynamic range of the gamma scatter gauge is quite wide, extending well under 50% quality. However, Figure 19 shows an optional boss directly across from the detector. Moving the source to this boss will produce a highly accurate transmission gauge when operating near zero percent quality. The calibration function f is, of course, different, but sensitivities of the order of $\pm 0.1\%$ or $\pm 0.01\%$ quality would not be difficult, due in part to the definition of quality.

The actual weight of the gauge of Figure 19 is determined after detailed engineering. It should not be difficult to keep it under ten pounds.

In summary, the gamma scatter gauge appears well capable of meeting the specifications. Furthermore, it offers the possibility of an enormously wide dynamic range with great sensitivity at 0% quality as well as at 100% quality.

An additional benefit from its development is an accurate density gauge for low density cryogenic fuels. In the transmission mode of operation with the pressure signal disregarded, it can read liquid density very accurately, probably to $\pm 0.1\%$.

A ten millisecond response time presents no difficulty. The standard deviation of the statistical error necessarily increases by a factor of 3.2.

Increasing the source size decreases the statistical error and provides a means of compensation.

This gauge is applicable to larger diameter pipes. However, pipes less than three inches in diameter should be expanded before measurement.

Figure 19 is a true quality meter operating independent of the flow speed. This is desirable, since it is not limited to certain flow speeds. The most practical way to obtain a mass flow measurement is to use the quality meter determination of average density ($N' - N_0$) as a correction to the pressure drop across one orifice, perhaps a measurement of interest to NASA since it is understood these pressure measurements are being made. See Section 4 for further comments on implementation of this technique.

There is no particular advantage to taking the inverse of f of Equation (5-19). In fact, it is better to have f as the output electronic voltage adjusted so that $f = 0$ volts at 100% quality and $f = 5$ volts at 50%. Thus, lower than 50% quality will indicate a voltage greater than five. The following section covers the electronics in some detail.

5.4 Electronic Circuitry

The basic idea of the circuit to be described is to compare the pulse rate produced by the scintillation counter with a reference pulse rate and produce a DC output proportional to the first divided by the second. A potentiometric type absolute pressure transducer is made to vary the reference pulse rate in such a manner as to correct the quality gauge reading for absolute pressure. Details of the electronics are described below.

5.4.1 Basic Concepts

If N' is the scintillation counter pulse rate with the cryogenic fluid in the vent tube,

$$\text{Output} = K \frac{N - N_o}{\frac{p}{30} N_R + 0.06 N_R},$$

where

N_o (an adjustable constant set on the ground) is the count rate with the tube empty,

p is the tube pressure in psia,

N_R is the reference count rate at 30 pounds per sq. in. absolute, and

K is an arbitrary constant.

The equipment, shown in block diagram form in Figure 20, consists of a multiplier phototube crystal scintillation counter, a regulated power supply, a pulse amplifier, a pulse rate ratio computing circuit, a reference pulse rate generator, and an absolute pressure potentiometer transducer.

The pulses from the scintillator are amplified to about one volt

BLOCK DIAGRAM
 CRYOGENIC VENT
 QUALITY GAUGE WITH
 SCINTILLATION PHOTOMULTIPLIER

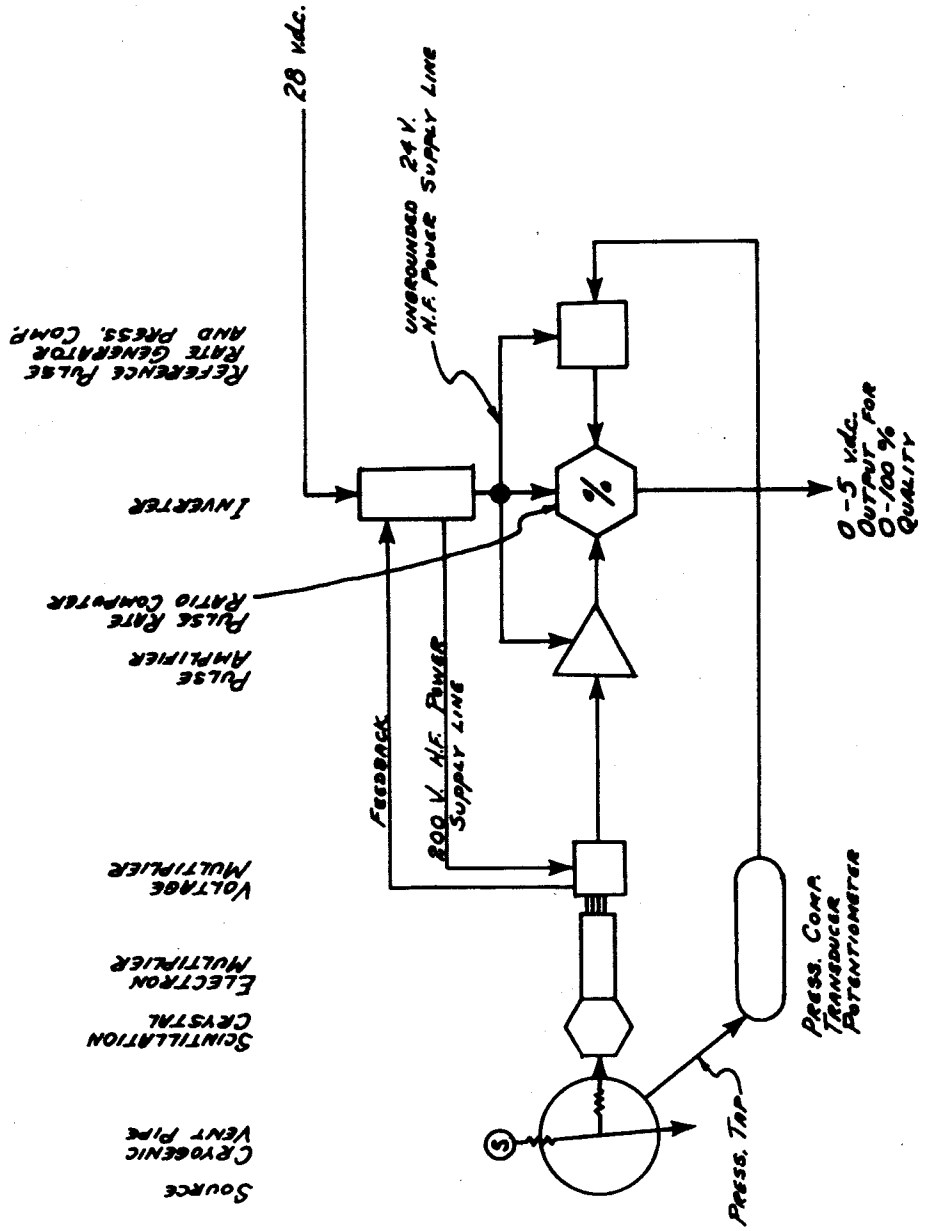


FIGURE 20

amplitude and fed to the ratio circuit where they reset a tunnel diode transistor flip-flop circuit which has been set by the reference pulse frequency. Under the set condition, a negative constant current, I_o , flows into an output circuit; under the reset condition, an equal positive constant current flows into the output circuit.

The average value of the output current, I_a , is then given by,

$$I_a = -I_o + \frac{N_1}{N_R} I_o$$

where

N_1 is the frequency of the pulses from the scintillation counter

N_R is the reference frequency

I_o is the constant current.

The statistical variations of this output are smoothed by a capacitor and produce a voltage across an output resistor. The negative offset voltage is balanced out by a potentiometer to provide

$$e_a = K \frac{N_1}{N_R}$$

By causing N_R to increase linearly with the absolute pressure and including a factor x to account for the nonideal behavior of the vent gas,

$$e_a = K_1 \frac{N_1}{N_R + xN_R}$$

Adjustment of the zero bias to account for " N_o ," the scintillator count

rate under empty tube conditions gives

$$e_a = K_1 \frac{N_1 - N_0}{N_R (1 + x)}$$

or

$$\% \text{ Quality} = K_2 \frac{N_1 - N_0}{N_R (1 + x)}$$

where K_1 and K_2 are constants.

5. 4. 2 Specific Description

The specific electronics system design recommended is described in more detail in the following sections.

5. 4. 2. 1 Scintillator Assembly

The scintillator consists of an RCA Type 4438 ruggedized multiplier phototube with head-on construction. The tube is operated at a current gain of 600,000 with an overall peak voltage of 1250 volts. It is to be coupled to an NaI(Tl) crystal with a plastic lightpipe and special bonding agent to reduce internal reflections. The encapsulated voltage multiplier section of the power supply is to be mounted integral on the bottom of the phototube with the leads soldered directly to the voltage outlets of the voltage multiplier.

The whole assembly is to be mounted into an aluminum container and encapsulated in silicone rubber in such a manner as to withstand the high acceleration forces to be encountered and the pressure variations.

5. 4. 2. 2 Regulated Power Supply

The regulated power supply shown in Figure 21 consists of a high frequency inverter feeding a diode capacitor voltage multiplier and filter that feeds each electrode of the multiplier phototube directly.

Voltage regulation and control is to be accomplished by a differential operational amplifier acting as a summing amplifier. The control signal is obtained from the last multiplier phototube dynode. The control signal is compared to a precision Zener diode voltage through a resistance network.

A remote negative coefficient resistor mounted in the multiplier phototube assembly provides a rising voltage to compensate for the negative gain coefficient of the multiplier phototube with rising temperature.

5. 4. 2. 3 Pulse Amplifier

The pulse amplifier shown in Figure 22 consists of a four-stage, high frequency silicon transistor amplifier with gain per stage severely limited by local feedback. The overall voltage gain is approximately 126 db.

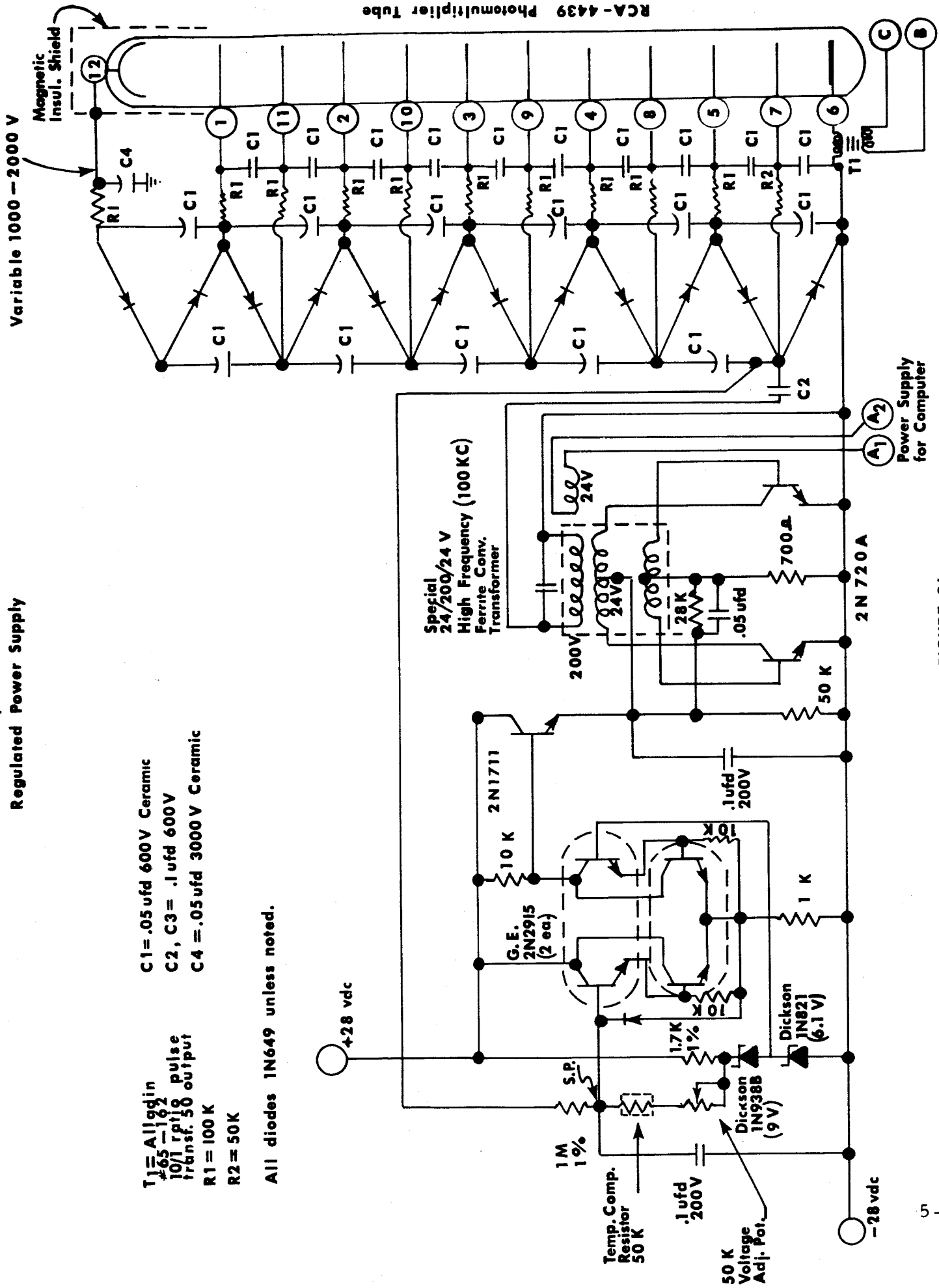
The first stage is a grounded base voltage amplifier with low input impedance to match the pulse transformer output of the multiplier phototube section.

The second and third stages use emitter follower feedback, while the fourth stage is an emitter follower to give a low output impedance.

5. 4. 2. 4 Ratio Computer

The computer is a prior Industrial Nucleonics development and a patent application is pending thereon.

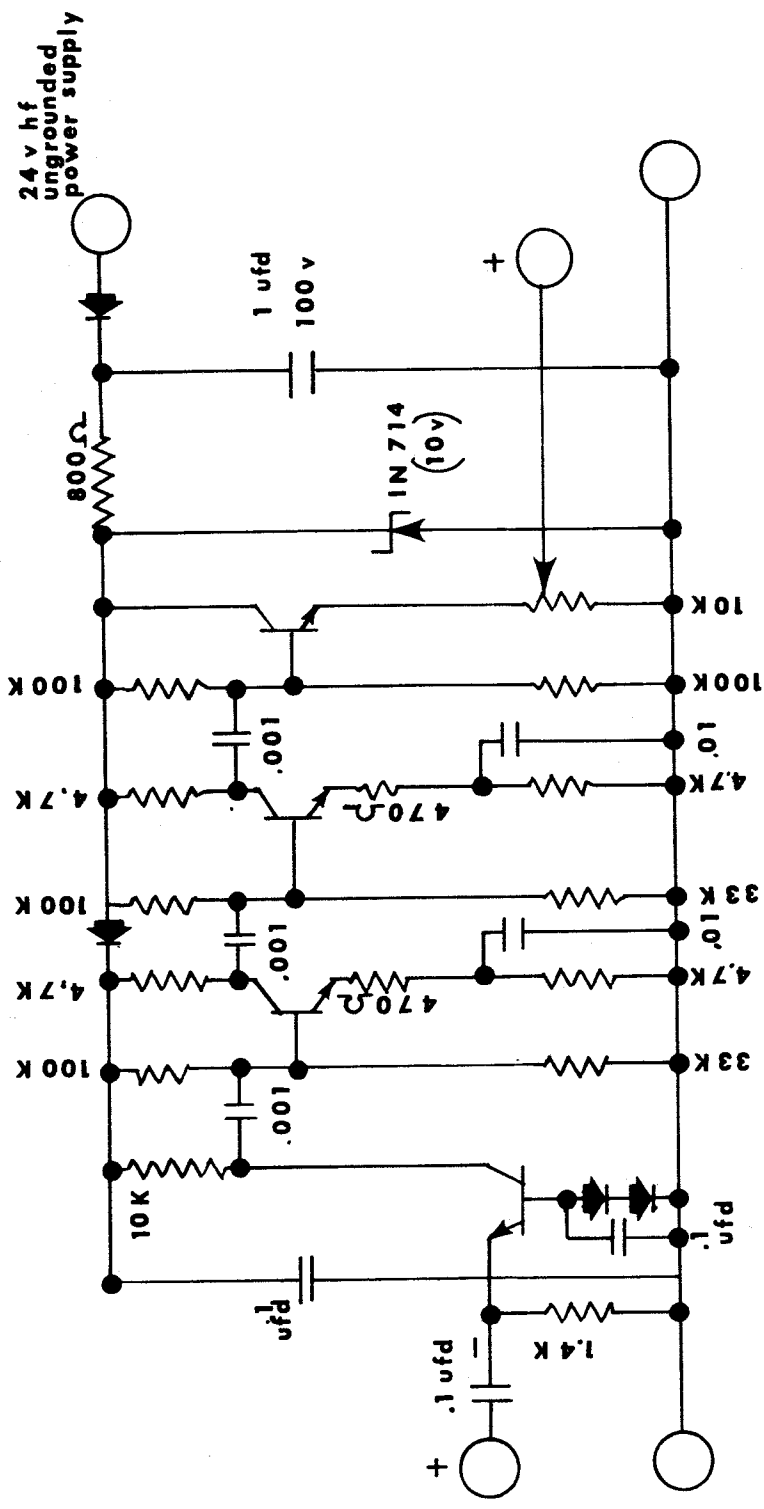
Photomultiplier and Regulated Power Supply



- T1 = Alligoin #65-162 10/1 rpf 10 pulse transf. 50 output
- C1 = .05 ufd 600V Ceramic
- C2, C3 = .1 ufd 600V
- C4 = .05 ufd 3000V Ceramic
- R1 = 100 K
- R2 = 50 K

All diodes 1N649 unless noted.

FIGURE 21



ALL TRANSISTORS 2N 930
 ALL DIODES IN 676

PULSE AMPLIFIER

Figure 22

The pulse rate ratio computer shown in Figure 23 consists of a special random pulse rate ratio divider developed by Industrial Nucleonics. The theory of operation of this device is treated in Appendix E.

The heart of the system is a flip-flop (tunnel diode in this case) gating a positive regulated current into a capacitor resistance network in the "one" position and an equal negative current in the "zero" position.

The amplified pulse signal from the scintillation counter pulse amplifier sets the flip-flop into the one position while a reference pulse signal sets it into the zero position. The average DC output is then proportional to the ratio of the two pulse rates.

The reference pulse generator consists of a unijunction diode relaxation oscillator having a constant current feed to its discharge capacitor so that the pulse rate is linearly proportional to this current and the voltage regulating this current. This reference frequency is controlled by the remotely located absolute pressure transducer to effect pressure compensation of the quality signal output. Temperature coefficient adjustment is provided.

5.4.2.5 Temperature Control

In view of the wide range of ambient temperatures to be encountered by this equipment, it is proposed to have two temperature regulators, one for the multiplier phototube voltage multiplier assembly and the other for the inverter-amplifier-computer encapsulation. These are to maintain these units at a minimum of 25°C to a maximum of 65°C for operation and 25°C to 70°C maximum for survival. These can be of a simple

thermostat relay type working from the 28 volts DC general power supply.

5.4.2.6 Grouping of Units

It is proposed to mount the multiplier phototube scintillation crystal, lightpipe voltage multiplier section of the power supply with temperature compensation resistor in an aluminum case with silastic potting compound in such a manner as would be suitable for the high accelerations to be experienced.

The inverter regulator section of the power supply, the pulse amplifier, and the ratio computer-reference frequency generator are to be encapsulated together in a high acceleration resistant package. Both are to have the aforementioned temperature regulation.

5.4.2.7 Errors

It is expected that the power supply to the multiplier phototube can be maintained within 0.1% for the regulated temperature range. Variations in this will have little effect on the accuracy of the output as long as the change in sensitivity does not cause the loss of pulses by lowering their amplitude below the triggering point.

The inherent accuracy of the ratio computer is dependent on variation of reference pulse rate and the accuracy of the constant current regulators providing the output signals. The first can be controlled to 0.1% and the second to about 0.5%, so it may be assumed that the overall accuracy can be adjusted to less than $\pm 1\%$.

5.4.2.8 Weight

Scintillation counter assembly	1.5 lb.
Power supply-amplifier-computer assembly	<u>1.0 lb.</u>
Total	2.5 lb.

5.4.2.9 Solid-State Detector System

As illustrated in Figures 18 and 24, a beta transmission gauge utilizes a solid-state detector, a charge sensitive preamplifier, a pulse amplifier, a pulse rate ratio computer with reference pulse rate generator, an absolute pressure compensator transducer, and a suitable power supply.

The solid-state detector and the charge amplifier represent the main difference between this and the multiplier phototube system. The other units, such as the pulse amplifier, the ratio computer, the reference generator, and the absolute pressure compensator, will be essentially the same. The power supply will also have differences in that it will produce a voltage of 400 volts maximum for the solid-state detector instead of 1250 volts required for the multiplier phototube. Its inverter and regulator are of the same type.

The charge sensitive amplifier may be of the microminiaturized silicon type, such as the Electro-Nuclear Laboratories Type 305N. The pulse amplifier must have its gain improved by a factor of ten to make up for the lower output of the charge amplifier.

BLOCK DIAGRAM
 CRYOGENIC VENT
 QUALITY GAUGE WITH
 SOLID STATE DETECTOR

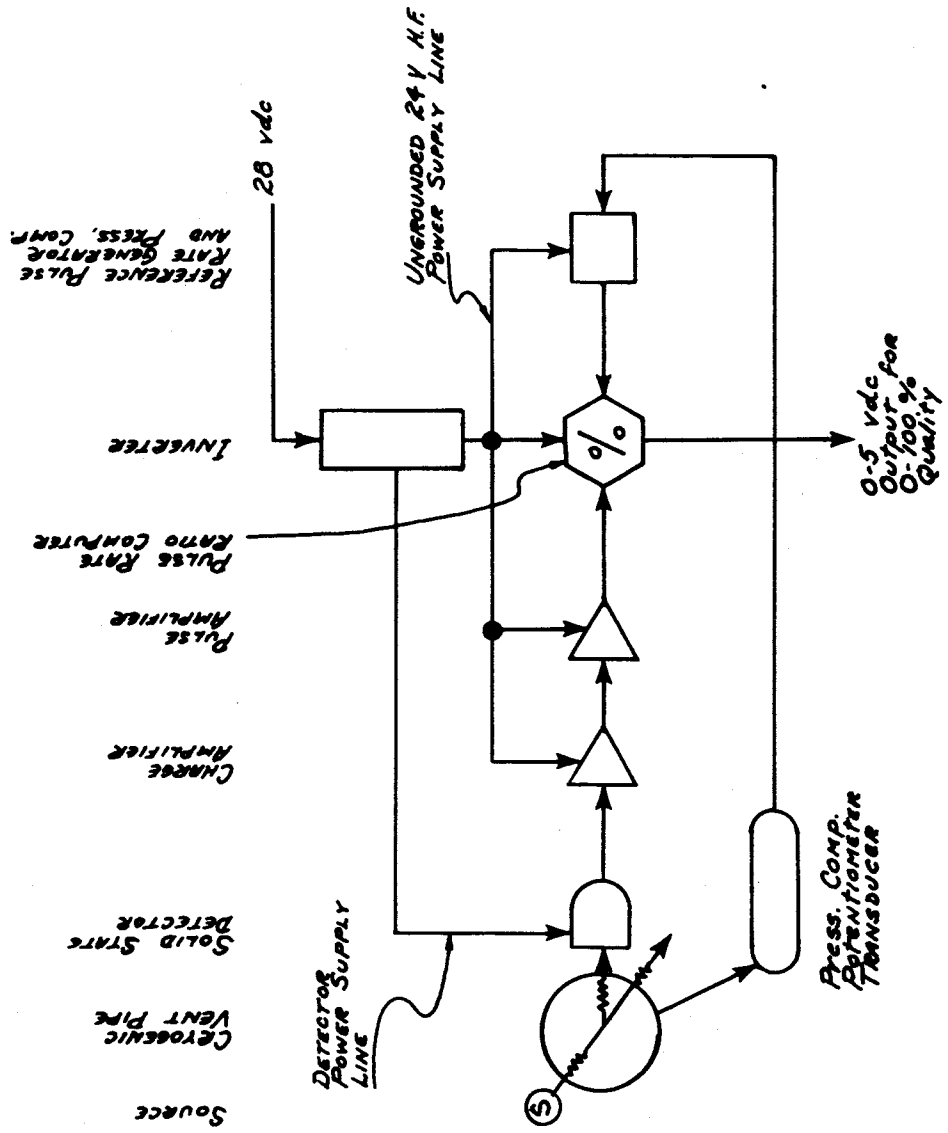


FIGURE 24

6. CONCLUSIONS

This report includes a general study of the measurement of quality and specific analyses of many possible approaches. In Section 5, three methods were recommended. All three appear capable of meeting the specifications over the 100% to 50% quality range. In addition, each method has some additional distinctive attributes.

The gamma ray scatter gauge is recommended for the application because of its unique ability to make very accurate measurements at low quality when the line is mostly filled with liquid. On several occasions, it has been indicated that this requirement is desirable. An additional requirement of this study was to select the one best method offering most promise to the application. Therefore, the gamma ray scatter gauge is selected as the most promising approach.

If, however, optimum measurement in the 100% to 50% quality range only is the overwhelming consideration, then some additional experimental work on the other two approaches might be recommended to assure their application capabilities are within the necessary requirements. These two approaches should be given further contractual consideration.

BIBLIOGRAPHY

1. Space/Aeronautics, August 1964.
2. Pippard, A. B.: The Elements of Classical Thermodynamics, Cambridge University Press, 1961.
3. Vance, R. W. and Duke, W. M.: Applied Cryogenic Engineering, John Wiley & Sons, Inc., New York, 1962.
4. Washburn, E. W.: International Critical Tables, Volumes I - VII, McGraw-Hill, New York, 1926.
5. Hodgman, Charles D. (Ed.): Handbook of Chemistry and Physics, Chemical Rubber Publishing Company, Cleveland, Ohio, July 15, 1950.
6. Maryott, Arthur A. and Smith, Edgar R.: Table of Dielectric Constants of Pure Liquids, United States Department of Commerce, National Bureau of Standards, August 10, 1951.
7. Gray, Dwight E. (Ed.): American Institute of Physics Handbook, McGraw-Hill Book Company, Inc., New York, 1963.
8. Ramsey, N. F.: Nuclear Moments, John Wiley & Sons, New York, 1953.
9. Grodstein, Gladys White: X-Ray Attenuation Coefficients from 10 kev to 100 mev, United States Department of Commerce, National Bureau of Standards, April 30, 1957.
10. Shumilovskii, N. N. and Mel'ttser, L. V.: Radioactive Isotopes in Instrumentation and Control, The Macmillan Company, New York, 1964.
11. Hughes and Schwartz: Neutron Cross Sections, BNL 325, U. S. Government Printing Office, Washington, D. C. 1958.
12. Herzberg, G.: Spectra of Diatomic Molecules, Second Edition, D. Van Nostrand Co., Inc., Princeton, New Jersey, 1950.
13. Binder, R. C.: Fluid Mechanics, Prentice Hall, New York, 1950.
14. Streeter, Victor L. (Ed.): Handbook of Fluid Dynamics, McGraw-Hill Book Company, Inc., New York, 1961.
15. Considine, Douglas M.: Process Instruments and Controls Handbook, McGraw-Hill Book Company, New York, 1957.

16. Cusick, C. F.: Flow Meter Engineering Handbook, Minneapolis-Honeywell Regulator Company, Philadelphia, Pennsylvania, 1961.
17. Addison, Herbert: Hydraulic Measurements, John Wiley & Sons, Inc., 1946.
18. Linford, A.: Flow Measurement & Meters, E. & F. N. Spon Limited, London, 1949.
19. Blechman, Seymour: "Techniques for Measuring Low Flows," Instruments and Control Systems, Vol. 36, pp 82-85, October 1963.
20. Driskell, L. R.: "How to Select the Best Flowmeter," Chemical Engineering, pp 83-90, March 4, 1963.
21. Norton, Harry N.: "Strain-Gage Pressure Transducers," Instruments and Control Systems, pp 85-88, March, 1963.
22. Nelson, R. C.: "Torque," Instruments and Control Systems, pp 77-83, March, 1963.
23. Damrel, J. B.: "Quartz Bourdon Gauge," Instruments and Control Systems, pp 87-89, February 1963.
24. Clark, Dudley B.: "Rare-Earth Pressure Transducers," Instruments and Control Systems, pp 93-94, February 1963.
25. Ball, S. J.: "Simulation of Plug-Flow Systems," Instruments and Control Systems, pp 133-140, February 1963.
26. Studier, Walter: "Quartz Pressure Sensors," Instruments and Control Systems, Vol. 35, pp 94-95, December 1962.
27. Stapler, Mead: "Drag-Body Flowmeter," Instruments and Control Systems, pp 97-99, November 1962.
28. Hartmann, H. R.: "Micro Torque Measurement," Instruments and Control Systems, Vol. 35, pp 105-106, November 1962.
29. "Flowmeter Practice," Instruments and Control Systems, Vol. 36, pp 89-92, April 1963.
30. Rogers, Earl J.: "Semiconductor Pressure Transducer Features Mechanical Compensation," Instruments and Control Systems, Vol. 36, pp 128-130, April 1963.

31. Wood, Russell D.: "Steam Measurement by Orifice Meter," Instruments and Control Systems, Vol. 36, pp 135-137, April 1963.
32. Hughes, A. R.: "New Laminar Flowmeter," Instruments and Control Systems, Vol. 35, pp 98-100, April 1962.
33. Shichman, Daniel and Johnson, Jr., Ben S.: "Tap Location for Segmental Orifices," Instruments and Control Systems, Vol. 35, pp 102-105, April 1962.
34. Cartier, R. J.: "Precision Liquid Manometry," Instruments and Control Systems, Vol. 35, pp 114-117, April 1962.
35. Johnson, D. P. and Newhall, D. H.: "The Piston Gage as a Precise Pressure-Measuring Instrument," Instruments and Control Systems, Vol. 35, pp 120-123, April 1962.
36. "Dead-Weight Testers," Instruments and Control Systems, Vol. 35, pp 126-130, April 1962.
37. Muhleisen, Edward H.: "Digital Flow and Blending," Instruments and Control Systems, Vol. 35, pp 141-147, May 1962.
38. Siev, Robert: "Mass Flow," Instruments and Control Systems, Vol. 33, pp 966-970, June 1960.
39. Von Vick, George: "Transducer Evaluation," Instruments and Control Systems, Vol. 33, pp 979-981, June 1960.
40. "NBS Flow Program," Instruments and Control Systems, Vol. 33, p. 1011, June 1960.
41. Mathewson, C. W.: "The 'Dimensionless' Strain-Gage Transducer," Instruments and Control Systems, Vol. 34, pp 1870-1871, October 1961.
42. Epstein, Saul: "Variable-Reluctance Pressure Transducers," Instruments and Control Systems, Vol. 34, pp 1876-1877, October 1961.
43. Dowdell, Rodger B.: "The Dall Flow Tube," Instruments and Control Systems, Vol. 33, pp 1006-1009, June 1960.
44. Benson, James M. and Hawk, Charles E.: "Testing Small Orifices," Instruments and Control Systems, Vol. 33, pp 996-998, June 1960.
45. Hall, Clifford N.: "Subcritical, Controlled-Ullage, Cryogenic Tankage Concept," Journal of Spacecraft, Vol. 1, No. 4, July-August 1964.

46. Halsell, Charles M.: "Why Meter Mass Flow," ISA Journal, Vol. 7, No. 6, pp 48-62, June 1960.
47. Force Transducers, Clark Electronic Labs.
48. Digital Pressure Generator, Hass Instrument Corporation.
49. Pressure Transducer, Edcliff Instruments.
50. Flowmeter Probe, Ramapo Instrument Company, Inc.
51. Flow Transducer, Hydropoise, Inc.
52. Force and Pressure Sensors, Clark Electronic Laboratories.
53. Aerojet-General Corporation, "Cryogenic Flow Measurements," Air Force Contract AF 04(645)-8, January 17, 1962.
54. General Electric Company, Lynn, Massachusetts, and Wyle Laboratories, El Segundo, California, "Cryogenic Mass Fuel Flow Transmitters," Air Force Contract No. AF33-657-9786, December 1962.
55. Armour Research Foundation of Illinois Institute of Technology, "Feasibility Study of a New Mass Flow System," Atomic Energy Commission Contract No. AT(11-1)-578, January 31, 1962.
56. Lewis Research Center, Liquid-Hydrogen-Flowmeter Calibration Facility; "Preliminary Calibrations on Some Head-Type and Turbine-Type Flowmeters;" NASA Contract No. NASA TN D-577; October 1961.
57. Advisory Group for Aeronautical Research and Development, "The Thermal Laminar Boundary Layer on a Rotating Sphere," Report 283, April 1960.
58. The Marquardt Corporation, "Turbine Flow Meter and Calibration Facility Study," Air Force Contract No. AF04(611)-7548, August 1962.
59. Wyle Laboratories, "Liquid Hydrogen Mass Flowmeter Evaluation and Development," U. S. Army Contract No. NAS8-1526, March 31, 1961 through September 30, 1961.
60. Translation, "Use of Oscillator Quartz Crystals for Weighing Thin Layers and Micro-Weighing," by G. Sauerbrey, TIL/5282, February 1962.
61. Descriptive literature relating to turbine meters manufactured by Potter Aeronautical Corporation, Union, New Jersey; Hydropoise, Inc., Scottsdale, Arizona; Waugh Engineering, Van Nuys, California; Cox Instruments, Detroit; Space Instrumentation Co., Santa Monica, California; Fischer and Porter Company, Warminster, Pennsylvania; and Quasitomics, Inc., Tarzana, California.

62. Mason, Warren P. (Ed.): Physical Acoustics, Academic Press, New York, 1964.
63. Beranek, L. L.: Acoustics, McGraw Hill, New York, 1954.
64. Herzfeld and Litovitz: Absorption and Dispersion of Ultrasonic Waves, Academic Press, New York, 1959.
65. Brekhovskikh, L. M.: Waves in Layered Media, Academic Press, New York, 1960.
66. Sette, D. (Editor): Dispersion and Absorption of Sound by Molecular Processes, Academic Press, New York, 1964.
67. Morse, P.: Vibration and Sound, McGraw-Hill, New York, 1948.
68. Morse and Feshbach: Methods of Theoretical Physics, McGraw-Hill, New York, 1953.
69. Abramowitz, Milton and Stegun, Irene A.: Handbook of Mathematical Functions with Formulas, Graphs, and Mathematical Tables, National Bureau of Standards Applied Mathematics Series • 55, U. S. Government Printing Office, Washington, D. C., June 1964.
70. Irani and Callis: Particle Size: Measurement, Interpretation, and Application, John Wiley & Sons, New York, 1963.
71. Division of Engineering, Brown University, "The Attenuation of Acoustic Waves in a Two-Phase Medium," Prime Contract No. NOrd 16640, Bureau of Naval Weapons, Department of the Navy, May 1963.
72. Vigoreux, P.: Ultrasonics, John Wiley & Sons, Inc., New York, 1951.
73. Bohm, D.: Quantum Theory, Prentice Hall, New York, 1951.
74. Lamb, H.: Hydrodynamics, Dover Publications, New York.
75. Condon, E. U. and Odishaw, Hugh: Handbook of Physics, McGraw-Hill Book Company, Inc., New York, 1958.
76. Yeh, L.: "Phase Angle in Vibration Work," Instruments and Control Systems, Vol. 35, pp 88-90, December 1962.
77. Ultrasonic Flowmeter, Gulton Industries, Inc.

78. Watertown Arsenal Laboratories, "Ultrasonic Attenuation and Velocity in SAE 4150 Steel," D/A Project 5B93-32-004, December 1961.
79. University of California, Department of Engineering, Fluid Motion and Sound, Navy, Contract No. Nonr-233(62), May 1, 1960 - April 30, 1961.
80. Cornell Aeronautical Laboratory, Inc., "Analysis of Nonsteady Two-Phase Flow," Office of Naval Research, Department of the Navy, Contract Nonr 3623(00), NR-098-038, June 1964.
81. Scott: The Physics of Electricity and Magnetism, John Wiley & Sons, New York, 1959.
82. Space Sciences Incorporated, "Development and Testing of a Cryogenic Quality Meter," Air Force Contract No. AF33(657)-11750, March 1964.
83. Beechcraft Research and Development, Inc., "Flow Theory Development for a Cryogenic Liquid," WADC Technical Report 58-529, Contract Number AF33(616)-5178, September 1958.
84. Landau, L. D. and Lifshitz, E. M.: Statistical Physics, Pergamon Press Limited, Reading, Massachusetts, 1958.
85. Fraade, D. J.: "Measuring Moisture in Solids," Instruments and Control Systems, pp 99-101, February 1963.
86. Fraade, D. J.: "Measuring Moisture in Liquids," Instruments and Control Systems, pp 109-111, March 1963.
Fraade, D. J.: "Measuring Moisture in Gases," Instruments and Control Systems, Vol. 36, pp 100-105, April 1963.
87. Pake, G. E.: Paramagnetic Resonance, W. A. Benjamin, Inc., New York, 1962.
88. Abragam, A.: The Principles of Nuclear Magnetism, Oxford University Press, London, 1961.
89. Panofsky, Wolfgang K. H. and Phillips, Melba: Classical Electricity and Magnetism, Addison-Wesley Publishing Company, Inc., London, Reading, Massachusetts, 1962.
90. Schweber: An Introduction to Relativistic Quantum Field Theory, Row, Peterson and Co., Evanston, Illinois, and Elmsford, New York, 1961.

91. Strange, John P.: "Sensors for Automatic Analyses," Instruments and Control Systems, pp 91-95, November 1962.
92. "Optical Methods of Studying Pressure Effects," Instruments and Control Systems, Vol. 35, pp 107-108, December 1962.
93. Star, Joseph: "Hall-Effect Transducers," Instruments and Control Systems, Vol. 36, pp 113-116, April 1963.
94. "Capacitive Pressure Sensors," Instruments and Control Systems, Vol. 35, pp 119-122, May 1962.
95. Weiby, Paul: "The Versatile Capacitance Bridge," Instruments and Control Systems, Vol 35, pp 112-115, August 1962.
96. Grossman, Lawrence M. and Charwat, Andrew F.: "The Measurement of Turbulent Velocity Fluctuations by the Method of Electromagnetic Induction," The Review of Scientific Instruments, Vol. 23, No. 12, pp 741-747, December 1952.
97. Capacitive Pressure System, Omega Dynamics Corporation.
98. Measurement of Hypersonic Flow, Guggenheim Aeronautical Laboratory.
99. Conductive Plastic, Emerson & Cuming, Inc.
100. Electrostatic Generators, Société Anonyme de Machines, Electrostatiques.
101. Goddard Space Flight Center, "The Simultaneous Measurement of Ionospheric Electron Densities by CW Propagation and RF Impedance Probe Techniques," NASA, NASA TND-1098, January 1962.
102. Air Force Cambridge Research Laboratories, "Determination of Electron Density Using the Microwave Cavity Technique," Air Force AFCRL 765, September 1961.
103. Aerospace Corporation, Laboratories Division, "Some Effects of Fluid Motion on the Propagation of Electromagnetic Waves," Air Force, Contract No. AF04(647)-930, September 1961.
104. American Electronic Laboratories, General Biophysical Investigation and Instrumentation, "Measurement of Intracardiac and Intravascular Blood Velocity," Navy, Contract No. Nonr 2912(00), May 1963.
105. Astrosystems International, Inc., "Hot Gas Velocity Measuring Device," Air Force Contract No. AF04(611)-8157, April 10, 1963.

106. Kittle, Charles: Introduction to Solid State Physics, John Wiley & Sons, Inc., New York (Second Edition), February 1959.
107. Physics Today, Vol. 17, No. 9, September 1964.
108. Lazarew and Schubnikow: Phys. Z Soviet, Vol. 11, p. 445, 1937.
109. Messiah: Quantum Mechanics, John Wiley & Sons, Inc., New York, Vol. I, 1961; Vol II, 1962.
110. Rose, M. E.: Elementary Theory of Angular Momentum, John Wiley & Sons, New York, 1957.
111. Harvey, Arthur F.: Microwave Engineering, Academic Press, 1963.
112. Born and Wolf: Principles of Optics, Pergammon Press, 1959.
113. Southworth, George C.: Principles and Applications of Wave Guide Transmission, Van Nostrand Publishing Company, 1961.
114. Landan and Lifschitz: Electrodynamics of Continuous Media, Pergammon Press, New York, 1960.
115. Evans, The Atomic Nucleus, McGraw-Hill, New York.
116. Norton, H. N.: "Resistance Elements for Missile Temperatures," Instruments and Control Systems, Vol. 33, pp 992-994, June 1960.
117. Benson, James A.: "Thermal Conductivity Vacuum Gauges," Instruments and Control Systems, Vol. 36, pp 98-101, March 1963.
118. Cramer, S: "Thermal Transfer Standard Has Memory," Instruments and Control Systems, Vol. 36, pp 105-107, March 1963.
119. Morse, Philip M.: Thermal Physics, W. A. Benjamin, Inc., New York, 1964.
120. Faul, Joseph C.: "Thermocouple Performance in Gas Streams," Instruments and Control Systems, Vol. 35, pp 104-106, December 1962.
121. Hubbard, Philip G.: "Operating Manual for the IHR Hot-Wire and Hot-Film Anemometers," Bulletin 37, No. 432, State University of Iowa, 1957.

122. Wolf, O. C.: "The Hot-Wire Anemometer," Instruments and Control Systems, Vol. 33, pp 962-963, June 1960.
123. Bankoff, S. G. and Rosler, R. S.: "Constant-Temperature Hot-Film Anemometer as a Tool in Liquid Turbulence Measurements," Review of Scientific Instruments, Vol. 33, No. 11, pp 1209-1212, 1962.
124. Lumley, J. L.: "The Constant Temperature Hot-Thermistor Anemometer," Symposium on Measurement in Unsteady Flow, The American Society of Mechanical Engineers, pp 75-82, Presented at the ASME Hydraulic Division Conference, May 21-23, 1962.
125. Curtis: Introduction to Neutron Physics, Van Nostrand, Princeton, New Jersey, 1959.
126. Berkhoff, R. D.: "The Passage of Fast Electrons Through Matter," Encyclopedia of Physics, Vol. 34, pp 53-138, Springer-Verlag, Berlin, Germany, 1958.
127. Translation: "An Accurate Theory of Free Convection by A. A. Pomerantsev (A paper for presentation at the Heat Transfer Conference, June 5-10, 1961, at Minsk, USSR, pp 1-11), January 17, 1962.
128. Taylor, J. M.: Semiconductor Particle Detectors, Butterworth & Co., Limited, Washington, D.C., 1963.
129. New York University, College of Engineering, "The Diffusion of Polydisperse Particulate Clouds," Army, Contract No. DA18-108-CML-6392 and Contract No. DA18-108-405-CML-256, November 15, 1961.
130. Dew Point Hygrometer, Cambridge Systems, Inc.
131. Timmerhaus, K. D.: Advances in Cryogenic Engineering, Vol. 1-8, Plenum Press, Inc., New York, 1960-1963.
132. Vance, Robert W.: Cryogenic Technology, John Wiley & Sons, Inc., New York, 1963.
133. Folsom, Richard G.: McGraw-Hill Series in Mechanical Engineering, McGraw-Hill Book Company, Inc., New York, 1958.
134. Brillouin, Leon: Science and Information Theory, Academic Press, Inc., New York, 1963.
135. Billington, D. S.: Radiation Damage in Solids, Academic Press, Inc., New York, 1962.

136. Dearnaley, G. and Northrop, D. C.: Semiconductor Counters for Nuclear Radiation, John Wiley & Sons, Inc., New York, 1963.
137. Fisher, G. T.: "Simulation of Liquid-Vapor Humidification," Instruments and Control Systems, pp 133-138, January 1963.
138. "Characteristics of Fine Particles," Chemical Engineering, p. 207, June 11, 1962.
139. Zuehlke, Arthur A.: "Error Bands," Instruments and Control Systems, Vol. 35, pp 132-133, April 1962.
140. Rasmussen, Robert A.: "Application of Thermistors to Measurements in Moving Fluids," The Review of Scientific Instruments, Vol. 33, No. 1, pp 38-42, January 1962.
141. Corruccini, R. J.: "Properties of Materials at Low Temperatures (Part I - III)," Chemical Engineering Progress; Vol. 53; No. 6, 7, and 8; pp 262-267, pp 342-346, pp 397-402; June, July, and August, 1957.
142. "Low Temperature Technology - What's the Latest," Chemical Engineering, pp 77-82, November 30, 1959.
143. Kamal K. Seth, Northwestern University, and R. M. Wilenzick and T. A. Griffy, Duke University, "The Evaporation Model and the Shape of the Spectra of Inelastically Scattered Neutrons," Nonr(G)00069-62, 1962.
144. Lewis Research Center, Cleveland, Ohio, "An Empirical Relation for Predicting Void Fraction with Two-Phase, Steam-Water Flow, NASA Contract No. NASA TN D-1189, January 1962.
145. Rocket Propulsion Establishment, Westcott, Technical Memorandum No. 249, "Density of Liquid Oxygen Between 90° and 105°K as a Function of Pressure and Temperature," by B. W. A. Ricketson, February 1962.
146. Translation: "Diffusion of Slow Neutrons Through Liquid Oxygen," by S. V. Starodubtsev and B. I. Khrushchev, FTD-MT-63-82, September 24, 1963, Air Force Systems Command, Wright-Patterson Air Force Base, Ohio.
147. AID Report 61-130, Soviet Nuclear Instrumentation and Control for Propulsion, September 15, 1961.

148. AID Report 61-152, Soviet Nuclear Instrumentation and Control for Propulsion, December 11, 1961.

APPENDIX A

APPENDIX A

RESPONSE OF A PARALLEL PLATE CAPACITOR TO FUEL LOCATION

Section 4.3.1 described the capability of capacity measurements to measure quality of vented cryogenic fluids. Proof of the response described is given below.

1. RESPONSE BECOMES INSENSITIVE IN THE LIMIT $\epsilon \rightarrow 0$

The response of a parallel plate capacitor becomes insensitive to fuel location in the limit $\epsilon \rightarrow 1$. Reference Section 4.3.1 for definitions of symbols. For a homogenous fuel distribution,

$$S = (\epsilon - 1) \delta \quad (\text{A-1-1})$$

where

$$\delta = \frac{V_1}{V} \quad (\text{A-1-2})$$

In Equations 4-25 through 4-31, δ was taken as 1/2. For arbitrary δ ,

$$S_a = \delta\epsilon - \delta = (\epsilon - 1)\delta, \quad (\text{A-1-3})$$

which is the same as for the well-mixed case and

$$S_b = \frac{\delta(\epsilon - 1)}{\delta + \epsilon - \delta\epsilon} \quad (\text{A-1-4})$$

The error as a fraction of signal is

$$\frac{S_a - S_b}{S} = 1 - \frac{1}{\delta + \epsilon - \delta\epsilon} \quad (\text{A-1-5})$$

In the limit $\epsilon \rightarrow 1$,

$$\frac{S_a - S_b}{S} \rightarrow 0 \quad \text{as } \epsilon \rightarrow 1. \quad (\text{A-1-6})$$

Hence, for liquids with very small dielectric constants, the position error in a parallel plate capacitor becomes negligible. As shown by Equations A-1-1 and A-1-4, the signal is also very small.

2. FINITE ERROR IN RESPONSE AT $\delta \rightarrow 0$

A finite error due to fuel location exists even in the limit that the amount of liquid, $\delta \rightarrow 0$. For this case, the error as a fraction of signal is given by the $\delta \rightarrow 0$ limit of Equation A-1-5.

$$\text{as } \delta \rightarrow 0 \quad \frac{S_a - S_b}{S} \rightarrow 1 - \frac{1}{\epsilon} \neq 0 \quad (\text{A-1-7})$$

APPENDIX B

APPENDIX B

SOURCES OF STATISTICAL NOISE IN GAMMA RAY ATTENUATION OR SCATTER

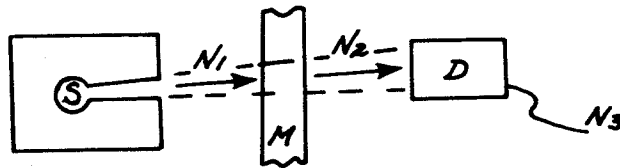
Calculations are made of statistical noise in a typical nucleonics density gauge. Errors associated with electronic data processing are not treated and are, thus, in addition to the transducer errors considered here.

1. INTRODUCTION

There is a commonly quoted thumb rule which states that due to the random Poisson¹¹⁵ nature of radioactive decay, an expected count of N pulses will have a standard deviation of \sqrt{N} .¹⁰ In an example, this rule is shown to give good results, but for reasons which are largely independent of the randomness of the decay rate. In general, it is shown that the randomness in N is a property of the transducer as a whole and could not necessarily be significantly reduced even by a hypothetical source of unvarying decay rate.

As shown in the figure, a source produces an average (or expected) number of photons, N_1 , in the solid angle subtended by the detector during a counting interval. N_1 is thus the average output count of the detector if the detector is 100% efficient and if there is no material between the source and the detector.

The presence of material, M , reduces the count N_1 to a lower value N_2 .



N_3 , the average number of pulses put out by the detector during the counting interval, is less than N_2 by the efficiency factor of the detector. Each element of this system will be separately analyzed before the total transducer is considered.

2. SOURCES OF STATISTICAL NOISE

It was intimated above that statistical noise is generated not only in the source but also in the material under measurement and in the detector. These noise sources are analyzed below with consideration being given to their effect on the measurement objective.

2.1 Source Statistics

The source puts out an average count N_1 into the solid angle subtended by the detector. Normally, one makes the approximation is made that the decay rate is characterized by Poisson statistics. This is an excellent approximation, but approximation it is, as can be seen by computing the probability that 10^5 atoms will produce 10^6 disintegrations. (The Poisson distribution¹¹⁵ gives a nonzero probability for n disintegrations during the next counting interval no matter how large n is. Physically, however, it is obvious that n cannot exceed the number of atoms present. Hence, the Poisson

description is not exact.) The binomial distribution¹¹⁵ is also a very good approximation and, in addition, it is very convenient for the purpose of this report. The binomial distribution is discussed below.

If a coin is flipped, there is some probability, p , of heads coming up (success) and some probability, q , of tails coming up (failure). Since either heads or tails must appear on this ideal coin, $p + q = 1$. If n flips (attempts) are made, the most probable number of heads is np and the standard deviation is

$$\sigma = \sqrt{npq} = \sqrt{np(1-p)} \quad (\text{B-2-1})$$

In general, the probability of an arbitrary number of heads coming up is given by the binomial distribution.

Similarly, radioactivity may be thought of as n radioactive atoms trying to decay into the solid angle subtended by the detector. Each atom has a probability p_s of success during the next counting interval. (Depletion of the source strength* due to decay is irrelevant to the statistics considered here which are written in terms of the current source strength.) Thus,

$$N_1 = np_s \quad (\text{B-2-2})$$

which describes radioactivity by the binomial distribution. It was, in fact, a model very much like this which led to the first quantitative understanding of nuclear decay.

To obtain an idea of the magnitude of n and p_s , let

$$N_1 = 10^4 \quad (\text{B-2-3})$$

and assume the source is cesium. (This value of N_1 is rather small for

*That is, from one counting interval to the next.

practical instrumentation. For demonstration purposes N_1 is assumed small. The corresponding errors are thus impractically large. Assuming the detector subtends 20% of the 4π solid angle around the source and the counting interval is 1/10 second, then the actual decay rate is 5×10^5 gammas/second or 5×10^5 decays per second if the source efficiency is unity.

The usual formula for depletion of source strength is

$$n' = n e^{-t/\tau} \quad (\text{B-2-4})$$

where τ is the characteristic life of the source (43 years or 1.4×10^9 seconds for cesium). Thus, at $t = 0$

$$\frac{dn}{dt} = -\frac{n}{\tau} \quad (\text{B-2-5})$$

or

$$n = (1.4 \times 10^9) (5 \times 10^5) = 7 \times 10^{14} \quad (\text{B-2-6})$$

radioactive atoms

and

$$p_s = N_1/n = 1.5 \times 10^{-11} \quad (\text{B-2-7})$$

which is not very probable.

According to the binomial distribution,¹¹⁵ (Equation A-2-1),

$$\sigma_{N_1} = \sqrt{np_s q_s} = \sqrt{N_1} \sqrt{1 - 1.5 \times 10^{-11}} \approx \sqrt{N_1} (1 - .75 \times 10^{-11}). \quad (\text{B-2-8})$$

The usual Poisson statistics yield:¹¹⁵

$$\sigma_{N_1} = \sqrt{N_1}. \quad (\text{B-2-9})$$

The fact that the two distributions differ in their estimate of the standard deviation by less than one part in 10^{11} is good evidence for the suitability of the binomial description.

If the source fluctuation is the only source of the statistical error, the relative standard deviation is

$$\frac{\sigma_{N_1}}{N_1} = \frac{10^2}{10^4} = 1\%, \quad (\text{B-2-10})$$

since the material and the detector act just as scalars without changing the percentage statistical fluctuations.

There is good reason to think that the binomial description of nuclear decay is actually more accurate and general than the Poisson.

The least complex description⁷³ of radioactive decay starts with a picture of an alpha particle inside a nuclear potential. The particle moves back and forth, striking the potential barrier about 10^{21} times per second. There is a small probability of penetration (tunneling) each time, which is independent of the number of previous attempts. Eventually, the alpha particle escapes and gamma ray production occurs immediately as the nucleus readjusts.

p_s is the probability of any one preselected nucleus decaying during the counting interval. If p_s is small, then a binomial description of the decay process results.¹¹⁵ In the limit of a large number of atoms, n , and small p_s , the binomial distribution approaches the Poisson distribution for most calculations.¹¹⁵ This limit is closely approached in most nucleonic applications and is the basis for the generally accepted Poisson description of nuclear decay.

Although this report illustrates an exception, it is normally more convenient to work with the Poisson distribution. However, the binomial

description is more fundamental and is valid for a large or small number of atoms.

2.2 Mass Absorption Statistics

The material itself has a very interesting effect on the statistics. Suppose the material transmissivity is just sufficient to permit half the photons to reach the detector--i. e., $N_2 = 1/2 N_1$. If 10^4 photons fall on the material, $1/2 \times 10^4$ will, on the average, reach the detector. This is just an average, however. Certainly, exactly half the photons are not transmitted during each counting interval as can be seen by considering the possibility of an odd number of photons reaching the material--e. g., $N_1 = 9$ or even 1. Fifty percent transmissivity actually means that each photon has a fifty percent chance of penetrating the material. Since the separate photons are uncorrelated, it is again similar to the coin-tossing experiment, a series of uncorrelated events each of which has a fifty percent chance of a successful outcome. The binomial distribution should thus be an excellent description of the statistics of transmission. Poisson statistics is unsatisfactory, however, as can be seen from the case of a negligible amount of mass in the path. In that case, N_2 approaches N_1 , and for fixed N_1 the variations in N_2 approach zero. Certainly, N_2 does not exceed N_1 . A Poisson estimate, namely $\sqrt{N_2}$, implies that the statistical fluctuations increase as the material is removed, reaching a 50% probability that N_2 exceeds the fixed N_1 .

Assuming that mass absorption in the material is the only cause of statistics, examination is made of its effect on the system performance.

$$N_2 = p_m N_1 \quad (\text{B-2-11})$$

where p_m is the probability of a photon penetrating the material and reaching the detector. According to Equations (B-2-1) and (B-2-11),

$$\frac{\sigma_{N_1}}{N_2} = \frac{\sqrt{N_1 p_m (1-p_m)}}{p_m N_1} = \frac{1}{\sqrt{N_1}} \sqrt{\frac{1-p_m}{p_m}} \quad (\text{B-2-12})$$

this shows that the percent deviation in N_2 becomes as small as desired as the material becomes very transparent. However, this conclusion is rather misleading as the following analysis will show.

The probability of transmission through the material is fairly well represented by

$$p_m = e^{-\mu \rho t} = e^{-\mu a} \quad (\text{B-2-13})$$

where μ is the cross section, ρ the density, and t the thickness of the material. It is actually $a = \rho t$ that we wish to measure.

As a function of N_2 , a is given implicitly by

$$N_2 = p_m N_1 = N_1 e^{-\mu a}. \quad (\text{B-2-14})$$

For small errors, the error in a , namely Δa , is related to the error in N_2 by

$$\sigma_a = \Delta a = \frac{\partial a}{\partial N_2} \Delta N_2 = \frac{\partial a}{\partial N_2} \sigma_{N_2} \quad (\text{B-2-15})$$

Solving for the percent error in a from Equations (B-2-11) through (B-2-15) yields:

$$\frac{\Delta a}{a} = \frac{1}{\sqrt{N_1}} \frac{1}{\ln(p_m)} \sqrt{\frac{1}{p_m} - 1}. \quad (\text{B-2-16})$$

For either limit, $p_m \rightarrow 0$ or 1, the percent error in a becomes infinitely large; hence, there is some value of p_m which produces a minimum relative error in a for fixed N_1 .

If, for convenience, k is defined as

$$k = \frac{1}{p_m}, \quad (\text{B-2-17})$$

the inverse of the p_m dependent part of Equation (B-2-16) becomes

$$\frac{\ln k}{\sqrt{k-1}} \quad (\text{B-2-18})$$

which is here designated g . The minimum relative error in a occurs at the extreme value of g . This is obtained by setting the derivative of g equal to zero and results in the following equation for k :

$$2 \frac{k-1}{k} = \ln k. \quad (\text{B-2-19})$$

The trial value of $k = 5$ is very close to the solution. Linear extrapolation from $k = 5$ gives $k = 4.92$. From Equation (B-2-17),

$$p_m = 0.203. \quad (\text{B-2-20})$$

For convenience, use $p_m = 0.2$. From Equation (B-2-14)

$$0.2 = e^{-1.6}. \quad (\text{B-2-21})$$

That is, the material thickness-photon energy combination should be set at 1.6 characteristic lengths for best accuracy in the hypothetical case that the material is the only source of statistical error.

Arriving at a reasonable p_m for the material, the corresponding noise level may be computed assuming that transmission is the only source of statistics. Exactly N_1 photons attempt to penetrate

the material. According to Equations (B-2-1) and (B-2-14),

$$\frac{\sigma_{N_2}}{N_2} = \frac{\sqrt{N_1 p_m (1-p_m)}}{N_1 p_m} = \frac{1}{\sqrt{N_1}} \sqrt{\frac{1-p_m}{p_m}} . \quad (\text{B-2-22})$$

Under the assumption that the material transmission is the only source of noise, the detector acts as an exact scalar and

$$\frac{\sigma_{N_3}}{N_3} = \frac{\sigma_{N_2}}{N_2} . \quad (\text{B-2-23})$$

2.3 Detection Statistics

Finally, the detection should be considered as a source of statistical error. The method of data processing becomes important here. The average energy rather than the number of transmitted alpha particles might be counted. An ionization chamber integrates the pulses and, thus, is influenced by the variation in pulse sizes as well as the number of pulses. Statistical treatments of these cases can certainly be performed. However, for this example, it is sufficient to consider straightforward pulse counting. Lost counts will be ignored and variations in trigger height will be left to an electronic error analysis. Thus, each photon has a probability of being detected which is independent of the other photons. By these assumptions, it becomes practical to describe the detection process with a binomial distribution.

The detector efficiency is the probability that an individual photon will be detected. This is p_d the probability of success at the detector. On the average,

$$N_3 = p_d N_2 = p_d p_m N_1 = p_d p_m p_s n. \quad (\text{B-2-25})$$

The standard deviation in N_3 , assuming the detector is the only source of statistics, is

$$\frac{\sigma_{N_3}}{N_3} = \frac{\sqrt{N_2 p_d (1-p_d)}}{N_3} = \frac{1}{\sqrt{N_2}} \sqrt{\frac{1-p_d}{p_d}}. \quad (\text{B-2-26})$$

In contrast to the other components, it is theoretically practical to remove the statistical error (in this case, by letting p_d approach unity).

Suppose N_3 is held fixed as p_d is increased--i. e. , the cross sectional area of the detector is decreased as the efficiency is increased. By the usual Poisson estimate of the standard deviation, namely $\sqrt{N_3}$, there is no reason to expect a reduction in statistical error. However, from Equations (B-2-25) and (B-2-26),

$$\frac{\sigma_{N_3}}{N_3} = \frac{1}{\sqrt{N_3}} \sqrt{1-p_d} \quad (\text{B-2-27})$$

indicating the statistical error of detection still approaches zero as the detector efficiency approaches 100%. This is a good illustration of the difference between binomial and Poisson statistics which occur at large values of p . It shows the gross inappropriateness of Poisson statistics for an efficient detector.

Equation (B-2-27) was derived assuming the detector is the only source of error. The point will be considered again when the system as a whole is analyzed to see whether these implications carry over.

For the numerical example, ($N_1 = 10^4$, $N_2 = 2 \times 10^3$), assume $p_d = 20\%$ as a typical detector efficiency. From Equation (B-2-26)

$$\frac{\sigma_{N_3}}{N_3} = 4.47\%. \quad (\text{B-2-28})$$

Thus, on an individual component basis, the detector is the principal source of statistical error. Recall that the source produced 1% error and the transmission 2%.

2.4 Statistics of Transmission Plus Detection

Comparison is made of the statistical variations of the output, N_3 , for two cases. In one case, there is the randomly varying output of the radioactive source with an average count of 10^4 per counting interval and the usual statistical variations of transmission and detection. This will be covered under the analysis of the whole system in the next section.

In the other case, the source is replaced by an ideal source which emits exactly 10^4 photons in each counting interval. The statistical errors come from transmission and detection only. N_1 photons attempt to be transmitted and detected and their probability of success is

$$P_{md} = P_m P_d \quad (\text{B-2-29})$$

This is a typical binomial process and, thus, from Equations (B-2-1), (B-2-2), and (B-2-25)

$$\frac{\sigma_{N_3}}{N_3} = \frac{\sqrt{(np_s) (p_m p_d) (1-p_m p_d)}}{np_s p_m p_d} = \sqrt{\frac{1-p_m p_d}{np_s p_m p_d}} \quad (\text{B-2-30})$$

Substituting $N_1 = 10^4$ and $p_m = p_d = 0.2$, yields

$$\frac{\sigma_{N_3}}{N_3} = 4.90\% \quad (\text{B-2-31})$$

This is the relative standard deviation of the system with an unvarying source, but with a realistic mass absorber and detector. In the next section, the source is treated as random and the system as a whole is analyzed and compared with Equation (B-2-31).

Any nonradioactive source of photons such as an X-ray machine is,

of course, subject to the statistical errors considered in this section.

In addition, each source of photons has its own statistics of photon production.

2.5 Integrated Transducer Statistics

With the characteristics of each component identified, it is now possible to analyze the system as a whole. A photon in a nucleus has a probability p of escaping the nucleus, penetrating the material, and being detected.

$$p = p_s p_m p_d \quad N_3 = np. \quad (\text{B-2-32})$$

Thus, a single binomial description of the whole system is appropriate and yields

$$\frac{\sigma_{N_3}}{N_3} = \frac{\sqrt{np(1-p)}}{np} = \sqrt{\frac{1-p}{np}}. \quad (\text{B-2-33})$$

Since p is of the order of 10^{-11} in the example and is negligibly small in almost any practical nucleonic gauge,

$$1-p \approx .999999999999 \approx 1.$$

Thus, to an extremely high accuracy

$$\frac{\sigma_{N_3}}{N_3} = \frac{1}{\sqrt{np}} = \frac{1}{\sqrt{N_3}} \quad (\text{B-2-34})$$

which is the usual Poisson estimate of the error. It is significant that Equation (B-2-34) includes the statistics of transmission and detection as well as those of radioactive decay.

For the numerical example considered,

$$N_3 = .2 \times .2 \times 10^4 = 400 \quad (\text{B-2-35})$$

$$\frac{\sigma_{N_3}}{N_3} = \frac{1}{\sqrt{400}} = 5\% \quad (\text{B-2-36})$$

The total system error of 5% is thus made up of 1% from the random decay of the source, 2% the randomness of transmission, and 4.47% from the randomness of detection.

In particular, as stated in the introduction, a comparison is made of the performance with a typical random source versus the performance with an ideal constant rate source. As seen from Equations (B-2-31) and (B-2-36), an ideal statistics-free source would reduce the standard deviation of the statistical errors a mere 0.1%, from 5% to 4.9%. This confirms the statement that the source can by no means be treated as the essential cause of the statistical error.

The various numerical standard deviations computed in this report are obviously related to each other by root mean square relations--e. g. ,

$$1^2 + 2^2 + (4.47)^2 = 5^2$$

and

$$2^2 + (4.47)^2 = (4.90)^2$$

(B-2-37)

The question thus arises whether this is fortuitous, approximate, or exact. The standard deviation of the source alone as seen at N_3 after exact scaling by the material and the detector is

$$\sigma_s = p_m p_d \sqrt{np_s (1-p_s)} \quad (\text{B-2-38})$$

where $p_n p_d$ is the scaling factor; n , the number of attempts; and p_s , the probability of successful escape from the nucleus. Similarly, the contributions of the transmission and detection, each computed assuming no other statistical error are

$$\sigma_m = p_d \sqrt{(np_s) p_m (1-p_m)} \quad (\text{B-2-39})$$

$$\sigma_d = \sqrt{(np_s p_m) p_d (1-p_d)} \quad (\text{B-2-40})$$

Taking the root mean square of the three standard deviations yields

$$\sigma = \sqrt{\sigma_s^2 + \sigma_m^2 + \sigma_d^2} = \sqrt{np_s p_m p_d (1-p_s p_m p_d)} = \sqrt{np(1-p)} \quad (\text{B-2-41})$$

which is indeed the exact binomial standard deviation for the integrated system. This could probably have been anticipated because the three sources of statistical error are independent.

Notice that Equation (B-2-27) appears to contradict Equation (B-2-34). The former equation seems to indicate that performance is improved by a more efficient detector with a smaller area, even though the output count rate does not increase. Equation (B-2-34) shows that in the system as a whole, the advantage is completely lost--i. e., Equation (B-2-34) is independent of the detector efficiency. The reason is, of course, that if N_3 is held constant while the efficiency is increased, then N_1 and N_2 must decrease. Thus, the statistical error of the source and the material increase to compensate for the decreased error from the detector.

In a similar vein, the derivation of 1.6 characteristic lengths of material as optimum did not consider the effect of changing the number

of characteristic lengths on the statistics of detection. The usual derivation¹⁰ of two characteristic lengths for best signal-to-noise ratio is based on Equation (B-2-34) and is preferable to the 1.6.

The most important formula of this discussion is Equation (B-2-34) which reaffirms the usual Poisson estimate of the statistical error. It is a very general formula describing the minimum statistics of the transducer. Its cause includes the statistics of transmission and detection as well as the random decay rate of the nuclei.

2.6 Alternative Approaches

In the preceding sections, it was possible to calculate the statistical fluctuations of an integrated nucleonic density transducer as well as the contribution from each of the elements of the transducer. The critical step which facilitated this calculation was the description of the radioactive decay by a binomial rather than the usual Poisson distribution.

Alternatively, it would have been possible to start out with a Poisson distribution from the source and show that the processes of transmission and detection might contribute significantly to the statistics but would not invalidate the Poisson description.

Another approach starts from some rather general assumptions of equal probability of pulses at the detector. By this method, it is possible to derive a Poisson description of N_3 without detailed reference to the mechanisms which produce the statistics.

For large n , both of these methods justify Equation (B-2-34). However,

they leave the impression that the nuclear source is somehow the principal cause of the $\sqrt{N_3}$ error. By performing a more exact derivation and then making the Poisson approximation at N_3 rather than at N_1 , it is possible to derive some additional results such as the output statistics starting with an idealized statistics-free source. The result (Equations B-2-30 and B-2-31) shows that the principle causes of the statistical errors are typically the transmission and detection rather than the nuclear source.

3. SUMMARY AND CONCLUSION

The output count, N_3 , of the detector in a nucleonic gauge has statistical fluctuations with a standard deviation of $\sqrt{N_3}$. The usual explanation is similar to the following paragraph excerpted from Ref. 10. "The probability of a given number of particles or quanta being emitted from a nuclear source in a finite interval of time is governed by Poisson's law. Hence, under counting conditions the absolute value of the standard deviation in the number of pulses $[N_3]$ at the output of the radiation counter will be equal to

$$\left[\sigma_{N_3} = \sqrt{N_3} \right].'' \quad (B-3-1)$$

This explanation may appear to imply that random decay is the principle source of statistical error. As this discussion has shown, Equation (B-3-1) includes the randomness of transmission and detection which may be more important.

The relative contributions to the $\sqrt{N_3}$ from the source, the material and the detector depend on the transmissivity of the material p_m and the

efficiency of the detector p_d , but are independent of the source size. This can be seen from the ratios of Equations (B-2-38), (B-2-39), and (B-2-40). The source statistics become dominant as p_m and p_d approach unity. Conversely, for a LH_2 scatter gauge, p_m (the probability of scatter into the detector) is very small and the source is an insignificant contributor to the statistical error.

This discussion was directed toward a nucleonic thickness gauge. However, the principles covered are rather general. For example, little more than a redefinition of symbols is necessary for the analysis to apply to a gamma-ray scatter gauge.

Although a fixed output count, N_3 , was considered in most of the report, the value of increasing N_3 is not questioned.

Equation (B-3-1) has been shown to be an accurate and versatile estimate of the minimum statistical error. However, the derivation shows that $\sqrt{N_3}$ arises from the transducer as a whole and is not necessarily largely due to the radioactive source.

APPENDIX C

APPENDIX C

SCATTERING OF GAMMA RAYS BY LIQUID VS.

SCATTERING BY VAPOR

The average density of a vapor may be doubled either by doubling the amount of vapor in the same volume or by adding liquid droplets having a total mass equal to the vapor mass. In the latter case, if the liquid density is orders of magnitude greater than the vapor density (which is normally the case), there may not be a doubling of the attenuation or scattering of the gamma rays.

This can be seen in either of two ways. First, in the limit that the density of droplets is very large, the cross section of the droplets, πa^2 , must become very small since the liquid mass is presumed equal to the constant vapor mass. In the limit that the droplet cross sections become vanishingly small, a vanishingly small fraction of the gamma rays will even hit a droplet. Since the liquid can only scatter those gamma rays which hit a droplet, this proves that the amount of scattering by the liquid can be arbitrarily small and, hence, not necessarily equal to the fixed and finite scattering by the vapor.

A second way to look at this same problem is to consider the low vapor density case, where the attenuation of the gamma flux may be neglected.

Every atom in the vapor is then irradiated by the same flux intensity and, hence, scatters an equal number of gamma rays on the average. If the liquid is introduced as one large sphere, it may shield part of itself, namely, the atoms on the side away from the source. Thus, these atoms do not have an equal chance of scattering and the net result is that the liquid does not contribute a signal equal to the signal from an equal weight of vapor or even equal to the signal which would come from the liquid if it were well dispersed.

Under the conditions of this study, the solution to these problems and to a similar problem for beta ray transmission is to disperse the liquid into drops smaller than a half thickness for the radiation used. This restriction is in no case impractical and, for the gamma ray quality meter, it is no restriction at all because of the large half thicknesses involved.

APPENDIX D

APPENDIX D

THE RELATION BETWEEN THE SOURCE STRENGTH AND DETECTOR COUNT RATE FOR THE GAMMA RAY SCATTER DETECTOR OF FIGURE 19 (SECTION 5.3)

At 100% quality and 22 psi, the density (ρ) hydrogen vapor is about 2×10^{-3} gm/cm.³ The sixty kev cross section (μ) is $0.326 \text{ cm}^2/\text{gm}$ and is due almost exclusively to scattering rather than absorption of the gamma rays.⁹ The collimator angles should be so adjusted that a sample volume about three inches on a side (7.6 cm) falls within the common field of view of the source and detector collimators. The probability of any 60 kev photon scattering in a 7.6 cm path length (t) of material (hydrogen vapor) is given by^{9, 69}

$$P_m = 1 - e^{-\mu\rho t} \approx \mu\rho t \quad (\text{D-1})$$

where the second equality is quite accurate due to the low value of P_m .

For the values given

$$P_m = 2 \times 10^{-3} \times .326 \times 7.6 = 5 \times 10^{-3} = \frac{1}{200} \quad (\text{D-2})$$

or one gamma in every two hundred passing through the sample volume will be scattered.

Of all the gamma rays scattered, only a certain fraction, p_d , is detected. First, the detector efficiency is less than one. At these low energies, the efficiency is quite high, however, 85% being a reasonable value. Secondly, of all the scattered photons, only a certain percent, p_c , Compton scatter into the detector. If the scattering were isotropic, p_c would be equal to the percent of the 4π solid angle subtended by the detector as seen from a typical point in the middle of the sample volume. The distance from the typical point to the detector is about 3.5 inches and a three inch diameter detector is a good size for this application. Thus,

$$p_d = .85 p_c = .85 \frac{\pi 3^2}{16\pi(3.5)^2} = 4.6 \times 10^{-2}. \quad (D-3)$$

Finally, there is the probability, p_θ , that a gamma ray from the source will be emitted in the direction of the sample volume. This is proportional to the fraction of the 4π solid angle subtended by the sample volume as seen from a typical atom in the source about 3.5 inches away.

$$p_\theta = \frac{3^2}{4\pi(3.5)^2} = 5.8 \times 10^{-2} \quad (D-4)$$

The overall probability of detection of an emitted gamma ray is p .

$$p = p_\theta p_m p_d = 5 \times 10^{-3} \times 4.6 \times 10^{-2} \times 5.8 \times 10^{-2} = 1.3 \times 10^{-5} \quad (D-5)$$

A curie of a radioactive material is defined⁷ as 3.7×10^{10} disintegrations per second. Many nuclei emit an average of the order of one particle per disintegration or 3.7×10^{10} particles per second per curie. It is the number of particles or photons emitted per second rather than the number of disintegrations which determines the effects of the radiation, and thus it is convenient to work in units of effective curies, C, where one effective curie is 3.7×10^{10} emanations per second.

For a source of C effective curies, the count rate per 1/10 second counting interval is

$$N = \frac{pC \times 3.7 \times 10^{10}}{10} = 4.8 \times 10^4 C . \quad (D-6)$$

Actually, the scattering is not exactly isotropic. At high energies (1 mev), forward scattering is strongly preferred.¹¹⁵ At 60 kev, the scattering is considerably more isotropic, although 90° scattering still falls below the average cross section per solid angle.¹¹⁵ Hopefully, the backscatter contribution to the flux will compensate for the lack of isotropy but to be on the safe side, take

$$N = 3 \times 10^4 C , \quad (D-7)$$

which should give satisfactory results.

APPENDIX E

APPENDIX E

THEORY OF PULSE RATE RATIO COMPUTER

The basic divider circuit is shown schematically in Figure E-1.

Consider two pulse frequencies, f_1 and f_2 , either random to each other such that their phase angle relationships fall with equal probability within any point from 0 to 2π radians, or two clock frequencies not in harmonic relationship which will permit one to advance on the other with uniform phase distribution. The frequencies, f_1 and f_2 , operate the switch in Figure E-1 in opposite directions. The switch remains in the thrown position until the next opposing pulse throws it in the opposite direction.

The average current, I_R , through the meter, M, is the sum of a series of positive and negative rectangular current waveforms that vary linearly between two extreme shapes. Figure E-2A shows the current waveform for the pulse of f_2 which occurs an infinitesimally small time (Δt) after the nearest pulse f_1 . Figure E-2B is that waveform which occurs when pulse f_2 occurs an equally small time before the nearest pulse f_1 . The extremes of these waveforms are averaged over a period $1/f_2$ of the lowest frequency f_2 , thusly,

$$A_1 = i_c \left[1/f_2 - (1/f_1 - \Delta t) - (1/f_1 - \Delta t) \right] \quad (\text{E-1})$$

$$= i_c (1/f_2 - 2/f_1 + 2\Delta t).$$

$$A_2 = i_c (1/f_2 - \Delta t - \Delta t) \quad (\text{E-2})$$

$$= i_c (1/f_2 - 2\Delta t).$$

$$I_R = \frac{(A_1 + A_2)f_2}{2} = i_c \frac{2/f_2 - 2/f_1}{2/f_2} = + i_c (1 - f_2/f_1) \quad (\text{E-3})$$

for

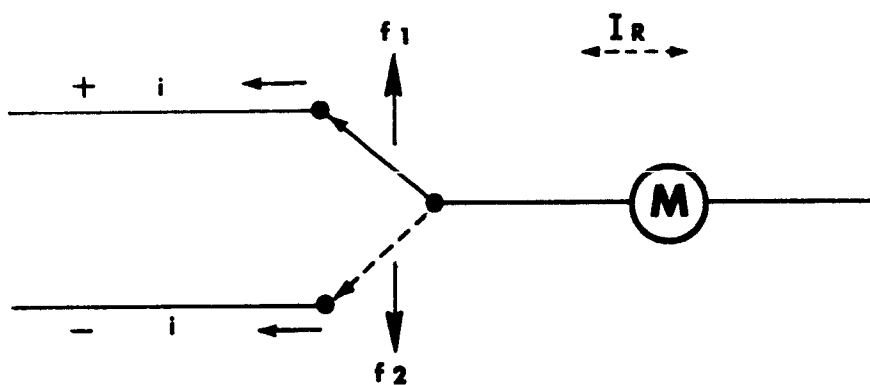
$$f_1 > f_2$$

and,

$$I_R = -i_c (1 - f_1/f_2) \text{ for } f_2 > f_1.$$

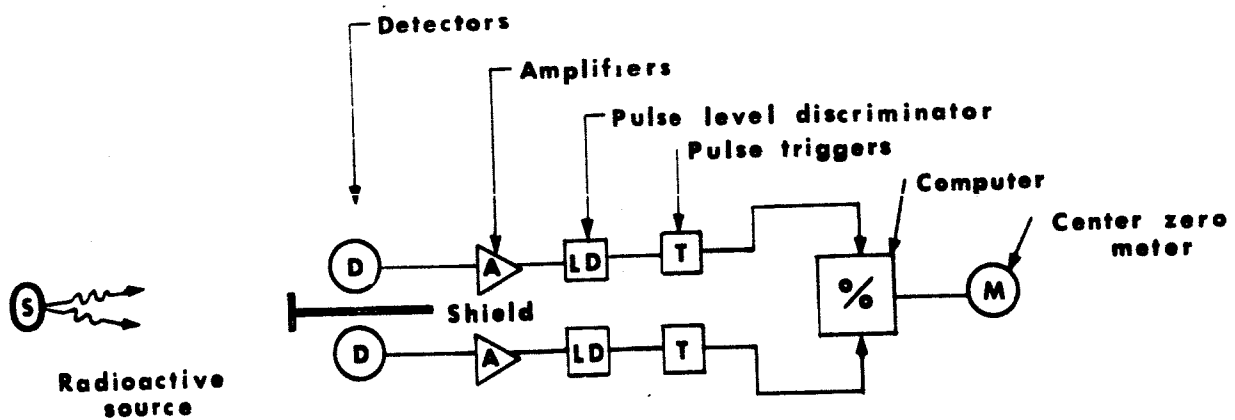
The average current, I_R , is zero when $f_1 = f_2$ and the bidirectional meter M is at its midpoint. When either frequency is absent, the meter needle will assume an extreme position. This is effectively dividing the other frequency by zero, a mathematical indeterminate. This is illustrated in the calibration curve of Figure E-3.

$f_2, f_1 =$ Pulse frequencies



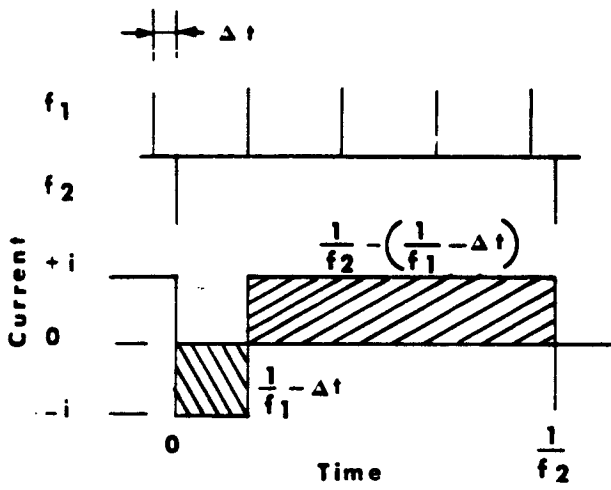
BASIC DIVIDER CIRCUIT

Figure E-1

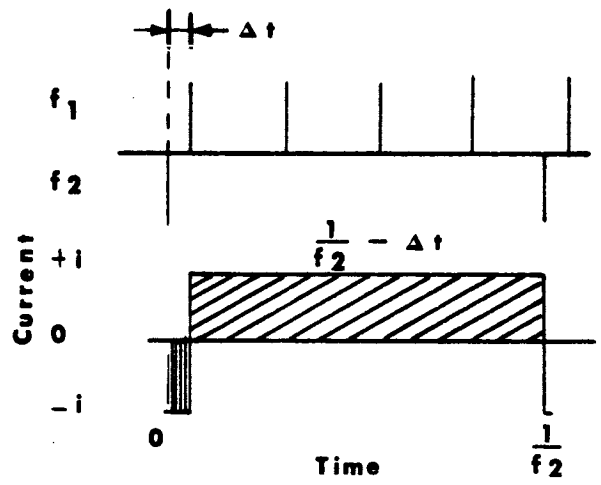


DIRECTION INDICATOR

Figure E-2



(A)



(B)

CURRENT WAVE FORMS

Figure E-3